BASIC AND PRACTICAL INVESTIGATIONS OF AUTOMATED STOPPED-FLOW MIXING SYSTEMS

Ву

Floyd James Holler

A DISSERTATION

Submitted to

Michigan State University

in partial fulfillment of the requirements

for the degree of

DOCTOR OF PHILOSOPHY

Department of Chemistry

ABSTRACT

1. 3 26 3

BASIC AND PRACTICAL INVESTIGATIONS OF AUTOMATED STOPPED-FLOW MIXING SYSTEMS

By

Floyd James Holler

Several elements of automated stopped-flow mixing systems have been investigated and are described. A critical study of temperature effects in stopped-flow mixing systems has been carried out. Special emphasis was placed on the determination of the signs and magnitudes of the temperature changes which occur before and during mixing when the modules are maintained at 20-30°C. Based on the results of these experiments, guidelines are suggested for minimizing the effects of the temperature changes which occur during mixing, particularly when the modules are utilized in routine reaction-rate methods of analysis.

The computerized temperature circuit utilized in the above study is described in detail. The operation and calibration of the circuit are presented, and a brief description of the software which was used for data acquisition and analysis is given. Experiments are presented which demonstrate the accuracy (±0.05 K), the precision (±0.002 K per sample), and the sampling rate (5 kHz) of the

system. A thermistor plunge test is presented in order to demonstrate the utility of the instrument.

A computerized version of the bipolar pulse conductance instrument is presented, and its operation is described in detail. The instrument is capable of high speed data acquisition and analysis, computer control over circuit parameters, optimization of individual measurements, and correction of measurements for temperature changes. The accuracy (± 0.02 %) and precision ($S/N \ge 10^4$ with signal averaging) make the instrument a useful tool for conductometric analysis. The system is applied as a detection system in stopped-flow mixing, and a multi-detector observation cell is described. Studies of the dehydration of carbonic acid and the reaction of nitromethane with base are presented to demonstrate the applicability of the instrumental system.

Two new designs for a computer controllable, stepping motor driven buret are presented, and the operating characteristics of the prototype models are presented. A 50 ml buret demonstrated accuracy and precision of ca. 0.05% for 10 ml increments. For 1 ml increments the accuracy and precision were ca. 0.1%. A second buret which features interchangeable syringe barrels is described and is shown to be precise to ca. 0.06% for 1 ml increments. A completely automated reagent preparation system is proposed which will utilize the precision burets. The system is intended to function as the front end to an automated stopped-flow mixing system.

Finally, a simple method is described for directly determining the relative position of the syringe drive block in a stopped-flow mixing system as a function of time. The principles of the method as well as experimental results which indicate its accuracy and ease of application are presented.

To Vicki

Brian, Brad, and Scott

With Love

ACKNOWLEDGMENTS

I wish to express appreciation to Professor S. R. Crouch and Professor C. G. Enke for guidance, encouragement, and friendship over the course of this work. I am particularly grateful for the many unique educational opportunities which they have provided. I also owe special thanks to Professor Ralph D. Joyner of Ball State University whose encouragement prompted my return to graduate school.

I am indebted to the Michigan State University Chemistry
Department for providing excellent research facilities
throughout the course of this work and a teaching assistantship during most of my tenure in graduate school. The
research support provided by the National Science Foundation is greatly appreciated. I am grateful for technical
support provided by the staffs of the machine shop, the
electronics shop, the glass shop, and the library of the
Chemistry Department.

In addition, I would like to thank the many members of C. G. Enke & Company and the S. R. Crouch Research Group for fellowship and assistance. I am especially indebted to Tim Nieman, Ed Darland, Keith Caserta, Phil Notz, and Tom Last for their friendship and their many positive contributions to this work. Also deserving special thanks are Sandy Koeplin and Roy Gall for assistance in the preparation of this manuscript and Tom and Arden Atkinson

for their assistance and hospitality during the final days.

I would also like to thank my parents and parents-inlaw for their support and encouragement during my education. Finally, I am most grateful to my wife, Vicki, for
her love and encouragement. During the past four years
she has maintained our home, raised three fine sons, and
provided financial and moral support, often under very
difficult conditions. Through it all, she has remained
my best friend and staunchest supporter.

TABLE OF CONTENTS

Chapter	P	age
LIST OF	TABLES	ix
LIST OF	FIGURES	×
INTRODUC	CTION	1
	STOPPED-FLOW TECHNIQUE IN CAL CHEMISTRY	3
Α.	INTRODUCTION	3
В.	REACTION-RATE METHODS OF ANALYSIS	5
	1. General Considerations	5
	2. Fast Reaction Techniques	10
C.	AUTOMATED STOPPED-FLOW MIXING SYSTEMS	16
-	ITICAL STUDY OF TEMPERATURE EFFECTS PED-FLOW MIXING SYSTEMS	20
Α.	INTRODUCTION	20
в.	EXPERIMENTAL	24
	1. Instrumentation	24
	2. Software	30
c.	RESULTS AND DISCUSSION	33
	1. Thermostatting Efficiency	33
	2. Temperature Changes During the Mixing Process	35
	3. Multiple Pushes	48
D.	SUMMARY AND CONCLUSIONS.	50

Chap	ter																		Page
III.	PI	RECIS	TERIZ SE ME RATUR	ASU	REM	ENT	· 0	F		ΡI		•	•	•	•	•	•	•	55
	Α.	INT	RODUC	TIO	N.	•	•	•		•	•				•	•	•	•	55
	в.	THE	TEMP	ERA	TUR	E M	ION	II	'OF	≀.	•	•	•		•	•	•	•	56
		1.	Anal	.og	Cir	cui	.t	•			•		•	•	•	•	•	•	56
		2.	Sequ	enc	er.	•	•	•	•	•	•	•	•	•	•	•	•	•	64
		3.	Comp	ute	r.	•		•		•					•	•	•	•	66
		4.	Inte	rfa	.ce.	•	•	•	•	•	•	•	•	•	•			•	67
	c.	CIRC	CUIT	OPE	RAT	ION	1.	•	•	•	•	•	•	•		•	•	•	68
		1.	Circ	uit	. Ca	lik	ora	ti	.or	1.	•	•	•	•	•	•	•		69
		2.	Tran	ısdu	cer	Ca	ali	.br	at	ic	on	•	•	•	•	•	•	•	70
		3.	Data	ı Ac	gui	sit	ic	n	ar	nd	Ar	na]	Lys	sis	3.	•	•	•	76
	D.	EVA	LUATI	ON	OF '	THE	e T	EM	1PI	ERA	JTA	JRI	C						
		MON	ITOR.	•	• •	•	•	•	•	•	•	•	•	•	•	•	•	•	77
		1.	Accı	ırac	y a	nd	Pr	ec	cis	sic	on	•	•	•	•	•	•	•	77
		2.	Fred	quen	су	Res	gge	ns	se	•	•	•	•	•	•	•	•	•	80
	E.	CON	CLUS	ONS	. .	•	•	•	•	•	•	•	•	•	•	•	•	•	82
IV.			JTER TIVIT									_			•				
			MICAI													•	•	•	85
	A.	INT	RODUC	TIO	N.	•	•	•	•	•	•	•		•	•	•	•	•	85
	в.	THE	INST	RUM	ENT	•	•	•	•	•	•	•	•	•	•	•	•	•	87
		1.	The	Ana	log	In	ite	ra	ct	ic	ns		•	•	•	•	•	•	89
		2.	The	Dig	ita	1 1	nt	er	ac	ti	lor	s	•		•		•	•	93
		3.	Syst	em	Fle	xib	il	it	у (an	d :	So	ftı	wa:	re	•	•	•	95
		4.	Meas	ure	men	t C	nt.	im	1 j	at	-ic	'n	_				_		99

Cnap	ter																		Page
	c.	PERF	ORMAI	NCE.		•	•	•	•	•	•	•	•	•	•	•	•	•	101
		1.	\$cale	e Cl	hang	ges	3.	•			•	•	•	•	•	•	•	•	101
		2.	Linea	ari	ty a	ano	1 F	≀an	ge	•	•	•	•	•	•	•	•	•	103
		3.	Resol	lut:	ion	aı	nd	s/	N	•	•	•	•	•	•		•	•	104
		4.	Accui	cacy	y .	•	•	•	•	•	•	•	•	•	•	•	•	•	104
		5.	Pulse	e W	idtl	h S	Sel	.ec	ti	on	٠.	•	•	•	•	•	•	•	108
	D.	DEHY	DRAT	ON	OF	CZ	ARE	BON	D	10	ΧI	DE	•	•	•	•	•	•	110
		1.	Expe	cime	enta	al	•	•	•	•	•	•	•	•	•	•	•	•	112
		2.	Resul	lts	and	ı E	Dis	cu	ss	io	n	•		•	•	•	•	•	117
		THE	ERATU REACT	rioi															
		WITH	BASI	Ξ.	• •	•	•	•	•	•	•	•	•	•	•	•	•	•	120
		1.	Expe	cime	enta	a 1	•	•	•	•	•	•	•	•	•	•	•	•	122
		2.	Resul	lts	and	1 E	Dis	cu	SS	io	n	•	•	•	•	•	•	•	122
	F.	CONC	LUSIC	NC		•	•	•	•	•	•	•	•	•	•	•	•	•	127
V.			N STI MATEI										UR •	EI	'S	•	•	•	128
	A.	INTR	ODUCI	rioi	N .	•	•	•		•	•	•	•	•	•	•	•	•	128
	В.	MACR	O-BUI	RET		•	•	•		•	•		•				•	•	129
		1.	Detai	ils	of	De	esi	.gn	•	•	•	•	•			•	•	•	129
		2.	Perf	orma	ance	е.	•			•		•	•	•	•	•	•	•	134
			RCHAI							-	0	AN	D						137
			O BUI								•	•	•	•	•	•	•	•	
			Desig																
		2.	Perf	orma	anc	e.													138

Chap	ter																		Page
	D.	SOLU	JTIO	N PI	REP	AR	AT 1	ON	S	YS?	CEM	1.	•	•	•	•	•	•	142
		1.	Con	tro	l a	nd	Se	qu	en	cir	ng	•			•	•	•	•	142
		2.	Sys	tem	Co	mp	one	ent	s.	•	•	•	•	•	•	•	•	•	144
		3.	Sol	utio	on	Pr	epa	ıra	ti	on	•	•	•	•	•	•	•	•	145
		4.	Sys	tem	Pe	rf	orn	nan	ce	•	•	•	•	•	•	•	•	•	145
VI.	FLOV	NSDUC W RAT	res									INC	3						148
				• •	•	•	• •	•	•	•	•	•	•	•	•	•	•	•	
VII.	SOF	rwari	E DE	VEL(OPM	IEN'	r .	•	•	•	•	•	•	•	•	•	•	•	150
	A.	INT	RODU	CTI	NC	•	•	•	•	•	•	•	•	•	•	•	•	•	150
	B.	THE	COM	PUTI	ER	•	•	•	•	•	•	•	•	•	•	•	•	•	150
	c.	TEM	PERA	TURI	E M	ION:	ITC	R	SOI	FTV	VA I	Œ	•	•	•	•	•	•	152
	D.			PUI E.							•	•		•	•	•	•	•	155
	E.			he I				iv	e 1	Plo •	ott •	ir •	ng •	•	•	•	•	•	157
APPEI	XIDIX	- P1	rogr	am 1	Lis	ti	ngs	·	•	•		•	•	•		•	•	•	162
	Prog	gram	TCA	L.	•	•	•	•	•	•		•	•	•	•	•	•	•	162
	Prog	gram	TAC	1.	•	•	•	•	•	•		•	•	•	•	•	•	•	163
	Subi	routi	ine	PLO	r.	•	•	•	•	•		•	•	•	•	•	•	•	169
REFEI	RENCI	ES.			•		•		•	•		•				•			172

LIST OF TABLES

Table	Page
1	Accuracy of Temperature Circuit 78
2	Precision of Temperature Circuit 79
3	Performance Characteristics 105
4	Accuracy (in percent) for various
	conductance - series capacitance
	combinations. Allowed relaxation
	time is 30 μ seconds unless otherwise
	indicated 107
5	Calculated Rate Constants for the
	Dehydration of Carbonic Acid 118
6	Buret Delivery Accuracy and Pre-
	cision - Ten Millimeter Increments 135
7	Buret Delivery Accuracy and Pre-
	cision - One Millimeter Increments 136
8	Precision of Interchangeable
	Buret - One Milliliter Increments 141
9	Interactive Graphics Commands 159

LIST OF FIGURES

Figure		Page
1	Classification of Reaction Rate	
	Methods	. 11
2	Optimum Automated Stopped-Flow	
	Mixing System	17
3	Thermostating Arrangement of the	
	Stopped-Flow Modules	25
4	Observation Cells of Stopped-Flow	
	Modules	29
5	Thermostating Efficiency of Stopped-	
	Flow Modules: Tc-vs-Tt	34
6	Long-Term Return to Thermal Equi-	
	librium after Cessation of Flow	37
7	Reproducibility of ΔT : (a) MSU;	
	(b) Durrum; (c) GCA. Multiple	
	Pushes: (d) MSU; (e) Durrum;	
	(f) GCA	39
8	Temperature-vs-time: Durrum Module	42
9	Temperature-vs-time: GCA Module	43
10	Temperature-vs-time: MSU Module	44
11	Effect of T_t on ΔT	46
12	Analog Portion of the Computerized	
	Temperature Monitor	53

Figure		Page
13	Analog and Digital Waveforms for	
	the Temperature Monitor	59
14	Digital Section of the Com-	
	puterized Temperature Monitor	65
15	Typical Resistance-vs-Temperature	
	Data for the Calibration of a Fast	
	Thermistor	72
16	Fit of the Data of Figure 15 to	
	the Equation: $T^{-1} = A + B \ln R$	74
17	Residual Plot for the Curve-fit	
	of Figure 16	75
18	Rapid Temperature Change Simulated	
	by Switching Two Different	
	Resistors into the Feedback Loop	
	of OAl	81
19	Thermistor Plunge Test	83
20	Block Diagram of the Computerized	
	Conductance Instrument	88
21	Analog Circuits of the Conductance	
	Instrument	91
22	Analog-to-Digital Conversion Section	
	of the Conductance Instrument	94
23	Measurement Sequencer of the Con-	
	ductance Instrument	96

rigure		Page
24	Percent Error-vs-log (Resistance)	
	at Various Pulse Widths	109
25	Multidetector Observation Cell	
	for the Stopped-flow Module	114
26	Reaction Curve for the Dehydration	
	of Carbonic Acid by Conductometric	
	Detection	116
27	Arrhenius Plot of Rate Constants	
	Obtained at Various Temperatures	
	by Conductometry	119
28	Conductance-vs-Temperature	
	Circuit Response for a Mixture	
	of 5 x 10^{-5} M Nitromethane and	
	$3.36 \times 10^{-3} \underline{M} \text{OH}^{-}$	123
29	Conductometric Curve Showing	
	the Progress of the Reaction of	
	Nitromethane with Base	125
30	Photograph of Automated Burets	
	and Controller	130
31	Detail of Macro-Buret	132
32	Detail of Interchangeable	
	Buret	139
33	Automated Solution Preparation	
	Creation	142

Figure		Page
34	(Figure 1) - Displacement Trans-	
	ducer (a) Attachment to Stopped-Flow	
	Mixing System (b) Schematic Diagram	148
35	(Figure 2) - Upper Curve: Oscilloscope	
	Trace. (·) Experimental Points Ob-	
	tained from Upper Curve. (-) Fitted	
	Curve: Distance-vs-Time. () Velocity-	
	vs-Time	149
36	Block Diagram of Computer System	151
37	Block Diagram of Computer Soft-	
	ware	153

INTRODUCTION

Generally, this dissertation is organized around the rapidly growing area of reaction-rate methods of analysis and the technology which makes reaction-rate methods possible. More particularly, it involves the characterization of the stopped-flow mixing technique and the development and application of two new detection systems for stopped-flow mixing. Each chapter of this work with the exception of the final chapter is a completed project and appears in the form of a manuscript which may be read independently of other chapters.

The first chapter gives an overview of reaction rate methods of analysis and provides the rationale for the use of the stopped-flow technique in analytical chemistry. The material in this chapter appeared as the introductory section in an extensive review article which dealt with this subject (1). Chapter two is an attempt to characterize three different stopped-flow mixing systems with respect to the thermal changes which occur in the instruments during use. The instrument which was developed to carry out this study is described in considerable detail in Chapter III. In the fourth chapter, the application of the bipolar pulse conductivity technique is described with emphasis on its role as a detection system in stopped-flow experiments.

Chapter V presents two computer-controlled, steppingmotor driven precision burets, and tests demonstrating
their accuracy and precision are described. A completely
automated reagent preparation system is then proposed
as an accessory to the stopped-flow mixing modules. The
sixth chapter presents an interesting application of
optoelectronics technology that enables the determination of absolute velocities in flow systems and other
instrumentation involving moving parts. Finally, the
last chapter discusses the computer software that was
developed in the process of carrying out the projects
discussed above.

The first six chapters of this thesis are manuscripts or sections of manuscripts of articles that have been submitted for publication. Chapter VI appears in this thesis in its published form with the permission of Analytical Chemistry (2). Although Chapter III has been retyped, it appears exactly as it went to press in Chemical Instrumentation (3), and it is reproduced by permission of the publisher. It should also be mentioned that the author played a significant role in the development of a stopped-flow reaction-rate method for the determination of cyanamide (4). Since a large portion of that work appeared in another dissertation (5), it is not reproduced here.

CHAPTER I

THE STOPPED-FLOW TECHNIQUE IN ANALYTICAL CHEMISTRY

A. INTRODUCTION

The stopped-flow technique for the rapid mixing of chemical reagents has gained widespread importance in the measurement of the rates of rapid chemical reactions. Reaction-rate information can be obtained routinely on reactions with half-lives as short as a few milliseconds by using stopped-flow mixing in conjunction with a rapid reaction monitoring technique, such as UV-visible spectrophotometry. Stopped-flow mixing is most frequently used to obtain fundamental information about rapid chemical reactions (rate law information, rate constants, activation energies, etc.). However, in recent years the stopped-flow technique has been shown to be a valuable tool for analytical purposes. There are several reasons why the stopped-flow technique has considerable potential in the analytical laboratory. First, with moderately rapid reactions, stopped-flow mixing can provide analytical information in a very short time, often in a few seconds or less. The high information throughput provided by stopped-flow systems is particularly attractive because the demand for analytical information in such critical areas as clinical chemistry and environmental chemistry

is rapidly growing and threatening to outpace the ability of the laboratory to supply the desired information. A second reason why stopped-flow mixing should gain increasing acceptance in analytical chemistry is the extremely small solution volumes required to obtain analytical information. Often, reaction-rate or endpoint methods can be carried out with sample volumes as small as a few microliters. The stopped-flow technique can also be completely automated to eliminate manual manipulations of reagents and to provide rapid and reproducible mixing of reactants. These latter features are, of course, desirable even for measurements on reactions which are normally considered slow. Finally, the increasing use of minicomputers and microprocessors with stopped-flow systems for control, data acquisition and data processing should lead to a higher level of automation with significant increases in measurement throughput, accuracy and precision.

In this chapter, the stopped-flow technique is examined from an analytical perspective. After a brief discussion of the advantages and limitations of reaction-rate methods of analysis, automated stopped-flow mixing systems are described in order to provide a framework for the chapters which follow.

B. REACTION-RATE METHODS OF ANALYSIS

Reaction-rate methods of analysis have become increasingly popular in recent years. Their application to analytical problems in several areas of chemistry has been the subject of books (6,7) and numerous review articles (8-28). Rate methods utilize the kinetics of reactions rather than reaction stoichiometries to provide analytical information. In this section the advantages and limitations of reaction-rate methods are discussed first. Then fast reaction techniques are classified, and the reasons why the stopped-flow technique has become the dominant flow method are presented.

1. General Considerations

In reaction-rate method of analysis the desired result of the measurement is the initial concentration of analyte, designated here as [A]_O. Experimental conditions are usually chosen so that the reaction is either first-order or pseudo-first-order for the analyte A. For a reaction of this type, the rate of disappearance A, with time is

$$-\frac{d[A]}{dt} = k[A] \tag{1}$$

where k is the first-order or pseudo-first order rate constant. If this equation is integrated from t = 0

(the reaction initiation time) to t = t (the time of observation), the following relationship between the concentration of A at time t and the initial concentration of A, $[A]_0$ is obtained.

$$[A]_{+} = [A]_{0} \exp (-kt)$$
 (2)

If Equation (2) is substituted into Equation (1), the reaction rate at any time t can be expressed in terms of $[A]_{O}$.

$$-\left(\frac{d[A]}{dt}\right)_{t} = k[A]_{o} \exp(-kt)$$
 (3)

Equation (2) forms the basis of one type of reactionrate method of analysis. By making a measurement of the concentration of A at any time t the initial concentration [A] can be determined.

The other type of reaction-rate method, based on Equation (3), is more correctly called a reaction-rate method because it involves a measurement of the change in concentration of A, $\Delta[A]$, which occurs in a given time interval, $\Delta t = t_2 - t_1$. If the measurements of $\Delta[A]/\Delta t$ are performed during the initial portion of the reaction, the procedure is termed an initial reaction-rate method. In this case the exponential term in Equation (3) is approximately unity. Conditions for which this approximation is valid have been discussed

by Pardue (25), Ingle and Crouch (29), and Crouch (18).

One advantage of methods based on initial reaction rates is that measurements can be made in a small fraction of the time required for the reaction to reach equilibrium. Reaction-rate measurements may be obtained within a few seconds of the initiation of the reaction, even if the reaction has a half-life of a few hours. The time necessary for an equilibrium method based on the same reaction would be prohibitively long for routine analytical procedures.

Because reaction-rate measurements are usually obtained during the initial stages of the reaction, very complicated reactions such as reactions with unfavorable equilibrium constants, or nonstoichiometric reactions, can often be employed for analytical purposes. Although the equilibria for these reactions may be complicated, the initial reaction rates are often straight-forward and can be used for obtaining quantitative analytical information.

Another advantage of rate methods is that they are often more specific than the corresponding equilibrium-based methods. Specificity can result in an additional saving of time, since separations can often be avoided. In addition, simultaneous analysis of complex mixtures by differential reaction-rate measurements can often be accomplished (6,18,27). If a sample contains two or more substances which react with a common reagent

at significantly different rates, differences in the rates of the reactions rather than their thermodynamic differences can be exploited for analysis. By measuring the rate of the reaction when the species of interest is the major contributor to the overall rate, specificity can be achieved. If the reaction were allowed to reach equilibrium, all of the substances would react with the reagents to form a mixture of products and would interfere with the determination of the species of interest. Multicomponent determinations can be performed by making several rate measurements during time periods when different species are reacting (6).

One of the most important advantages of the reaction-rate method is that it involves a relative measurement. For a first-order or pseudo-first-order reaction, the quantity of interest is the rate of change of some parameter (proportional to the concentration of a reactant or product) with time. The absolute value of the parameter used to monitor the reaction does not have to be measured accurately. Therefore, rate methods may afford freedom from those interferences which contribute to the absolute value of the parameter, but which do not enter into the reaction and, hence, do not contribute to the rate of change of the monitored parameter. For the specific case of spectrophotometric measurements, the absolute value of the absorbance of a solution at the analytical wavelength depends on factors such as

the presence of impurities which absorb radiation at that wavelength, turbidity in the solution, and cell imperfections. In a reaction-rate method, these factors do not interfere if they do not change as the reaction proceeds (30).

Although the advantages of rate methods are most apparent when slow reactions are considered, the enhanced specificity, increased speed and relative freedom from reaction monitor interferences are also advantageous when fast reactions are employed.

Reaction-rate methods of analysis are also subject to several limitations. One is imposed by the rate of the reaction. In order for a reaction to be analytically useful, it must occur at a measurable rate. To date the fastest reactions which have been analytically useful have half lives of several ms (31,32). The use of reactions with half lives of more than a few hours is clearly undesirable.

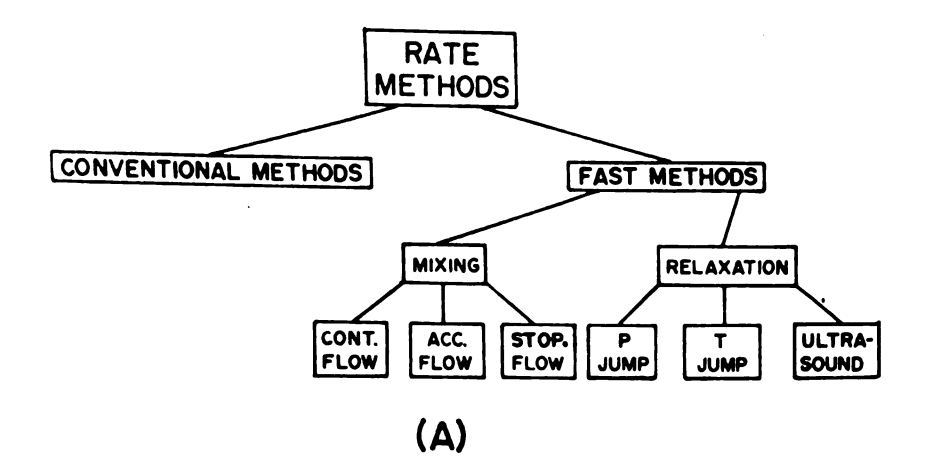
Since initial rate methods depend on the precise measurement of the reaction rate, a second limitation is that experimental conditions must be carefully controlled. The rate of a reaction is dependent on factors such as pH, ionic strength, and temperature. If these factors are not carefully controlled, reliable results will not be obtained. Often such parameters need not be as carefully controlled in stoichiometric methods as in rate methods.

Another limitation of rate methods is that lower signal-to-noise ratios are obtained than with equilibrium-based determinations, since only a small portion of the total available signal is measured. In many cases only very small changes in signal in a given measurement time are monitored. Thus, the detection system must have very high sensitivity.

In summary, it should be pointed out that for selected reactions the advantages of reaction-rate measurements can outweigh the limitations of control of reaction conditions and lower signal-to-noise ratios. In addition, new improvements in instrumental detection systems and the introduction of computerized instrumentation are rapidly minimizing the limitations of rate methods (18, 22).

2. Fast Reaction Techniques

a. Classification of Methods - Reaction-rate methods of analysis may be classified by first separating them into "conventional" and "fast" techniques as is illustrated in Figure 1(a). Although the distinction between these two classes is somewhat nebulous, it may be quantified to some extent if we consider that the time necessary to mix two reagents by manual (conventional) means is usually 2-10s. The further stipulation that the mixing time must be somewhat shorter than the half-life



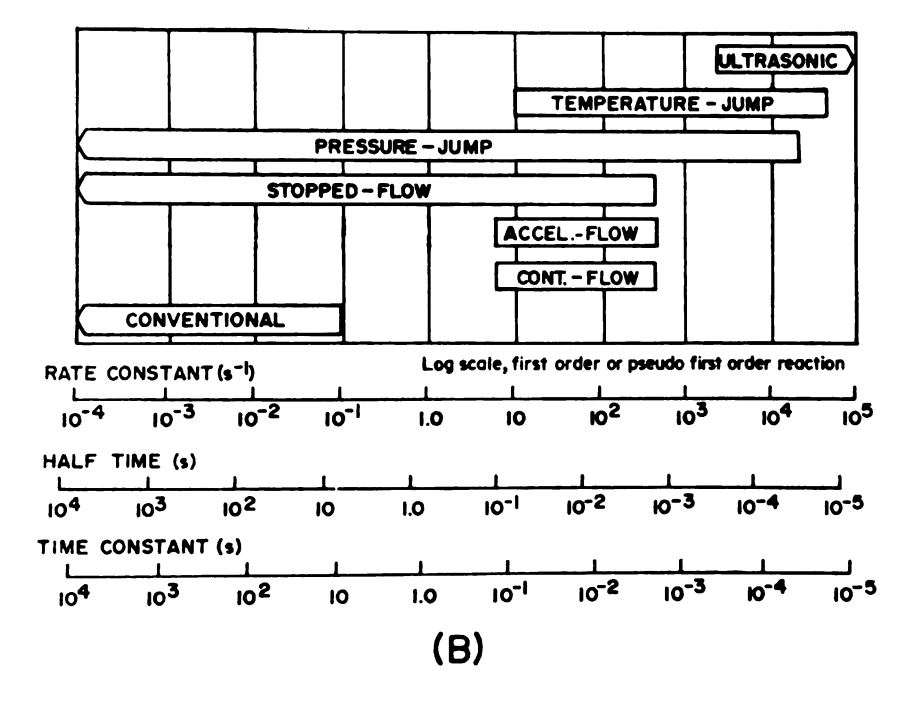


Figure 1. Classification of Reaction Rate Method.

of the reaction of interest limits first-order or pseudo-first order rate constants accessible by conventional means to $\approx 10^{-1} \, \mathrm{s}^{-1}$. The position of conventional rate methods in the range of available reaction-rate techniques is shown in Figure 1(b). "Fast" reactions may then be classified as those whose rates cannot be measured by "conventional" means at "ordinary" temperatures and concentrations, <u>i.e.</u>, first-order or pseudo-first order rate constants greater than $\approx 10^{-1} \, \mathrm{s}^{-1}$ (33).

Fast reaction techniques may be further divided into mixing and relaxation methods. The mixing methods are composed of three categories: continuous-flow; accelerated-flow; and stopped-flow methods. Flow methods all utilize initially separated reactants which flow in two or more different streams through a mixing chamber into an observation cell in which some physical property of the mixed solution is measured. The introduction of jet mixers has reduced times for complete mixing of reactant solutions to ~1 ms. This achievement has thus lowered the limit of half-lives of reactions observable by mixing methods to ~1 ms as is shown in Figure 1(b).

The continuous-flow method was first developed by Hartridge and Roughton in a pioneering series of studies in 1923 (34-36). In this method the two reagent solutions are allowed to flow from large reservoirs through a mixer into a long tube. Since the flow velocity may

be maintained constant, the distance along the tube from the mixer is proportional to the time of reaction. Observation of the physical property of interest at various distances along the tube gives a concentration-vs-time profile for the reaction.

The initial use of the accelerated- and stopped-flow methods was by Chance in 1940 (37). Briefly, the accelerated-flow method consists of forcing reagents through the mixing chamber at a rapidly increasing rate and simultaneously measuring the flow rate and a physical property of the solution. From the record of flow rate and the physical property of interest, a concentration-vs-time profile may be obtained. The technique requires only small volumes of solution, and reactions with half-lives of *1 ms may be observed.

In principle, the stopped-flow technique differs from the other mixing techniques only in that the observations are made after the flow is rapidly stopped (stopping time <1 ms). The lower limit of reaction half-lives accessible by this method is approximately the same as that of the other mixing methods as is illustrated in Figure 1(b). The advantages of this method over the other mixing methods are discussed in the next section.

Relaxation methods involve the application of a sudden perturbation to a chemical system initially at

equilibrium and subsequent observation of the relaxation of the system back to its equilibrium point. The most common of these methods are temperature-jump (t-jump), pressure-jump (p-jump), and ultrasonic absorption (33). Since these methods do not depend upon the mixing time of reactants, extremely rapid reactions ($t_{\frac{1}{2}} \approx 10^{-9}$ s for ultrasonic absorption), such as proton transfer reactions, may be studied. Although in principle relaxation methods could be used to obtain useful analytical information, they are not applicable to the majority of analytical reactions, which require separated reagents in order to obtain initial concentrations. Thus, the remainder of this chapter will focus on flow methods in general, and on the stopped-flow method in particular.

b. Advantages of the Stopped-Flow Method - There are several advantages of the stopped-flow method over the continuous- and accelerated-flow methods. The most obvious improvement over the continuous-flow method is the decreased volume of reagents required. The continuous-flow method requires from several milliliters to a few liters of solution, whereas most stopped-flow and accelerated-flow procedures involve less than one milliliter of each solution.

The slowest reaction time accessible to the continuous-flow method is limited by volume requirements and

the minimum velocity for turbulent flow. This sets the practical upper limit near 100 ms for the half life of the reaction. The lower limit is determined by the efficiency of mixing. With the accelerated-flow technique, the practical limits are 1-50 ms. The range is determined by the requirement that rapid observation must be made while the solution flow velocity is varied. In the stopped-flow procedure, however, the time range extends from about 1 ms to several minutes. The lower limit is determined by mixing efficiency, and the upper limit usually depends on the stability of the detection system.

Another advantage of the stopped-flow method is that the entire reaction curve is obtained from a single volume element of solution. In order to obtain the complete reaction curve from a continuous-flow experiment, observations at several different points along the reaction tube must be made.

The continuous-flow method is extremely sensitive to solution inhomogeneities within the reaction tube, particularly if spectrophotometric detection is employed. In stopped-flow experiments solution inhomogeneities are not serious problems because there is usually sufficient time between stopping the flow and the observation to allow the solution to become homogeneous.

C. AUTOMATED STOPPED-FLOW MIXING SYSTEMS

Figure 2 shows a pictorial diagram of a general stopped-flow mixing system with spectrophotometric detection. A controller is shown which directs the sequence of events in the system. The controller can be a manual sequencer, an electronic hard-wired sequencer, a minicomputer, or a microprocessor.

The sequence of operations necessary to obtain reaction-rate information begins with reagent preparation. Although this step is normally carried out manually, in principle all reagent preparation operations can be carried out under the supervision of the controller. After solutions are prepared, they must be introduced into the drive system, which normally consists of two syringes driven by a pneumatic cylinder or another mechanical device. Once solutions are introduced into the drive syringes, the drive system is actuated, and the two solutions flow into a mixing chamber. The mixed solution flows through an observation cell into a stopping device, which ceases the flow after a preset flow volume or time of flow. When the flow stops, the detection system is activated and data acquisition (e.g., absorbance vs time) begins. Data processing is often carried out in order to present the data in the desired format (initial rate, concentration of analyte, rate constants, etc.). Finally the desired information is presented

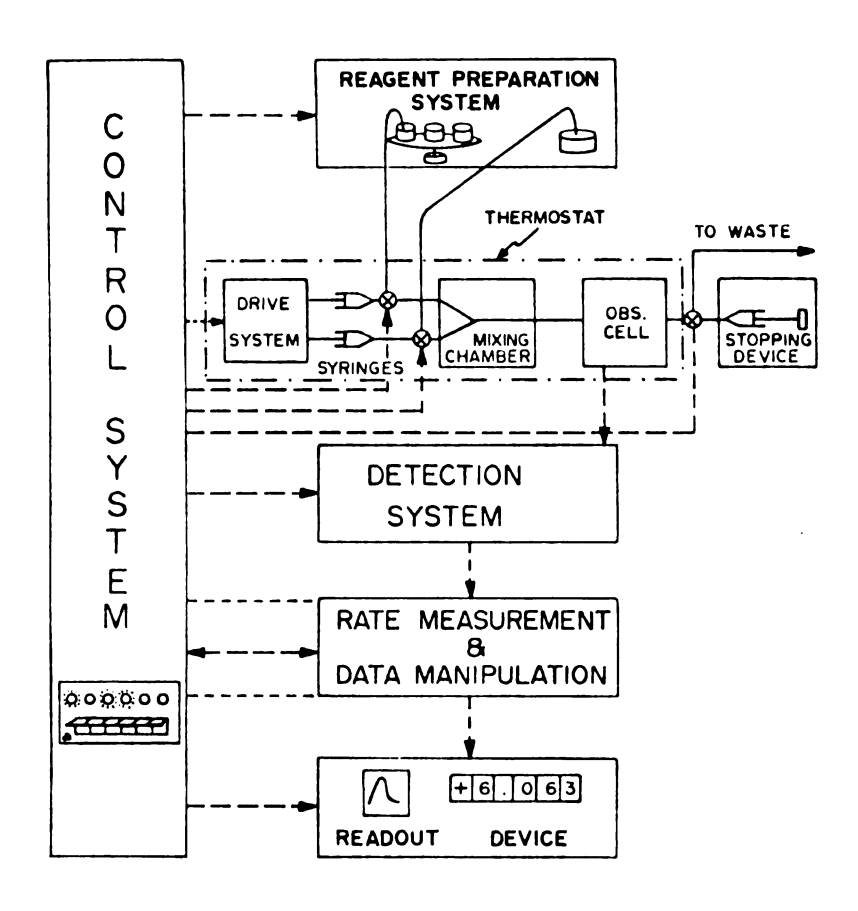


Figure 2. Optimum Automated Stopped-Flow Mixing System.

via a readout device (recorder, printer, plotter, etc.).

The stopped-flow mixing module of the generalized system is usually enclosed in some type of thermostatted housing as is shown in the figure. This is done in an attempt to insure that the temperature of the reaction medium under investigation remains constant to the extent that the measurement of the rate of the reaction is valid. Although the temperature of the observation cell is generally assumed to be the same as the thermostat, and temperatures in stopped-flow studies are sometimes reported to ±0.05°, actual temperature variations which occur on mixing are seldom measured or reported. As is discussed in Chapter II, these variations may amount to several degrees in extreme cases and thus should be of concern to investigators who wish to make high quality measurements of reaction rates for analytical purposes.

The operations of the generalized stopped-flow system can be divided into three parts: (1) sample and reagent handling; (2) mixing and stopping the flow; and (3) data collection and analysis. Automation of the entire system not only reduces human labor tremendously, but for fast reactions it reduces the analysis time by several orders of magnitude. The major time efficiencies occur in steps (1) and (3), but automation may result in significant human labor savings in step (2) as well.

Another inherent advantage of automation is increased sensitivity due to increased accuracy in data collection, rapid data treatment and signal-to-noise enhancement procedures. Automation can be accomplished by analog-digital hardware, but control of the entire system by a minicomputer or microprocessor greatly improves efficiency and flexibility, particularly in the research environment in which a great deal of flexibility is often necessary.

It is hoped that the work presented in the following chapters will contribute to the development of automated stopped-flow mixing systems both for fundamental research in the development of new reaction-rate procedures and for routine analysis.

CHAPTER II

CRITICAL STUDY OF TEMPERATURE EFFECTS IN STOPPED-FLOW MIXING SYSTEMS

A. INTRODUCTION

Until relatively recently the stopped-flow mixing technique has been a specialized tool for fundamental investigation of important reactions in chemistry and biochemistry. In this role, the technique has been characterized by rather poor accuracy and precision, the primary limitation being the precision of available detection systems and readout devices. Recent advances in electronics technology and the widespread availability of high quality computerized data acquisition systems have improved the quality of rapid reaction-rate data immensely. The magnitude of this improvement is exemplified by the data acquisition system of Malmstadt and O'Keefe (38) which is capable of acquiring fast kinetics data (5 ms measurement interval) with a signal-to-noise ratio of *450.

As a result of such improvements in accuracy and precision, the stopped-flow technique has received increased attention in the past few years, particularly with regard to its role in automated fast analysis (1). Along with this interest has come the necessity to

examine more carefully the operational characteristics of stopped-flow mixing systems in an effort to improve the quality of analytical data obtained with such equipment. A number of papers have appeared describing spurious results in stopped-flow systems due to inadequate control of temperature (39-41).

Several years ago Gibson noted absorbance anomalies caused by large temperature differences (≈20 K) between the drive syringes and cell block of his stopped-flow apparatus (39). He ascribed the anomalies to thermally induced refractive index changes in the observation cell. More recently, Miller and Gordon (40) have noted that the refractive index effect is much more pronounced with organic solvents which have larger temperature coefficients of refractive index. They have also shown that if the stopped-flow apparatus is thermostatted at temperatures different from ambient, the cell temperature differs from that of the thermostatting medium by an amount approximately in direct proportion to the difference between the temperature of the thermostat and ambient temperature. These workers indicate that the problem is compounded by the use of Kel-F as the construction material for observation cells and valve blocks. The low thermal conductivity of this material apparently makes the attainment of thermal equilibrium between the thermostatting medium and the reactant solutions more

difficult.

Chattopadhyay and Coetzee (41) have reported difficulties in the determination of activation energies from the results of stopped-flow experiments. They have suggested that these effects are due in part to the insulating properties of their Kel-F flow system and that the effects may be lessened by allowing a larger purge volume of reactants to flow through the observation cell. In this way the heat transfer between the observed solution and the valve block and the resulting temperature change may be minimized.

Temperature changes in stopped-flow systems may be a result of any of several different causes. If, as suggested above, the stopped-flow module is not adequately thermostatted or if some parts are thermostatted more efficiently than others, thermal gradients may exist between various components of the system. Thus, solutions passing from the drive syringes into the observation cell will undergo a temperature change.

Another cause of temperature change is the heat produced by viscous forces during the physical mixing of the reagents in the mixer. Calculations reveal (42) that under worst-case conditions this effect may amount to as much as 0.1 - 0.2 K for water alone in both syringes.

In addition to these sources, temperature changes may result from the enthalpy of dilution of the reagents.

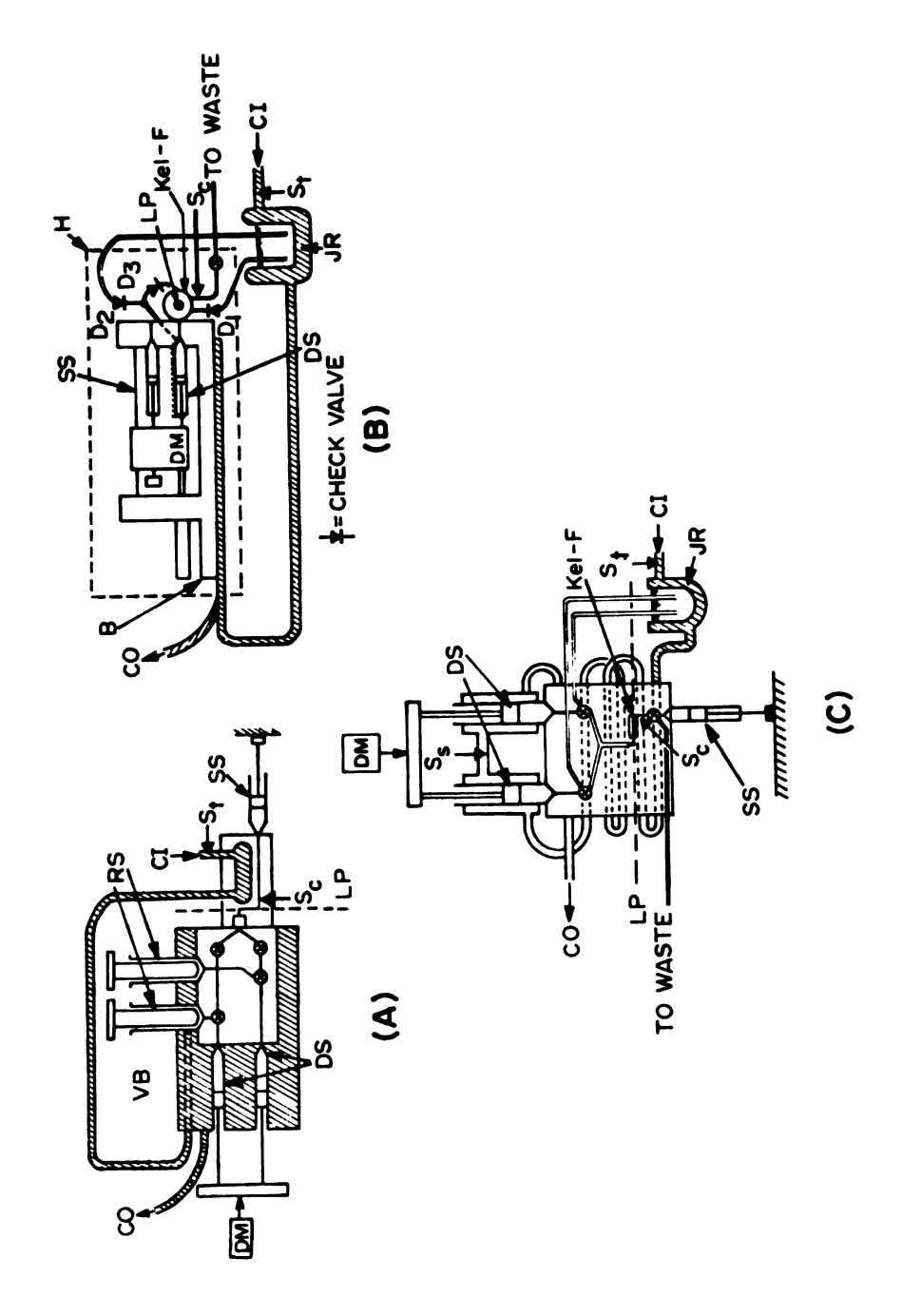
A contribution from the enthalpy of observed reaction itself may also be expected and could amount to several tenths of a degree for fairly concentrated solutions. Thus, the physicochemical process of combining reagents in a stopped-flow mixing system may produce temperature changes on the order of one tenth to several tenths of a degree. Clearly, such effects will induce undesirable changes in the rate of reactions under investigation which in turn will decrease the precision of analytical In this chapter, we describe the rate measurements. results of a critical study of the thermal behavior of three different stopped-flow mixing modules which are at our disposal; a Durrum Model 110 stopped-flow spectrophotometer, a GCA/McPherson Model EU 730-11 stopped-flow module and a stopped-flow mixing unit which was designed and built in this laboratory (43,44). Special emphasis is placed on the determination of the magnitudes and signs of the temperature changes which occur before and during mixing when the modules are maintained at 20-30°C. It is important to note that in order to characterize the thermal behavior of the stopped-flow mixing systems, all of the experiments which we describe have been carried out with only distilled water in the drive syringes. Based on the results of these experiments, we present guidelines for minimizing the effects of the temperature changes which occur during mixing, particularly when

the stopped-flow modules are utilized routinely in reaction-rate methods of analysis.

B. EXPERIMENTAL

1. Instrumentation

Figure 3 is a schematic representation of the 3 stopped-flow mixing systems which were utilized in this study. Figure 3(a) shows the Durrum Model 110 stoppedflow spectrophotometer which is based on the design of Gibson and Milnes (45). The reagents are stored in the reservoir syringes (RS) which are mounted in the valve block (VB). Upon proper rotation of the needle valves in the valve block, the reagents may be forced into the drive syringes (DS) where they remain until thermal equilibrium has been attained. The drive mechanism (DM) for the instrument is the same as for all three modules, a solenoid actuated pneumatic piston, which in this case was operated at an air pressure of 70 psi. The dead time of the Durrum instrument was found to be 3-5 ms both by the flow velocity method (2) and the extrapolation method (46). Thermostatting is provided by pumping water through a copper loop immersed in a constant temperature bath and into the coolant channel (CI) of the observation cell as shown in Figure 3(a). The coolant then passes from the channel to the reservoir surrounding



Thermostating Arrangement of the Stopped-Flow Modules. Figure 3.

the drive syringes and finally out of the stopped-flow module back to the circulation pump.

The stopped-flow mixing module of Figure 3(b) is the latest entry among the commercially available units. It is a prototype GCA/McPherson Model EU 730-11 Stopped-Flow module. This instrument has several interesting mechanical features which should be of utility to those interested in automated systems. The module has a single cycle operation with no manually manipulated valves. This is made possible through the use of fluid diodes $(D_1, D_2 \text{ and } D_3 \text{ in Figure 3})$. When the push cycle is initiated, the spent reagents from the previous cycle are expelled from the spring-loaded stop syringe (SS) through the solenoid valve (S). The drive mechanism (DM) then retracts and draws the reagents into the drive syringes (DS) through D_1 and D_2 . Air pressure (~35-40 psi) is then applied to the pneumatic cylinder which thrusts the drive plungers forward and forces the reagents through the mixer and observation cell and into the stop syringe. Just before the plunger of the stop syringe hits the stop block, a flag on the drive mechanism breaks the light beam of an opto-interruptor and produces a TTL signal for the initiation of data acquisition. The dead time of the module was found to be ≈ 5 ms (2, 46).

The thermostatting consists of a copper U-shaped

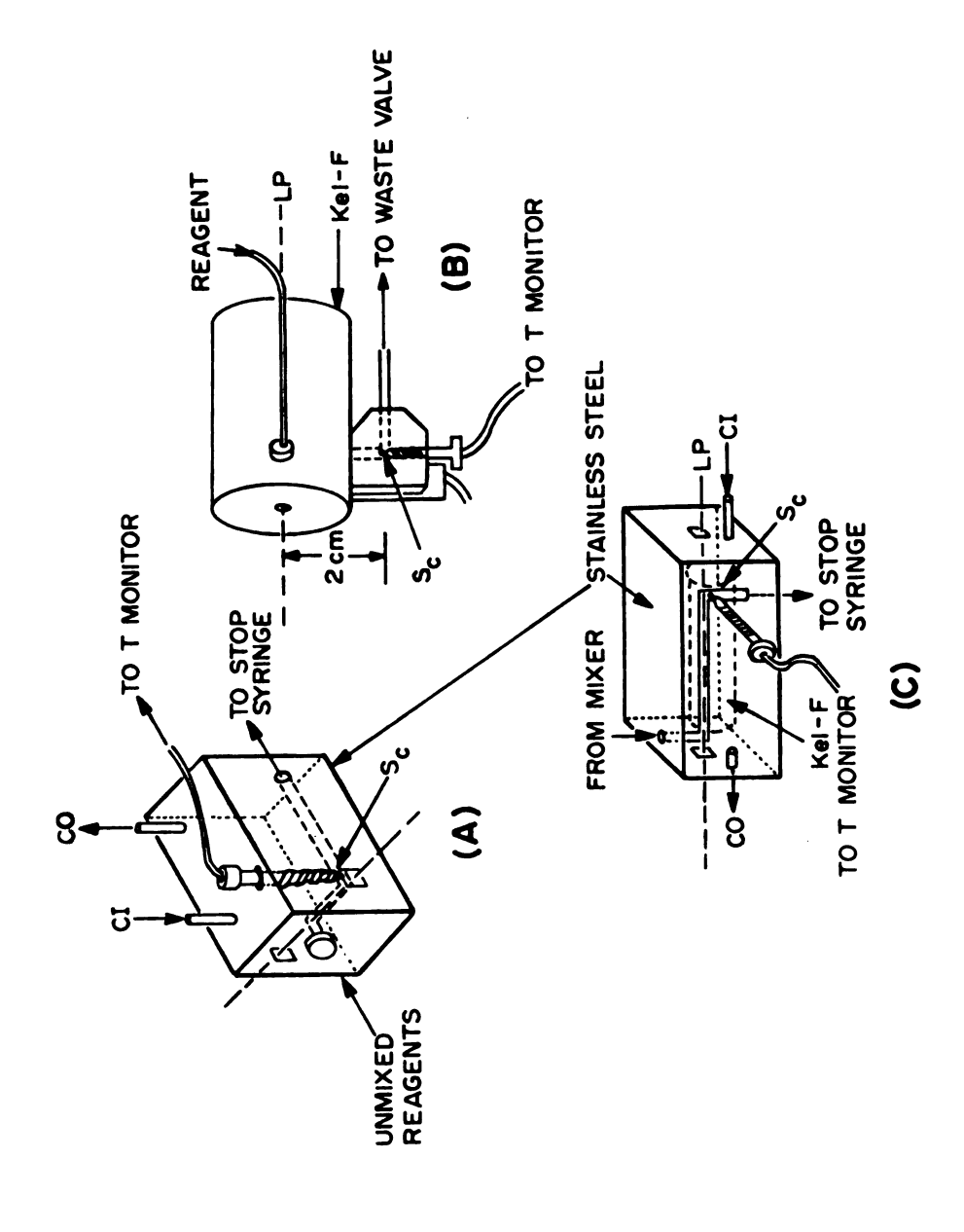
loop in contact with the bottom of the cast aluminum base (B). Coolant may be circulated through the loop in order to bring the base to the temperature of the bath. It should be noted that neither the glass syringes nor the Kel-F observation chamber come into contact with the thermostatting medium. The reagents are kept in jacketed reservoirs (JR).

The final stopped-flow mixing system which was investigated is illustrated in Figure 3(c), and it is referred to here as the MSU module. This unit was designed and built in our laboratory (43), and it has recently been refurbished in order to provide better temperature control, greater throughput of UV-visible radiation, and greater facility for the use of detection methods other than UV-visible spectroscopy (44,3). design of the flow stream is basically that of Gibson and Milnes (45), except that the valving has been completely automated. In addition, the stop syringe has been spring loaded so that spent solutions are automatically expelled when the outlet valve is thrown open. Temperature control is accomplished by circulating coolant through channels bored in the stainless steel blocks which make up the body of the module and through the brass jackets which surround the stainless steel drive syringes. Jacketed reservoirs (JR) have also been provided for the reagents. The dead time of the MSU

module is 3-4 ms at 70 psi drive pressure (2,46).

All temperature measurements within the stopped-flow systems were made with the computerized thermistor circuit previously described (3) (see Chapter III). measurements were accurate to ±0.05 K and precise to ±0.002 K for single measurements which require about The thermistors utilized in this work were fast bead-in glass thermistors with time constants of 7 ms (47) and 25 ms (48). The locations of the thermistors for the measurement of the temperature at various points in the stopped-flow modules are indicated in Figures 3 and 4 by the symbols S_s , S_t , and S_c where s, t, and c refer to locations near the syringes, near the thermostat, or near the observation cell. It should be noted that the GCA module includes as standard equipment a thermistor probe in the observation cell (49), but the time constant of the probe is ≈0.2 s, which is much too slow for measuring temperature changes on the millisecond time scale. We therefore elected to replace it with one of the 7 ms probes as shown in Figure 4(b). Identical probes were installed in the other units as shown in Figures 4(a) and 4(c). All room temperature measurements were made with a calibrated bomb calorimeter thermometer (50).

The temperature monitor (3) was under the control of a PDP 8/e minicomputer (51) equipped with 16K memory,



Observation Cells of Stopped-Flow Modules. Figure 4.

a dual floppy disk system, a cartridge disk, a real-time clock, graphics display terminals, and a general purpose interface buffer for communication with experiments.

2. Software

There are three major programs in the software set for the temperature monitor: a program for system calibration; a program for single static temperature measurements; and a program for timed data acquisition. During each experimental session, the temperature monitor was allowed to warm up for at least an hour, and then it was calibrated according to the procedure described previously (3).

In general, static temperatures were calculated by averaging 100 individual measurements made by the temperature monitor, although the operator may choose up to 2047 individual measurements. Since each measurement requires only 30 μs , the time required for a 100 point ensemble average to be determined is essentially the time required for the computer to print out the results. Any one of three different thermistors (S_t, S_s or S_c) may be connected to the temperature monitor by the operator via a rotary switch arrangement. The response characteristics for each thermistor are stored on a mass storage device and may be retrieved at any time by the software. Thus,

the operator need only specify the thermistor in use and the number of data acquisitions before the temperature measurement is initiated from the console. The computer then signals the temperature monitor that data acquisition may begin, retrieves the data from the interface, and calculates the temperature based on the previously determined thermistor characteristics (3).

The timed data acquisition program was designed to provide the operator maximum flexibility in fundamental investigations of rapid temperature changes. As in the program described above, the operator selects the thermistor and the number of points to be acquired per ensemble average. In addition the number of ensemble averages and the time between each data acquisition are operator selected. On a signal from the console, data acquisition is begun. Following the acquisition phase, the temperature data are calculated by the computer and plotted on the console device as a function of time. It is the interactive graphics mode of the data display routine which provides the degree of flexibility necessary to determine rapidly and accurately the temperature of the medium of interest at any point on the T-vs-t curve. After the plotting subroutine displays the data on the face of the storage tube of the console device (Tektronix 4006-1), the beam is returned to the first point where the beam blinks alternately off and on

waiting for a prompt from the operator. By typing control characters, the operator may then move the blinking dot (cursor) back and forth over the curve either continuously or a single point at a time until the point of interest has been reached. When this occurs, another control character is typed which causes the software index of the point to be stored so that the temperature value at the point may easily be retrieved. An interactive mode of data acquisition such as this is particularly advantageous when data profiles have unexpected shapes or when algorithms for numerical analysis of such profiles would be difficult or impossible to design (52). The interactive mode was used routinely to specify points on T-vs-t curves so that differences between the points could be easily determined.

Following the data acquisition and analysis phases of the program, the data may be written into a permanent file on one of the mass storage devices for retrieval and analysis at a later time, or another data acquisition sequence may be initiated. In addition, the investigator has the options of replotting the data, reanalyzing the data, chaining to other programs of interest, or returning to the keyboard monitor of the operating system (DEC OS/8).

In all experiments cited in this paper which involve the measurement of a single temperature or a change in temperature on the T-vs-t response curve, at least three determinations were made on three separate pushes of the stopped-flow unit under investigation.

C. RESULTS AND DISCUSSION

1. Thermostatting Efficiency

The thermostatting efficiency of a stopped-flow module may be defined in terms of the ability of the thermostatting arrangement to maintain the observation cell at or near the temperature of the thermostatting fluid as it enters the module. This property of the three systems was evaluated by measuring the temperature at the points labeled S_c and S₊ in Figure 3 and 4. The temperature of the constant temperature bath was varied over the range 20-30°C at approximately 1°C intervals. After a sufficient equilibration time (0.5 - 1 hr), at each setting, the temperature of the observation cell, T_{C} , the temperature of the circulating water, T_t , and ambient temperature, T_a , were measured. In Figure 5, T_c is plotted as a function of T_+ . The slopes, intercepts, and correlation coefficients (r) for linear least squares regression analyses of the curves for all three of the modules are shown in the figure, and the mean ambient temperature for each series of measurements is presented as well.

Clearly, the Durrum and the MSU modules track the

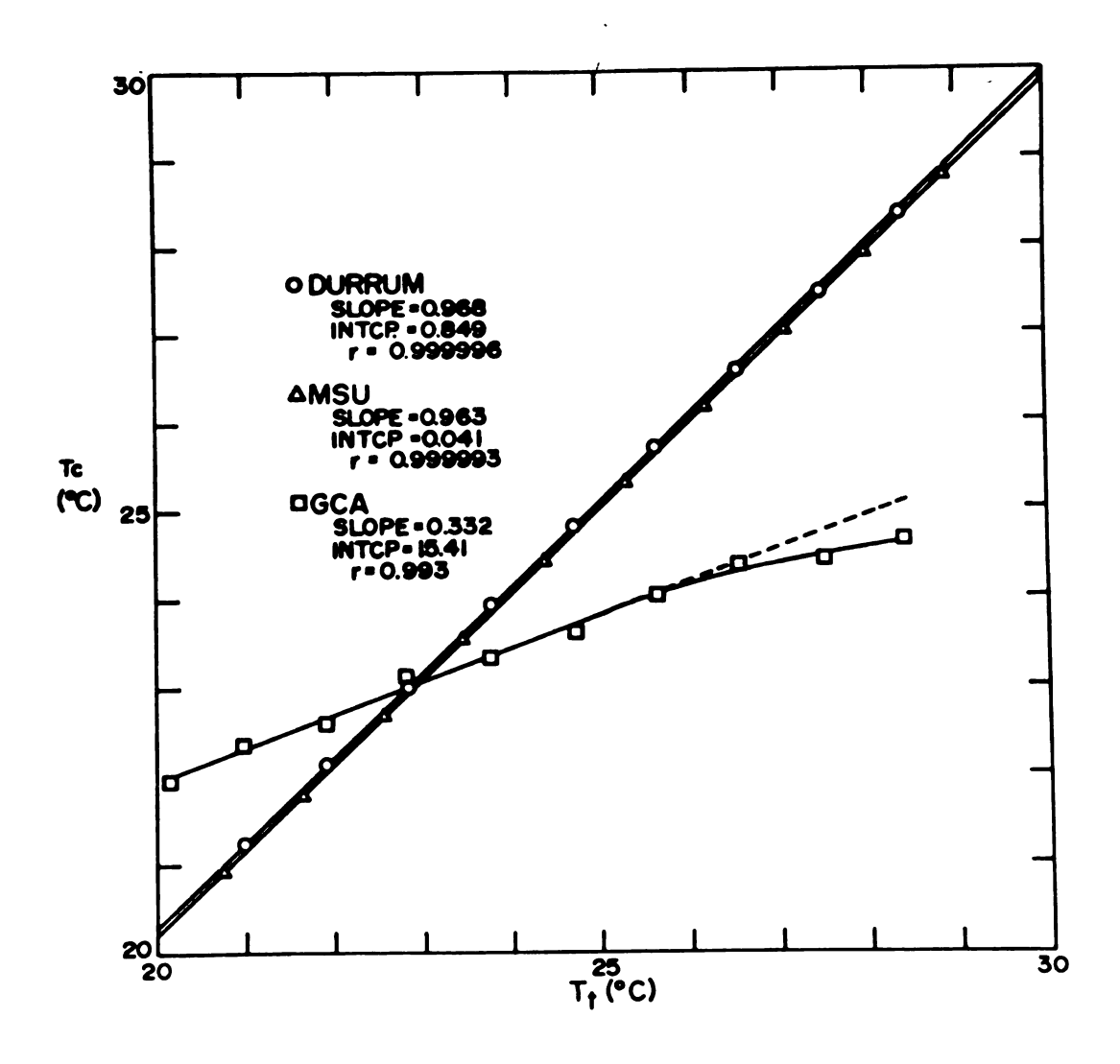


Figure 5. Thermostating Efficiency of Stopped-Flow Modules: T_c -vs- τ_t .

thermostat in a linear fashion over the temperature range shown. The slopes of the two curves are nearly identical, but the slope for the Durrum instrument is slightly greater, which indicates slightly better efficiency.

If the linear relationship holds over a somewhat larger temperature range, both the MSU and the Durrum modules would exhibit errors of approximately 1 K at 273 K.

The temperature of the observation cell of the GCA module does not linearly follow the temperature of the thermostat. Some of the reasons for this are apparent from Figures 3(b) and 4(b). In order for the Kel-F observation cell to attain the temperature of the thermostat, heat must be transmitted to or from the aluminum base, B, via thermal conduction. The cell is attached to the base only by two narrow copper strips and the end plate. The slope of less than 0.5 indicates that there is better thermal contact between the cell and the parts of the system at ambient temperature than between the cell and the thermostatting solution.

2. Temperature Changes During the Mixing Process

Very early in this investigation it became apparent that in the stopped-flow modules available to us, temperature changes occur during the mixing process under almost all combinations of ambient and thermostatted temperature. The task then was to assess not only the

magnitude of the changes as a function of the thermostatting temperature, but also the shape of the temperature-vs-time profile, the reproducibility of the changes and the time constant (τ) for achieving thermal equilibrium following mixing. The latter determination was necessary in this investigation in order to set a lower limit on the length of time necessary between pushes to achieve reproducibility of the temperature changes.

For these experiments, each stopped-flow module (configured as shown in Figure 2) was allowed to come to thermal equilibrium at a T_{+} of \underline{ca} . 20°C. In each case the flow cycle was initiated and data acquisition with the fast thermistor circuit was carried out for 50 s following the cessation of flow. The reattainment of the equilibrium temperature following the step temperature change, AT, which occurs upon mixing should be a function of the heat transfer properties of the solvent and the construction material of the observation cell. This is borne out by the data illustrated in Figure 6 for the three stopped-flow modules. The Durrum and MSU curves were offset vertically by a few tenths of a degree so that the curves could be compared easily; thus, the temperature scale is relative. The symbols for the curves are shown in the figure as are the time constants (τ's) for the return of the temperature of each module to its initial value.

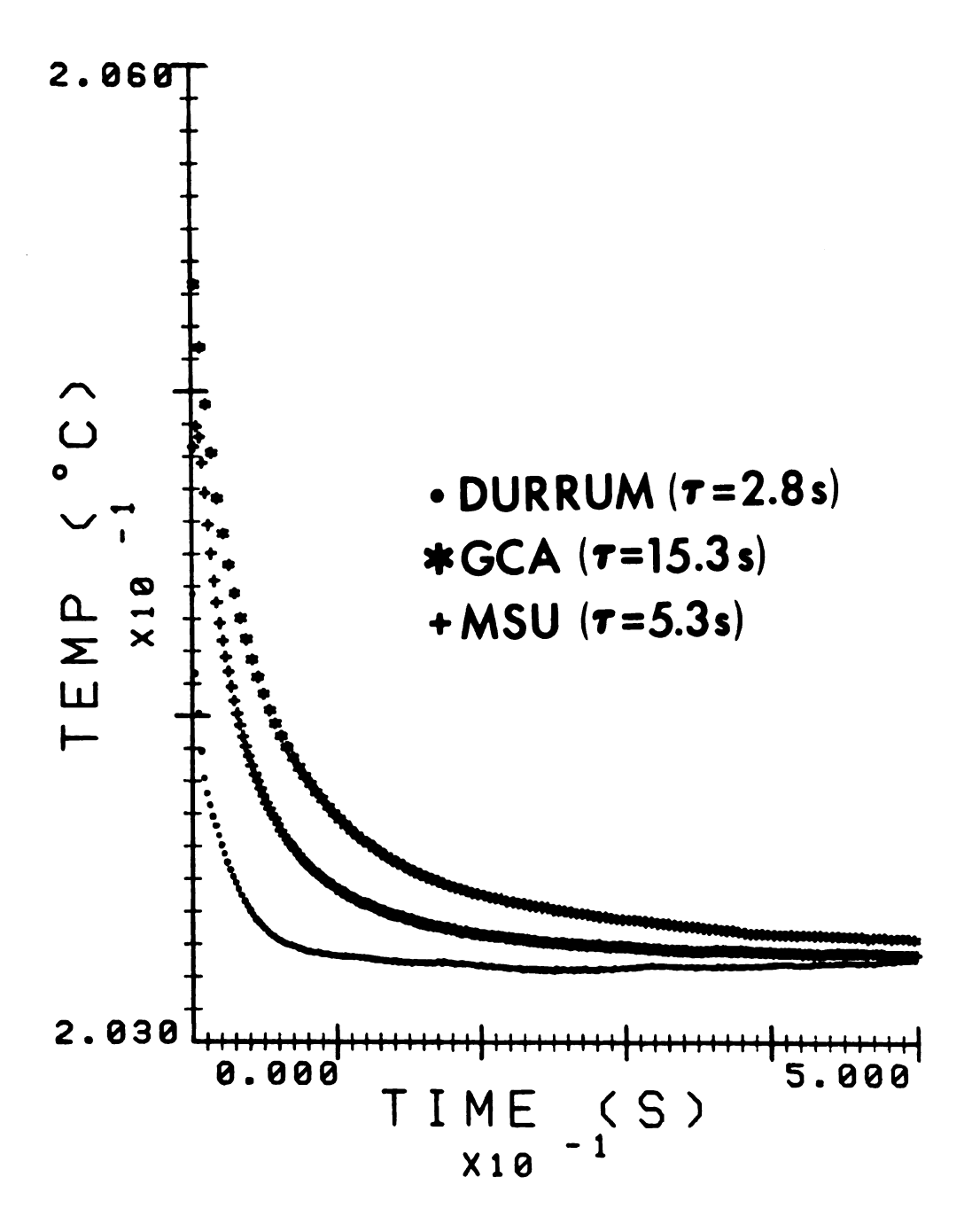


Figure 6. Long-Term Return to Thermal Equilibrium after Cessation of Flow.

The bottom curve (·) represents the response of the Durrum instrument which has an observation cell constructed entirely of stainless steel. The temperature in this cell returns to equilibrium approximately 10 - 15 s (ca. 5T) after the stop, which occurs at zero on the time axis. The construction material for the MSU module is stainless steel except for the observation cell channel itself, which contains a Kel-F insert (see Figure 3(c) and 4(c)) for the installation of conductance electrodes (53). As the middle curve (+) shows, about 25-30 s is required for the cell in the MSU module to reach equilibrium. As might be expected, based on the fact that the observation cell of the GCA module is constructed entirely of Kel-F, the establishment of equilibrium in that cell requires a longer period than that required by the Durrum module. As the top curve (*) illustrates, the GCA module requires more than 50 s to return to equilibrium. As a result of these preliminary results, at least 2-3 minutes was allowed between pushes in subsequent experiments to ensure reestablishment of thermal equilibrium. time delay was usually fixed by the time required to analyze and record the data.

The reproducibility of the temperature changes which occur during the push in each of the modules is illustrated in Figure 7(d), 7(e) and 7(f) for the Durrum,

GCA and MSU modules respectively. These experiments

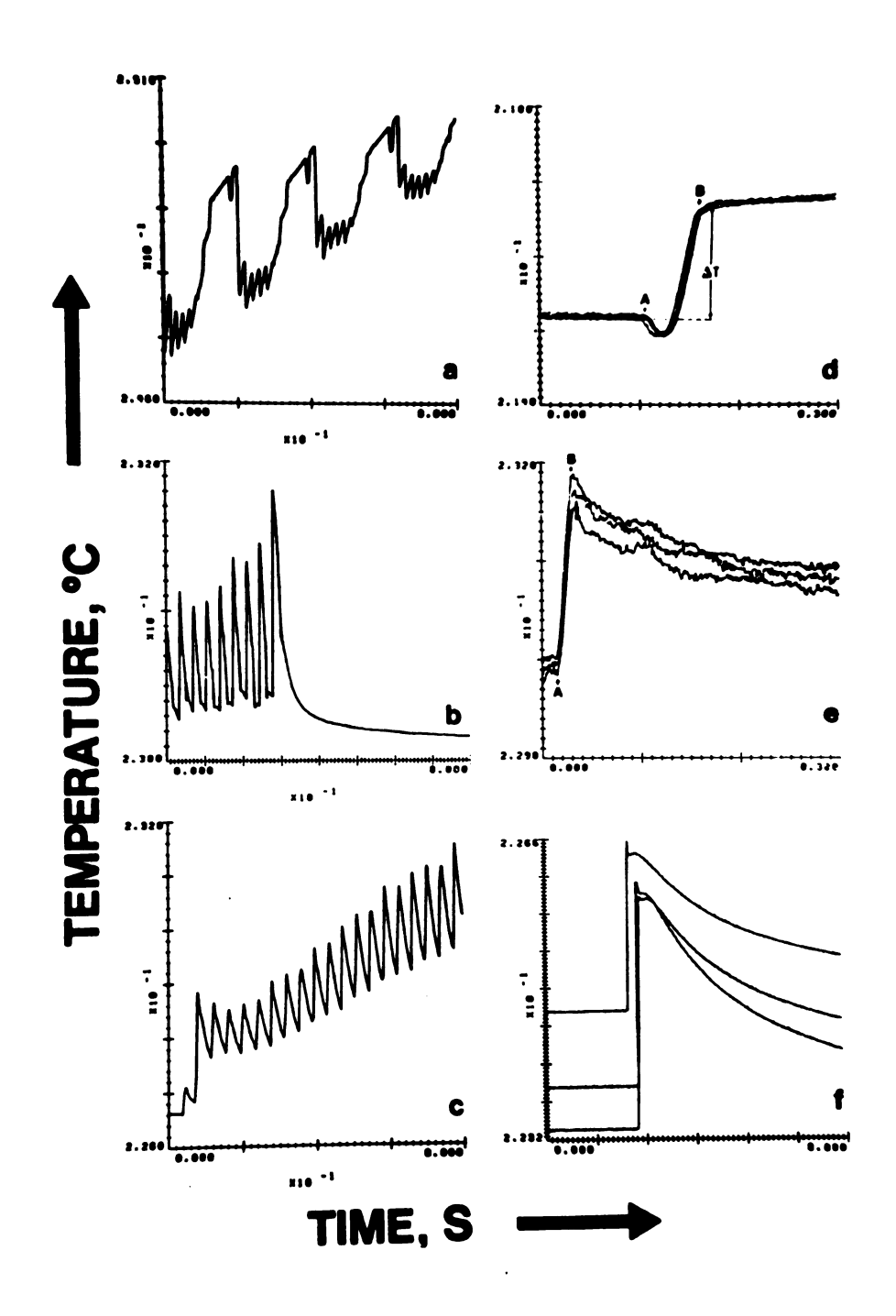


Figure 7. Reproducibility of T: (a) MSU; (b) Durrum; (c) GCA. Multiple Pushes: (d) MSU; (e) Durrum; (f) GCA.

were carried out as in the previous example except that data acquisition was initiated <u>ca</u>. 200 ms before the stop. This was accomplished by using the push signal rather than the stop signal to trigger the data acquisition. It is apparent from the curves that the Durrum and MSU modules are quite precise in this regard while the GCA is somewhat less so. For temperature changes measured over the range 20-30°C, the mean precisions were 0.0082 K, 0.0050 K, and 0.030 K for the Durrum, MSU and GCA modules.

It should be noted that the data for the GCA was collected for a considerably longer period of time than for the other modules with a correspondingly larger amount of signal averaging. This resulted in increased S/N in the data of Figure 7(f). These data were not collected in the normal cycle mode of the GCA. The module has a cycle interrupt control which was actuated after the contents of the stop syringe had been expelled and the drive syringes had come to thermal equilibrium, and only then was the push allowed to occur. The points denoted by A and B in Figure 7(d) and 7(e) indicate the beginning and end of the push.

As was noted in the opening paragraph of this section, it is advantageous to know how the temperature change (ΔT) during the push of a stopped-flow module varies as a function of the temperature of the constant

temperature bath. We have taken ΔT to be the difference between the static temperature of the observation cell before the push and the maximum (or minimum) temperature attained after the push (see Figure 7(d)). For the GCA module this occurs at point C in Figure 9. This quantity is readily obtained via the interactive graphics mode of the computer software. In order to determine this relationship for each of the modules, the thermostat temperature was varied over the range 20-30°C and ΔT was found at each of 9 or 10 different temperatures. For the Durrum and the MSU modules, this experiment was also carried out at two different ambient temperatures. The results of these experiments are shown in Figures 8, 9 and 10 for one data set at each different bath temperature.

It is clear from the families of curves that the Durrum module exhibits the smallest ΔT 's over the temperature range. It is also interesting to note that ΔT is always positive for the Durrum and GCA modules, in contrast with the MSU module which exhibits ΔT 's of both signs. The reader should again be reminded that the GCA curves were obtained at a slower data rate in order to record all of the temperature changes which occur during the cycle. The temperature change denoted by A in Figure 9 occurs when the stop syringe is purged, while the small bump at B occurs when the drive syringes are

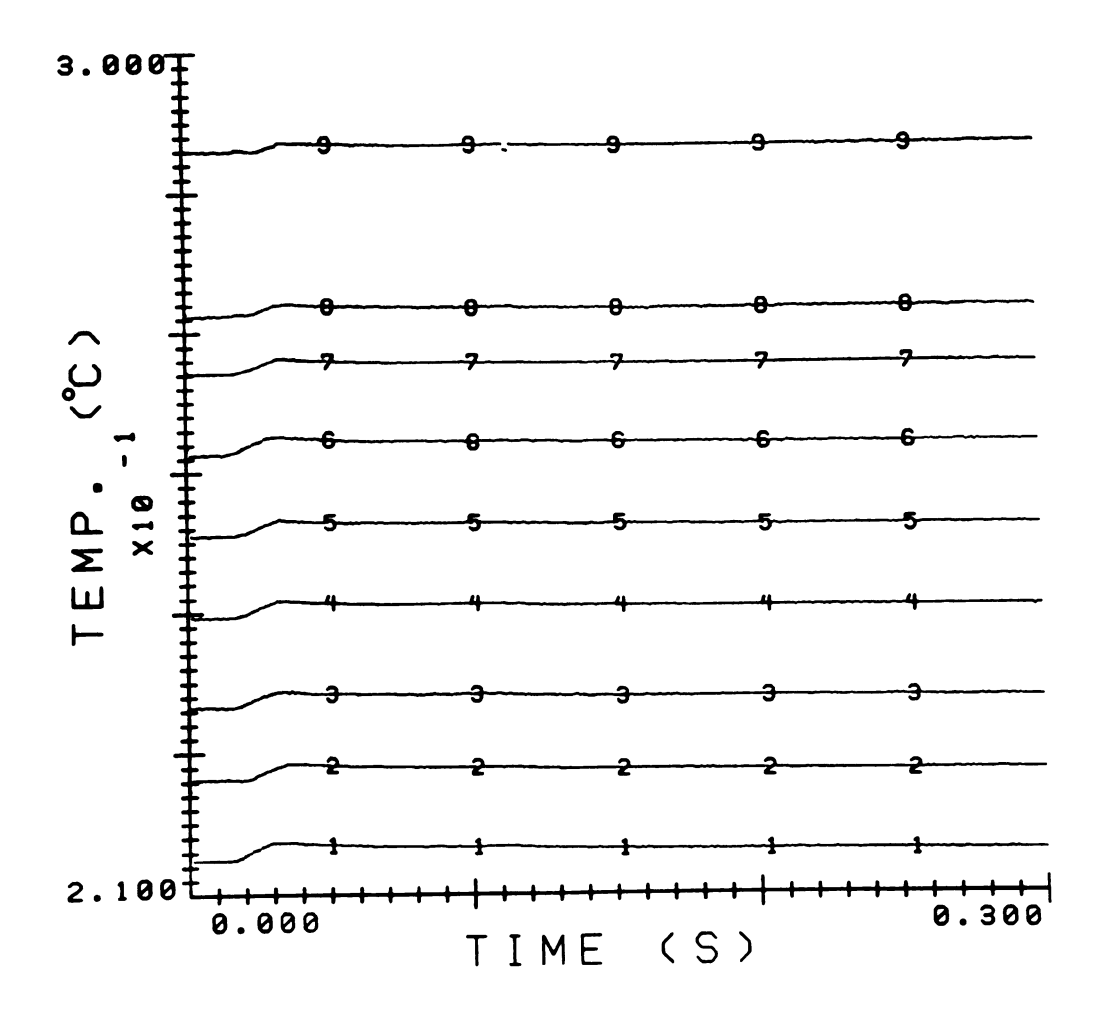


Figure 8. Temperature-vs-time: Durrum Module.

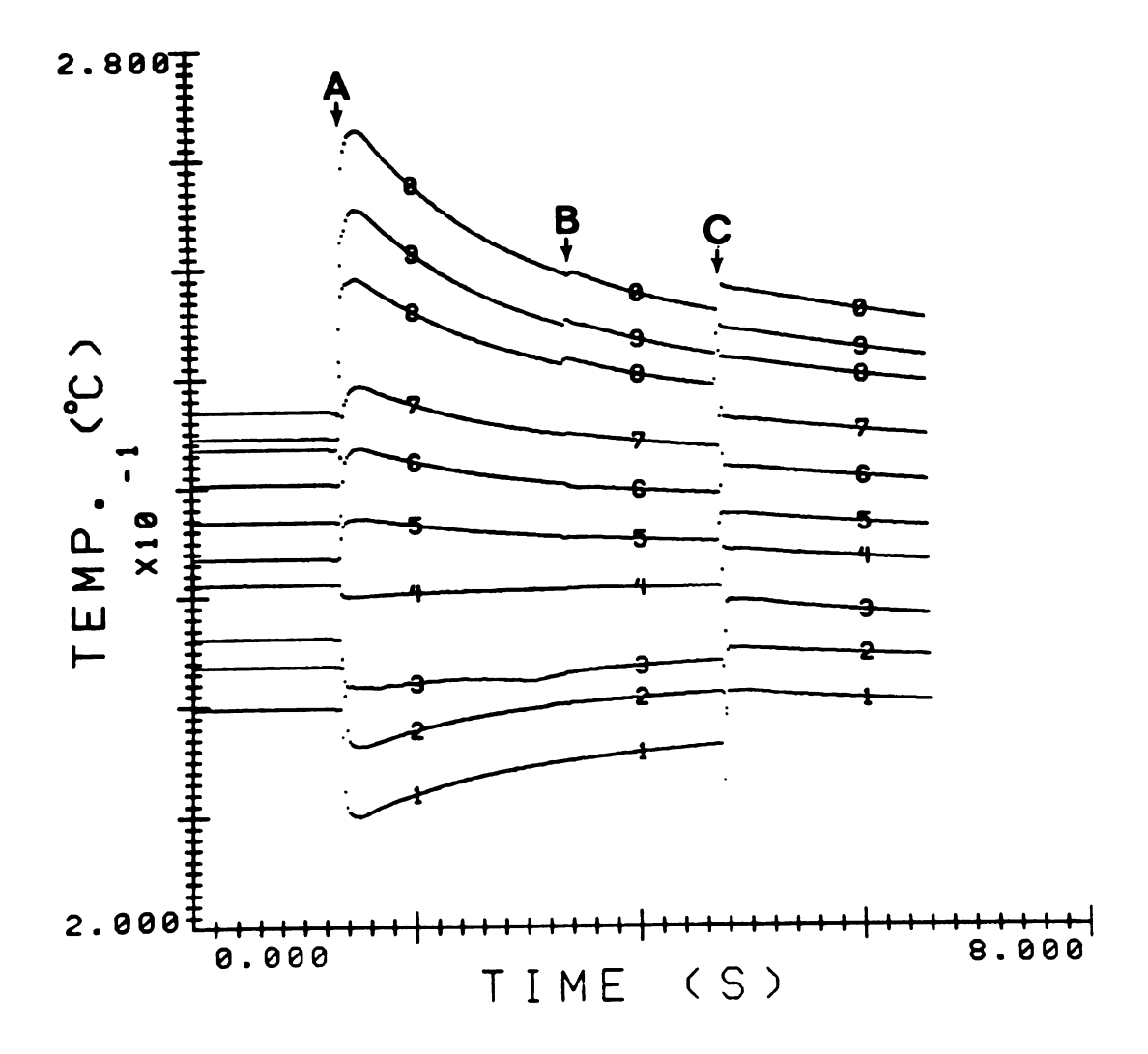


Figure 9. Temperature-vs-time: GCA Module.

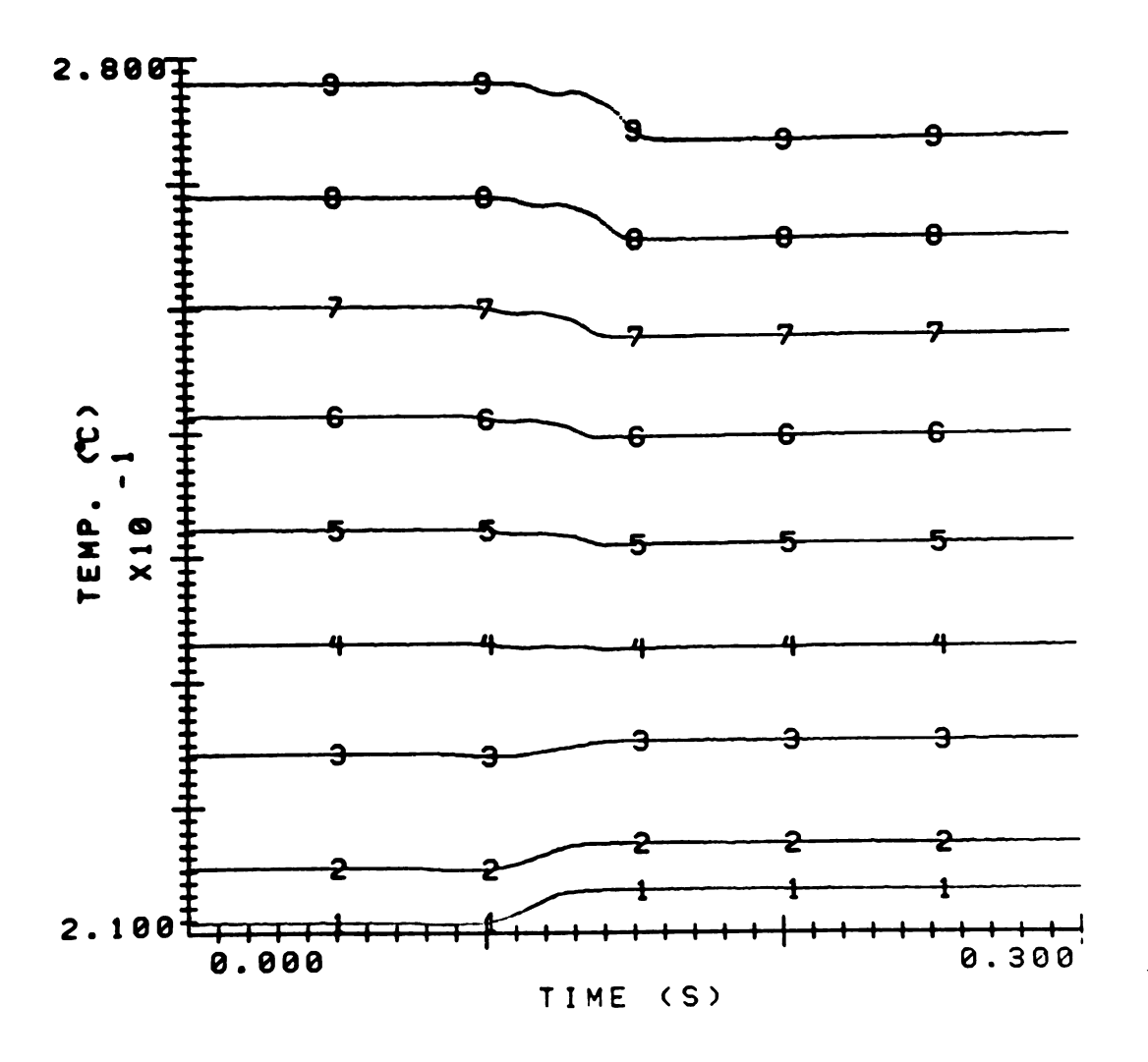


Figure 10. Temperature-vs-time: MSU Module.

filled. The ΔT at C is of the most importance since it occurs during the push. The ΔT 's at A and B were found to be a result of the fact that the fluid diodes shown in Figure 3 require a small flow of solution in order to seat. When the stop syringe is expelled, enough solution is drawn in through D₁ to cause the solution in the vicinity of T_C to approach the temperature of the reagent in JR, thus causing the spike at A. A similar situation occurs during the filling of DS and causes the bump at B.

It is informative to consider the plots of ΔT -vs- T_t shown in Figure 11 for each of the modules. The data were extracted from sets of data similar to those of Figures 8-10 via the interactive software routines described above. Data sets were collected for the Durrum and MSU modules at two different ambient temperatures (averaged over 6-8 hour period required to perform the experiments) and for the GCA module at one ambient temperature. The average ambient temperature ($\pm 2S$) are indicated by the horizontal bars near each plot.

The susceptibilities of the modules to changes in the thermostat temperature are clearly illustrated in Figure 11. The effect of a changing thermostat temperature is particularly marked for the MSU module. The slopes for the two lines representing experiments carried out at two different ambient temperatures are very nearly

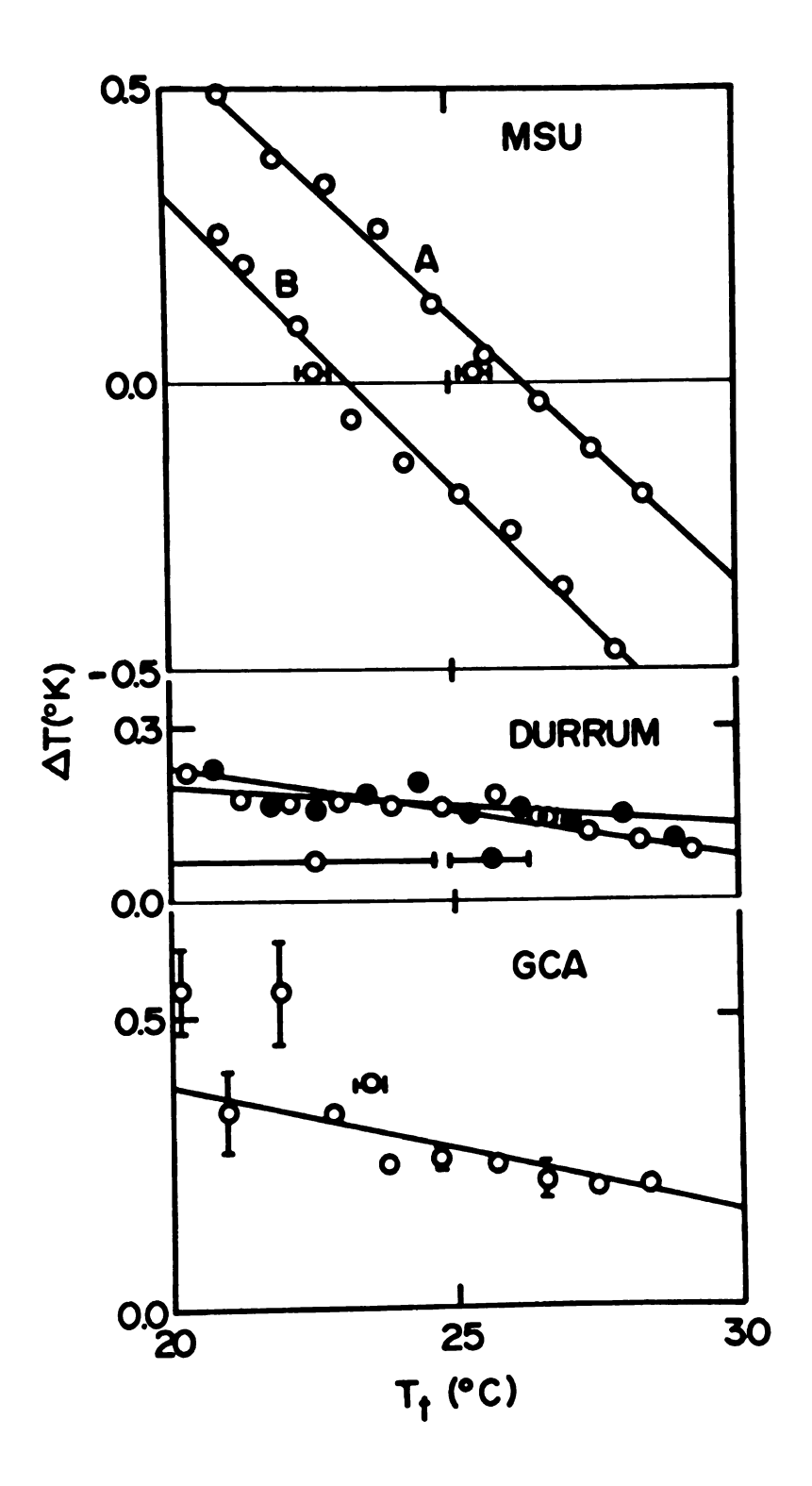


Figure 11. Effect of T_t on ΔT .

equal; -0.100 for curve A and -0.094 for curve B. The difference between the average ambient temperatures for curves A and B is ≈ 2.8 K which corresponds closely to the calculated value of ≈ 3.1 K for the difference between T_t values at a value of $\Delta T = 0$. This suggests that a change in the ambient temperature produces a horizontal shift in the ΔT -vs- T_+ curve for the MSU module.

It is also interesting to consider the AT values which correspond to $T_{+} = T_{a}$. These are 0.076 K and 0.057 K for curves A and B respectively. It is tempting to attribute at least part of these two values to viscous heating of the solvent as it is mixed, especially since it is at ambient temperature that the stopped-flow module should be relaively free of temperature gradients in its stainless steel body. Unfortunately, it was not possible to measure the actual temperature of the mixer or the valve block either of which could transfer heat to the fluid as it passes to the observation cell. fact, Figures 10 and 11 clearly illustrate that for the MSU module AT is always in the direction of ambient temperature. This is not unexpected since as Figure 3(c) shows, the valve block and mixer are not well thermostatted and are therefore probably somewhat closer to room temperature than the thermostat.

The results for the Durrum module shown in Figure
11 reflect considerably less sensitivity to changes in

thermostat and in ambient temperatures. In fact, one data set (circles) was obtained over a 3-day period in 3 different experimental sessions under the influence of a wide range of ambient temperatures. These points correspond fairly well with the other data set (filled circles) which was collected in one session over a relatively narrow temperature range. The slopes and intercepts of the respective linear regression lines for the two data sets are statistically indistinguishable at the 80% confidence level.

The data for the GCA module were extracted from data sets similar to those shown in Figure 9. The temperature change at point C in Figure 9 is plotted in Figure 11 as a function of T_t . The error bars for the lower temperatures clearly show the lack of precision of ΔT , but at the higher temperatures the data are considerably more precise exhibiting a 0.2 - 0.3 K increase. The fact that ΔT is always positive even at low T_t again suggests a significant contribution from viscous heating.

3. Multiple Pushes

One of the most important advantages of stopped-flow mixing as an analytical tool is the capability of performing very rapid analyses and of averaging the results from multiple pushes in order to increase the S/N. If significant changes in temperature occur during the push,

rate constants will vary accordingly and greater imprecision in measured rates may result. In order to assess the effect of multiple pushes, each of the modules initially at thermal equilibrium was cycled as rapidly as possible for several seconds, and the temperature, $T_{\rm C}$, of the observation cell was measured as in previous experiments.

Figures 7(a), 7(b), and 7(c) illustrate that each of the modules undergo cumulative increases in temperature over the several pushes observed. The number of pushes was limited in the Durrum module by purge volume which was set to give ~8 pushes per filling of the drive syringes. The range of the temperature fluctuations of the Durrum module was ~0.2 K under the conditions of the experiment. It should be mentioned that the data have been distorted slightly as a result of the large amount of signal averaging in these long term experiments and that the range is probably even greater than that shown.

The GCA module exhibited a range of temperatures of ~0.5 K in 25 pushes. Presumably much of this change was due to the drive syringes and observation cell approaching the temperature of the thermostatted water evidenced by the fact that toward the end of the experiment the temperature began to level off. The MSU module exhibited similar behavior during the discharge of four

different syringe fillings. The range of temperatures was ≈0.4 K during the 25 or so pushes of the module. No attempt was made in this series of experiments to minimize the effects of these temperature changes. Rather, the experiments were carried out at convenient temperatures in order to illustrate the magnitude of the ΔT's which result.

D. SUMMARY AND CONCLUSIONS

The investigation of the thermal behavior of the three stopped-flow modules has revealed significant variations in the temperature of the solvent during and following the mixing process. Clearly, temperature changes nearly always occur in these systems and may amount to 0.1 - 0.5 K for the simple case of the mixing of water under normal operating conditions. These changes depend upon the thermostatting temperature as well as the arrangement of the thermostatting mechanism and the extent to which the parts of the module come in contact with the thermostatting medium.

The Durrum stopped-flow module exhibited the most stable temperature characteristics of those tested with an average of ΔT of 0.2 K over the range 20-30°C. The GCA module, though showing rather wide variations in temperature, shows promise in automated, rapid, reaction-

rate analysis because of its single cycle operation and automated valving. The built-in thermistor port facilities monitoring the temperature of reaction mixtures. The MSU module also exhibits rather large ΔT 's at temperature much different from ambient. The temperature changes which occur in the Durrum and MSU modules are very reproducible provided that the observation cell is allowed to equilibrate between pushes.

Recommendations

It is apparent that the most efficient method of thermostatting a stopped-flow module is to immerse it in a water bath (54-56). Unfortunately, this is often inconvenient particularly when the module must be frequently serviced; hence, the trend is away from such arrangements. For analytical uses of stopped-flow mixing, it is best to operate near room temperature so that all parts of the stopped-flow module are at approximately the same temperature. If large variations of ambient temperature are expected, thermostatting mechanisms such as those exemplified by the GCA and MSU modules may not be adequate for precise work. Whenever possible the cell temperature should be monitored so as to provide assurance that large changes do not occur.

As has been pointed out (40) studies involving determinations of Arrhenius parameters at temperatures

much different than ambient should be carried out very carefully, preferably with accurate measurement of the actual temperature of the reactant solutions and the observed mixture. It is common practice to report reaction temperatures in stopped-flow studies to ± 0.1 K. Obviously, such data should be viewed with a critical eye.

The practice of averaging results from consecutive pushes of stopped-flow mixing modules for S/N enhancement should be carefully examined. A 0.2 K change in the temperature of a reaction mixture which has a typical energy of activation of 2 x 10⁴ cal/mole produces a change in the measured rate of 2.2% (57). Because temperature variations from push to push often approach this amount, only an actual measurement of the observation cell temperature can verify that such changes do not degrade the quality of analytical rate determinations.

The control of temperature on the millisecond time scale with solutions which are mixed by stopped-flow techniques is difficult. Temperature stability on this time scale requires either extremely rapid heat transfer relative to the speed of the reaction being studied or slow heat transfer with measurement of the actual temperature of the reaction mixture. If a stopped-flow mixing system exhibits a very reproducible temperature change followed by a slow return to thermal equilibrium,

rapid reactions may be investigated with minimal error due to temperature effects. For systems constructed of more thermally conductive materials such as stainless steel, the return to thermal equilibrium is somewhat more rapid than in systems constructed of materials of lower thermal conductivity. This results in minimal error in slower reactions.

One possible solution to the temperature problem which deserves investigation is that of maintaining the observation cell at a temperature slightly above that of the drive syringes and mixer so as to match its temperature to the temperature of the reagents after mixing (58). This requires reproducibility of the temperature change on mixing and the capability of thermostatting different parts of the mixing system at different temperatures. These requirements are met by both the Durrum and MSU modules.

Minimizing temperature errors in stopped-flow mixing systems involves a number of trade-offs with respect to the speed of the reactions of interest, the construction materials of the system, and the availability of instrumentation for rapid temperature monitoring. Maintaining relatively constant temperature is based on a compromise between the chemical inertness and the thermal conductivity of construction materials and the desirability of complete immersion of the stopped-flow apparatus.

An awareness of these factors should aid workers in the area of rapid reaction-rate analysis as well as those involved in more fundamental kinetics studies in avoiding the problems of uncertain and/or varying reaction temperatures.

CHAPTER III

COMPUTERIZED CIRCUIT FOR THE PRECISE MEASUREMENT OF RAPID TEMPERATURE CHANGES

A. INTRODUCTION

Recent interest in the rapid and accurate measurement of temperature (59,60) has dictated the need for a monitor which is capable of tracking temperature changes occurring on the millisecond to sub-millisecond time The performance criteria for such a system inhigh speed; chemical inertness; especially in clude: applications in which the transducer must be immersed in solutions which contain very reactive components; negligible power dissipation in the transducer; direct temperature readout; and good accuracy and precision. In addition, many chemical experiments are carried out near ambient temperature, and therefore the range of such a temperature monitor need only extend a few degrees above and below ambient. A number of instruments have been presented with similar criteria in mind (61-63), and they have been utilized in stopped-flow studies (61), in calorimetry (62), and in the measurement of optical power (63).

In this chapter we describe a computerized temperature monitor which is capable of accurately and precisely following rapid temperature changes. First, a description of the circuit and the rationale which dictated our choice of components is presented. We then describe the sequencer which controls the circuit and the computer and interface which were utilized for data acquisition and analysis. Next, the operation and calibration of the circuit are detailed and a brief description of some of the software which was used for data acquisition and analysis is given. Experiments are presented which demonstrate the accuracy (±0.05°K), the precision (±0.002°K per sample), and the sampling rate (5 kHz) of the system. Finally, we present the results of a thermistor plunge test in order to demonstrate the utility of the instrument.

B. THE TEMPERATURE MONITOR

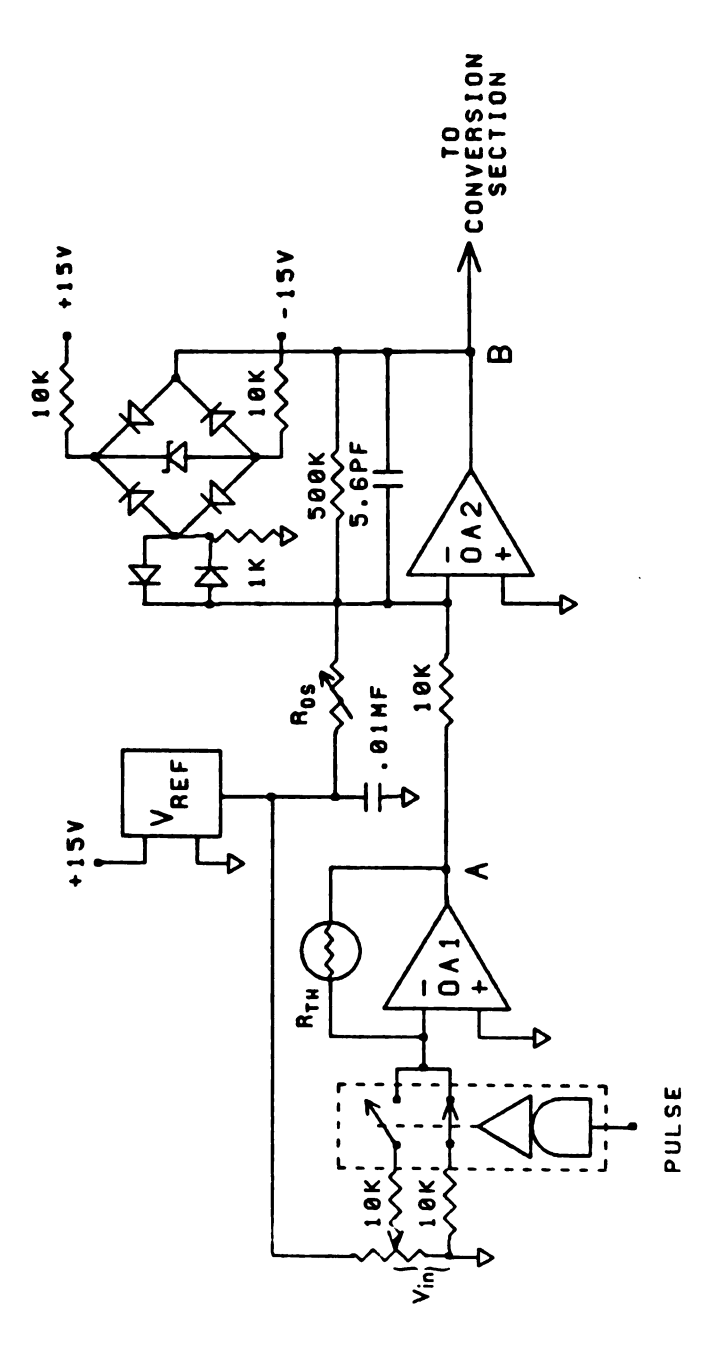
1. Analog Circuit

One of the most easily implemented temperature transducers is the coated semiconductor thermistor (64,65). The commercial availability of small, rapid response, chemically inert thermistors which have conveniently measurable resistances at temperatures of 200-600°K (47,48) makes them the optimum choice as the transducer in this application. The choice of the proper thermistor in any particular application must be based on a

compromise between the desired response time of the thermistor, the dissipation constant of the thermistor, and the response time of the measurement electronics for a given value of the thermistor resistance (66). If the dissipation constant is small and the power delivered to the thermistor is relatively large, the temperature measurement will certainly be affected by self heating of the thermistor. In addition, if the nominal value of the resistance of the thermistor is very large, the frequency response of the measurement electronics will be degraded to some extent.

We achieved a reasonable compromise among these factors by choosing a resistance and an excitation signal which are relatively small and by pulsing the thermistor with a low duty-cycle signal (67). A circuit which is capable of providing this type of excitation is presented in Figure 12.

Excitation of the thermistor, R_{TH} , is accomplished by asserting a TTL logic "l" at the PULSE input of the circuit as shown in the waveform diagram of Figure 13. The PULSE signal causes the upper 10 k Ω resistor to be switched into the summing point of OAl by a FET switch. A fraction of the stable voltage source V_{ref} produces a precise current through the 10 k Ω resistor and therefore through R_{TH} . Small fluctuations in the thermistor resistance due to changes in the temperature result in



Analog Portion of the Computerized Temperature Monitor. Figure 12.

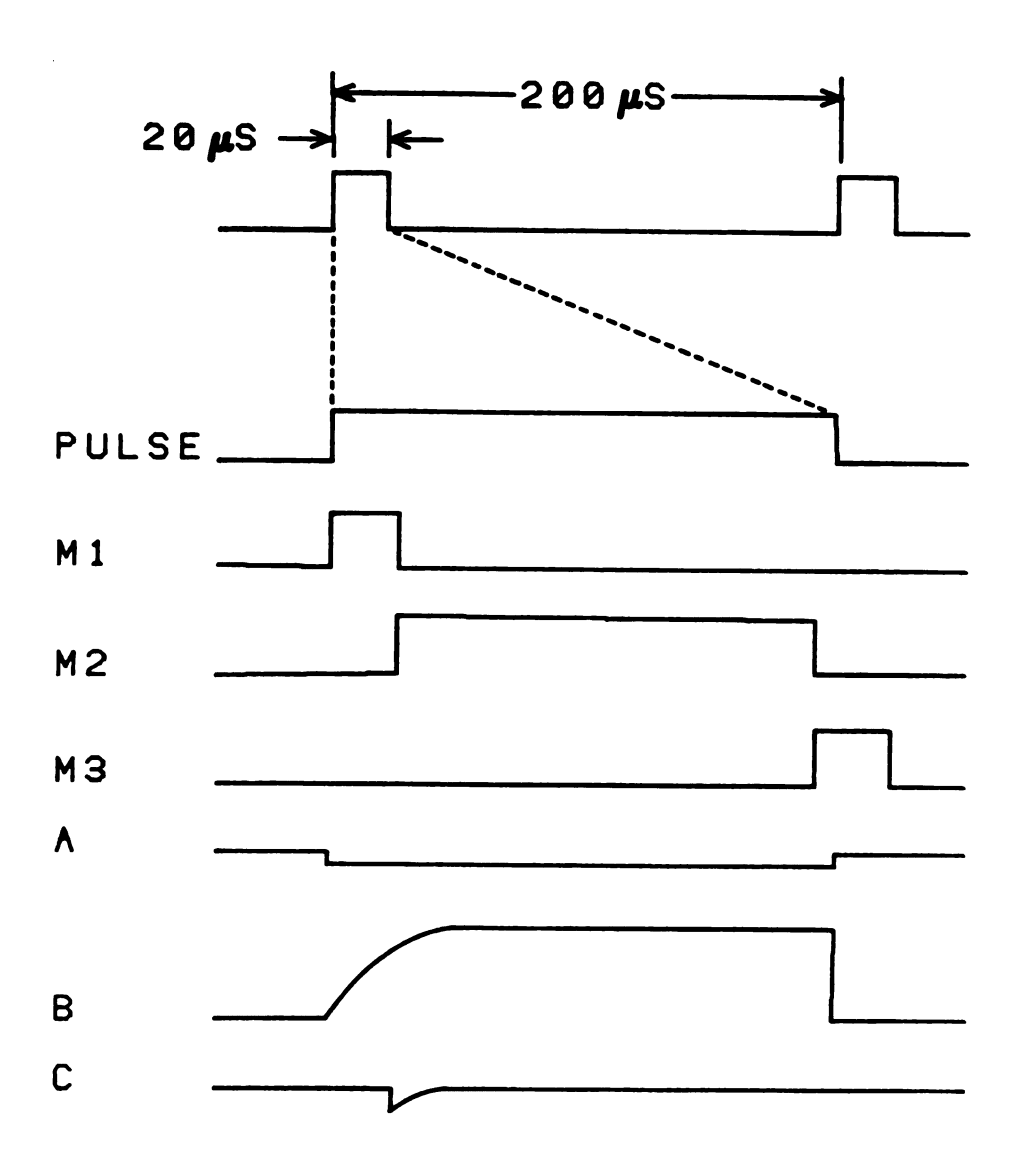


Figure 13. Analog and Digital Waveforms for the Temperature Monitor.

proportional changes in the output voltage of OAl. We chose R_{TH} to have a room temperature resistance of 10 $k\Omega$ and the excitation voltage, V_{in} , to be 0.5 V.

The analog output stage of the circuit of Figure 12 serves a threefold purpose. First, OA2 provides a gain of 50 to yield a full scale ±5 V response corresponding to approximately a 5 $k\Omega$ range of thermistor resistance. For the thermistors we have used, this translates into a temperature range of about 10°K (ambient ±5°K). addition, an offset current is applied to the summing point of OA2 through R to provide scale expansion. The offset sends CA2 into saturation between pulses of the input stage. This condition is undesirable since the overload recovery time of OA2 could be long enough to affect the accuracy of the measurement. Fortunately, this problem is easily overcome by the precision limiter array in the feedback loop of OA2 (68,69). The value of the zener diode limits the output of OA2 to ±6 V and ensures that the op amp does not saturate.

The operational amplifiers which we used were high quality, fast slewing (100 V/ μ s) FET input op amps (Analog Devices Model 149B). This model has been superceded by newer state-of-the-art op amps, but the principles of operation are, of course, the same. The voltage reference source is an AD 580 K (Analog Devices) 2.5 V integrated circuit, low-drift (0.6 mV typically) voltage

reference, and the FET switch is an Intersil IH 5042 SPDT analog switch with $t_{\rm on} = 500$ ns and $t_{\rm off} = 250$ ns (typical). All resistors are metal film 1% nominal values with ± 100 ppm/°K temperature coefficients (Dale MFF -1/4 - T-1).

It is possible to estimate an upper bound for the error, ΔT , in the measured temperature due to self heating of the thermistor by summing the average temperature increase, $\Delta T_{\rm ave}$, and the increase resulting from a single pulse. The power $P_{\rm cont}$, dissipated by the thermistor operated in the dc mode may be calculated as follows:

$$P_{cont} = \left(\frac{v_{in}}{10 \text{ k}\Omega}\right)^{2} \cdot R_{TH}$$

The power dissipated in the pulsed mode of operation (10% duty cycle) is then:

or

$$P_{\text{pulsed}} = 0.1 \times \left(\frac{0.5 \text{ V}}{10 \text{ k}\Omega}\right)^2 \times 10 \text{ k}\Omega = 2.5 \text{ }\mu\text{W}.$$

The dissipation constant, D, for the fastest thermistor which we used (τ = 7 ms) (47) was ≈ 0.5 mW°K⁻¹ in still water. Using this value, we calculate

$$\Delta T_{\text{ave}} = \frac{P_{\text{pulsed}}}{D} = \frac{2.5 \text{ W}}{0.5 \text{ mW}^{\circ} \text{K}} - 1 = 5 \text{ x } 10^{-3} \text{ s}.$$

The temperature increase due to a single pulse, ΔT_{pulse} , is given by the heat imparted to the thermistor per pulse divided by the heat capacity of the thermistor, C_p . We therefore have

$$\Delta T_{\text{pulse}} = \frac{Q_{\text{pulse}}}{C_{\text{p}}} = \frac{P_{\text{cont}} \times t_{\text{pulse}}}{C_{\text{p}}}$$

where t_{pulse} is the pulse width (20 μs). Thus,

$$\Delta T_{\text{pulse}} = \frac{2.5 \times 10^{-5} \text{ W} \times 2.0 \times 10^{-5} \text{ s}}{3.5 \times 10^{-6} \text{ J}^{\circ} \text{K}^{-1}}$$

$$= 1.4 \times 10^{-4} \circ K.$$

The maximum error in the temperature can be no greater than

$$\Delta T_{ave} + \Delta T_{pulse} = 5.1 \times 10^{-3} \, \text{oK}.$$

This value is sufficiently small for most purposes and is approximately twice the resolution of the circuit for a single data acquisition. It is important to note that in order to achieve the same error in the dc mode of operation, V_{in} would have to be reduced by the factor $1/\sqrt{10}$.

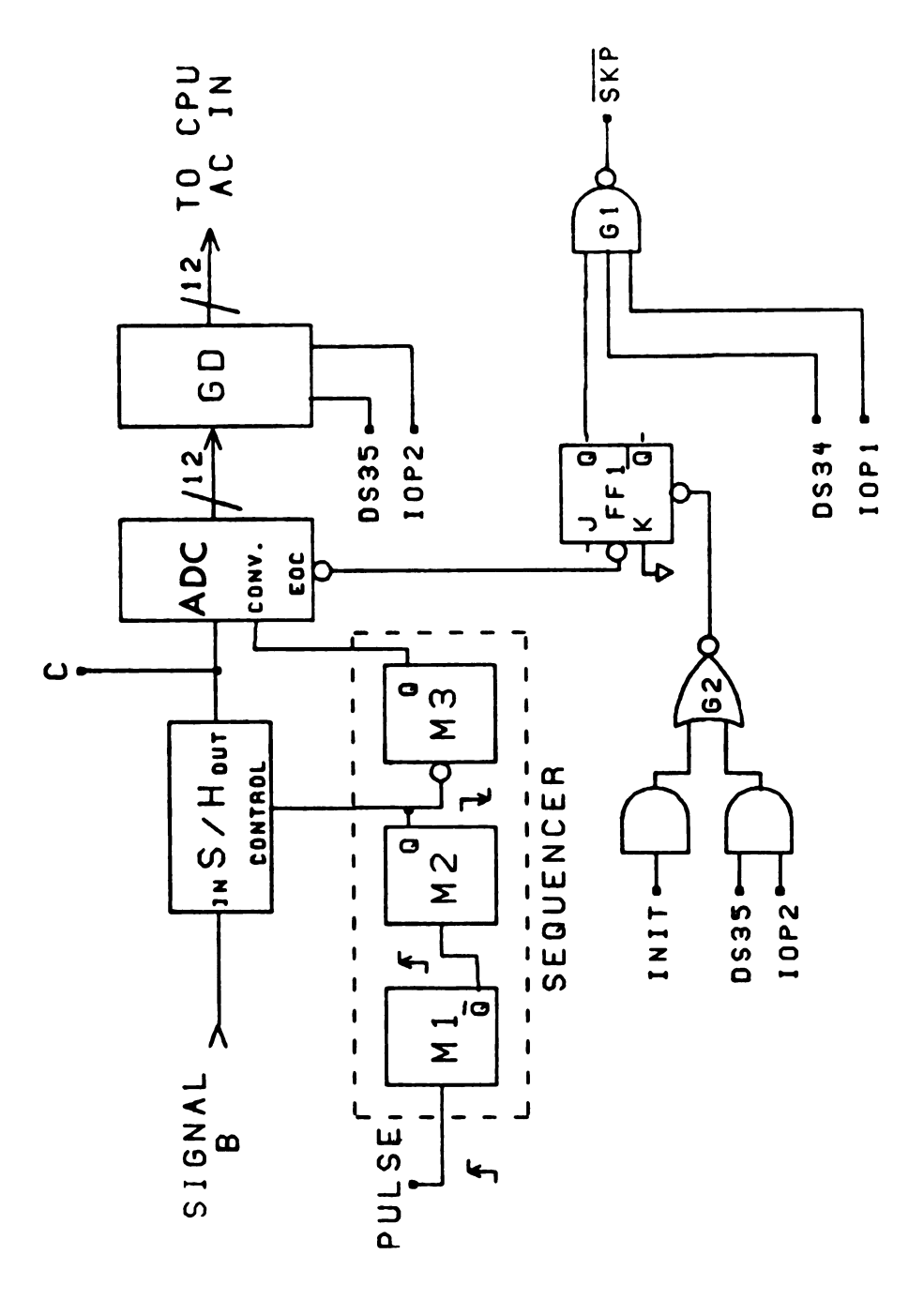
The advantages of pulsing are not obtained without some sacrifice. Since the signal is measured for 1/10 as long in the pulsed circuit, the S/N is reduced by $\sqrt{10}$ from that of continuous excitation. In computerized data acquisition, the time required to obtain one data point is usually 20-40 µs including software overhead to perform signal averaging. For data acquisition systems tracking more than one parameter (absorbance-temperature, conductance-temperature, etc.), this "dead time" may be 100-200 us. The pulsed technique has the advantage of keeping the thermistor "off" during these times. addition, the optimum analog filter for the continuous mode circuitry requires retuning for each different sampling rate and thermistor time constant. On the other hand the pulsed mode provides much flexibility in the choice of sampling rate and the amount of signal averaging.

Finally, it should be noted that the increased bandwidth of the pulsed system over the continuous excitation mode results in increased Johnson noise in the thermistor. With signal averaging the resolution of the circuit is within an order of magnitude or so of the Johnson noise limit.

2. Sequencer

The sequencing for the computerized temperaure monitor is provided by the monostable sequencer enclosed within the dashed lines of Figure 14. This type of sequencer was chosen for simplicity and convenience in adjusting the sampling delays which we will describe now. As previously mentioned, a 10% duty cycle was chosen (see Figure 13). A 20 µs pulse was found to be the shortest pulse width that could be used that would allow the amplifiers to settle to their true values during the pulse duration.

The operation of the sequencer may be explained with the aid of Figure 13. The pulse train shown in the top of Figure 13 drives the sequencer and is derived from a 1 MHz crystal controlled clock oscillator (Heath EU-800 KC, 1 MHz Time Base Card). The 20 μs pulses are generated at 5 kHz and it is these pulses which generate the current pulses in R_{mH} . Since the output of OA2 is at its negative bound between pulses, it is advantageous to delay sampling until the signal is close to its final value. This is accomplished by monostable Ml which produces a short delay pulse (Ml in Figure 13) on the rising The falling edge of Ml fires M2 which edge of PULSE. controls the sample and hold amplifier (S/H in Figure 14). The length of the sampling pulse, M2, is about 15 us which is the acquisition time of the sample and hold



Digital Section of Computerized Temperature Monitor. Figure 14.

amplifier.

The length of M2 is adjusted so that it switches to the "hold" position a few tenths of a microsecond before PULSE goes to logic " \emptyset ". This ensures that switching transients do not affect the measured signal. The falling edge of M2 generates M3, the analog-to-digital converter (ADC) trigger pulse. Since the falling edge of M3 initiates the ADC conversion, its width is adjusted to be 2-3 μ s, again so that switching transients generated by M2 and PULSE are nullified.

The analog signals generated by this sequencer are represented by waveforms A, B, and C of Figure 13. The voltage waveform A is generated when the constant current pulse is applied to the thermistor. Since the op amps are arranged in the inverting configuration, A is proportional to the resistance of the thermistor and is negative in sign. The bounded op amp produces signal B, the final magnitude of which is directly related to R_{TH}. The analog signal produced by the sample-and-hold amplifier (Analog Devices SHA-5) is represented by waveform C. This signal is passed to the A/D converter for digitization and subsequent storage in the computer.

Computer

The computer utilized in this work for experimental control is a PDP 8/e (51) equipped with 16 K memory,

dual floppy disk, cartridge disk, real-time clock, graphics display terminal, and a Heath EU 801 Computer Interface Buffer for general purpose interfacing. The interface buffer provides 12 bits in and out of the computer via a KA8E positive I/O bus interface located in the CPU. A number of control signals are also provided which enable data to be passed in and out of the CPU through the accumulator (AC) register.

4. Interface

The interface we designed was chosen to operate under the programmed I/O mode of data transfer. In Figure 14 we present the additional hardware which is necessary to convert the analog output of the temperature monitor to a digital number which may be passed to the CPU. A/D converter (Datel Model ADC-HY12BC) is cleared on the rising edge of M3 (Figure 14), and the conversion is initiated on the falling edge of M3. The end-ofconversion signal, EOC, clocks FF1 at the end of the conversion cycle thus opening the three input NAND gate, The computer may then check the status of the con-Gl. version by producing a device select pulse (DS34) and an input/output timing pulse (IOP1). If all inputs of Gl are logic "1", a logic " \emptyset " is asserted on the \overline{SKP} line of the interface, and the computer skips an instruction enabling the data to be driven into the AC of the CPU.

This is accomplished by asserting DS35 and IOP2 on the control lines of the EU 800-JL gated driver card (GC in Figure 14). Note that this I/O signal from the CPU also clears FFl in order to prepare the circuit for the next data acquisition sequence. The flag (FFl) may also be cleared by the INIT signal input to G2, which is a short initialization pulse generated by the CPU at the beginning of each program.

C. CIRCUIT OPERATION

Unfortunately, most thermal transducers have nonlinear response characteristics. A vast amount of creative energy has been expended in devising schemes such as linearization networks (70) in order to provide a direct readout of temperature for a variety of transducers. One of the major advantages of computerization of circuits such as the one which we are describing is that nonlinear responses may be numerically corrected in order to provide a readout which is convenient for the experimenter.

It should be clear that the ease of operation of the temperature monitor and the usefulness of the resulting data are highly dependent upon the software which may be available for the acquisition and subsequent manipulation of the experimental data.

In general, we may classify the operation of the circuit into three major categories: (1) circuit

calibration; (2) transducer calibration; and (3) data acquisition and analysis. In the sections to follow we will describe these procedures in some detail.

1. Circuit Calibration

As mentioned previously, the output of the temperature monitor is linear with the resistance of the thermistor, which is the feedback element of OAl. A very convenient method for calibrating the circuit is to replace the thermistor with a precision decade resistance box (DRB) (ESI DB52) and to vary the resistance over the range of interest. A simple calibration program which allows the operator to accomplish this task easily was written. After being prompted by the console terminal, the operator sets the DRB at the desired value, types the value of the resistance on the keyboard, and initiates the data acquisition. The instrument acquires a preselected number of A/D conversions (up to 2047), averages them, and stores them for subsequent analysis. After the desired number of calibration points have been acquired, control is returned to the program.

The software then performs a linear regression analysis on the ADC output-vs-resistance curve (71), and the computer prints the data, the residuals from the regression analysis, and the linear correlation coefficient. Values of the correlation coefficient are

typically 0.99999 or better. The slope and intercept of the calibration curve are then stored on the mass storage device for subsequent retrieval and use by other programs. The long term stability of the circuit was evaluated by recording the slopes and intercepts of the calibrations over a two month period. The relative standard deviation of the slopes was 0.14% and that of the intercepts was 0.08%. This corresponds to a total variation in a measured temperature of ±0.02°K over the period with only the initial calibration. This variation is reduced to ±0.001°K if calibrations are carried out each time the instrument is used.

All programs except the data acquisition and plotting routines were written in FORTRAN II under the OS/8 operating system (51). The data acquisition and plotting routines were written in SABR (51), an assembly level language which may be imbedded within the text of FORTRAN programs and sub-programs.

2. Transducer Calibration

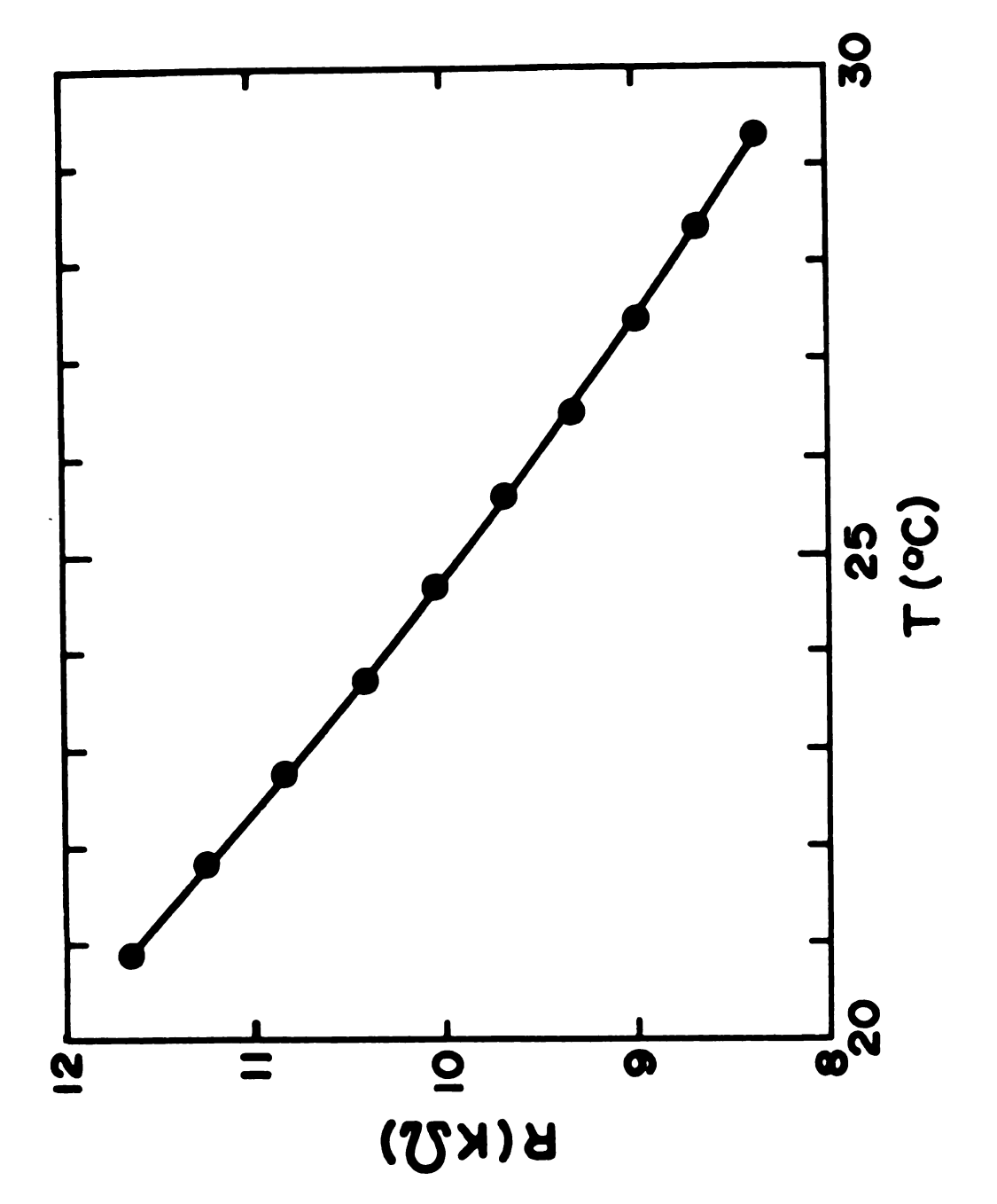
While it is possible to purchase calibrated thermistors, we have found it advantageous to calibrate them ourselves because of lower cost and greater convenience. The temperature accuracy of the monitor could be no greater than $\pm 0.01^{\circ} K$ since this is the value of the precision of the thermostated circulating bath which we

have available (Neslab TV 45/250). Unfortunately, the temperature standard available (a bomb calorimeter thermometer traceable to NBS standards) was only accurate to \underline{ca} . $\pm 0.05^{\circ}$ K, but this was deemed adequate for our own work.

A special computer program was written for this type of calibration which allows the operator to enter the temperature of the bath as read from the thermometer and initiate the acquisition of any number of R-vs-T data points. The data are acquired, the signal-to-noise ratio is evaluated and these values are printed for visual inspection by the operator. If the precision is acceptable, the operator indicates from the keyboard that the data should be retained, and the R-T pair is stored for further analysis at a later time. Following data acquisition at all temperatures which are of interest, the R and T values for all of the points are written into a permanent data file. A typical data set obtained with the temperature monitor is presented in Figure 15.

Trolander, et al. (72) have investigated a number of functional relationships for fitting T-vs-R curves for various semiconductor thermistors. With the function,

$$T^{-1} = A + B \log R + C(\log R)^3,$$



ಹ Typical Resistance-vs-Temperature Data for the Calibration of Fast Thermistor. Figure 15.

T-R data for a number of thermistors over a fairly wide temperature range. The fits are consistently accurate to within a few millidegrees over the range -20°C to 120°C. We have found that the first two terms of the series are sufficient to fit the T-R data obtained with the temperature monitor to within the experimental uncertainty over the range 20-30°C.

The R-T data obtained as discussed above are read into a general purpose nonlinear regression analysis program (71), and the coefficients resulting from the numerical analysis are printed out and written into a data file for later retrieval by other data acquisition routines. The curve resulting from a typical calibration run is illustrated in Figure 16. The correlation coefficient for this particular fit is 0.999991. The residuals from the calibration are plotted as a function of the temperature in Figure 17, and with one exception, they all lie within the range ±0.015°K.

Better absolute accuracy may be attained in a number of ways. A fast thermistor may be purchased from the manufacturer (47) which has been calibrated to $\pm 0.002^{\circ}$ K. Alternately an S-1 probe (47) may be purchased which is accurate to $\pm 0.01^{\circ}$ K and used to calibrate the thermistors locally as discussed above. A quartz thermometer could also be used if one were available. In any event, the

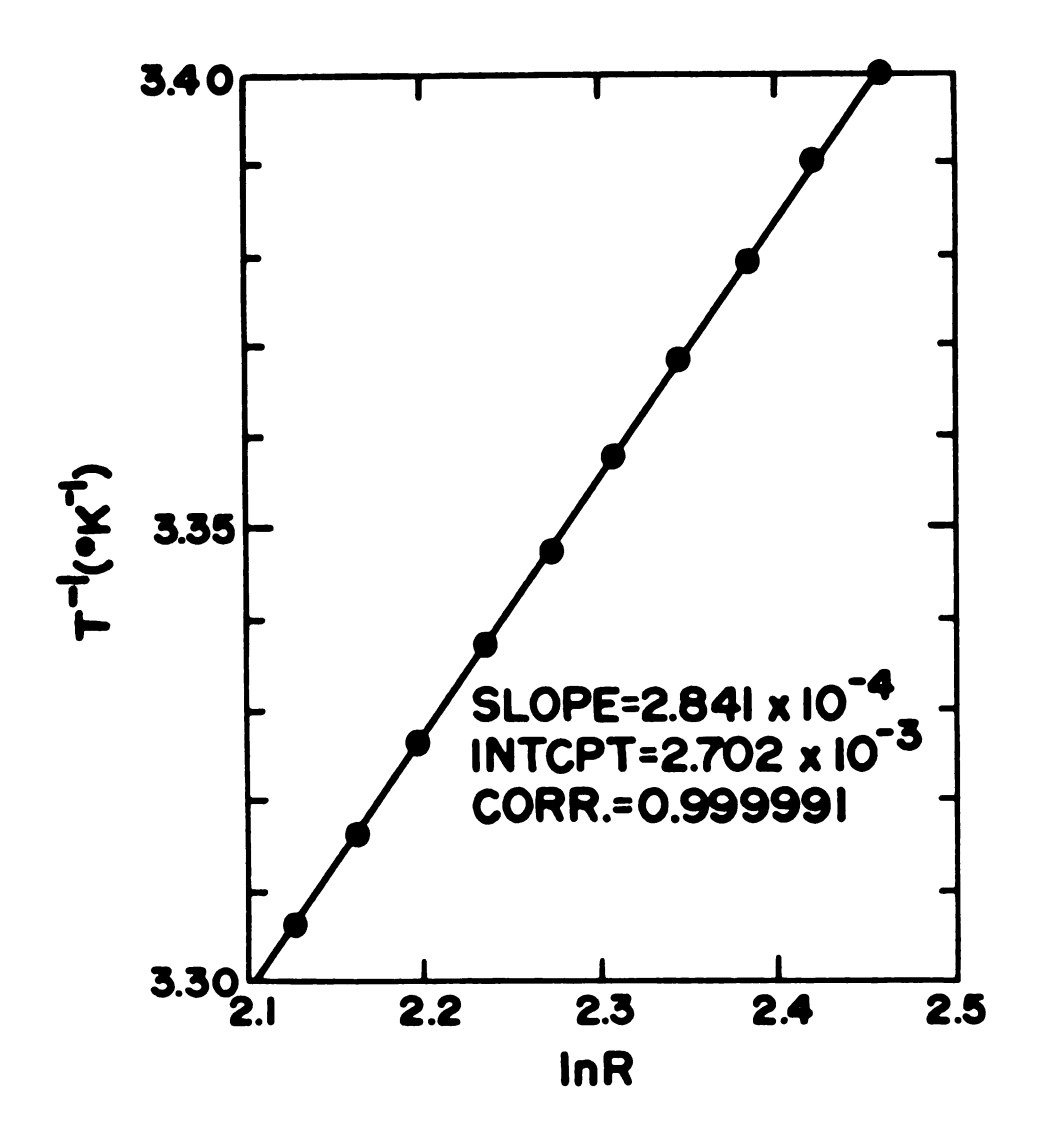
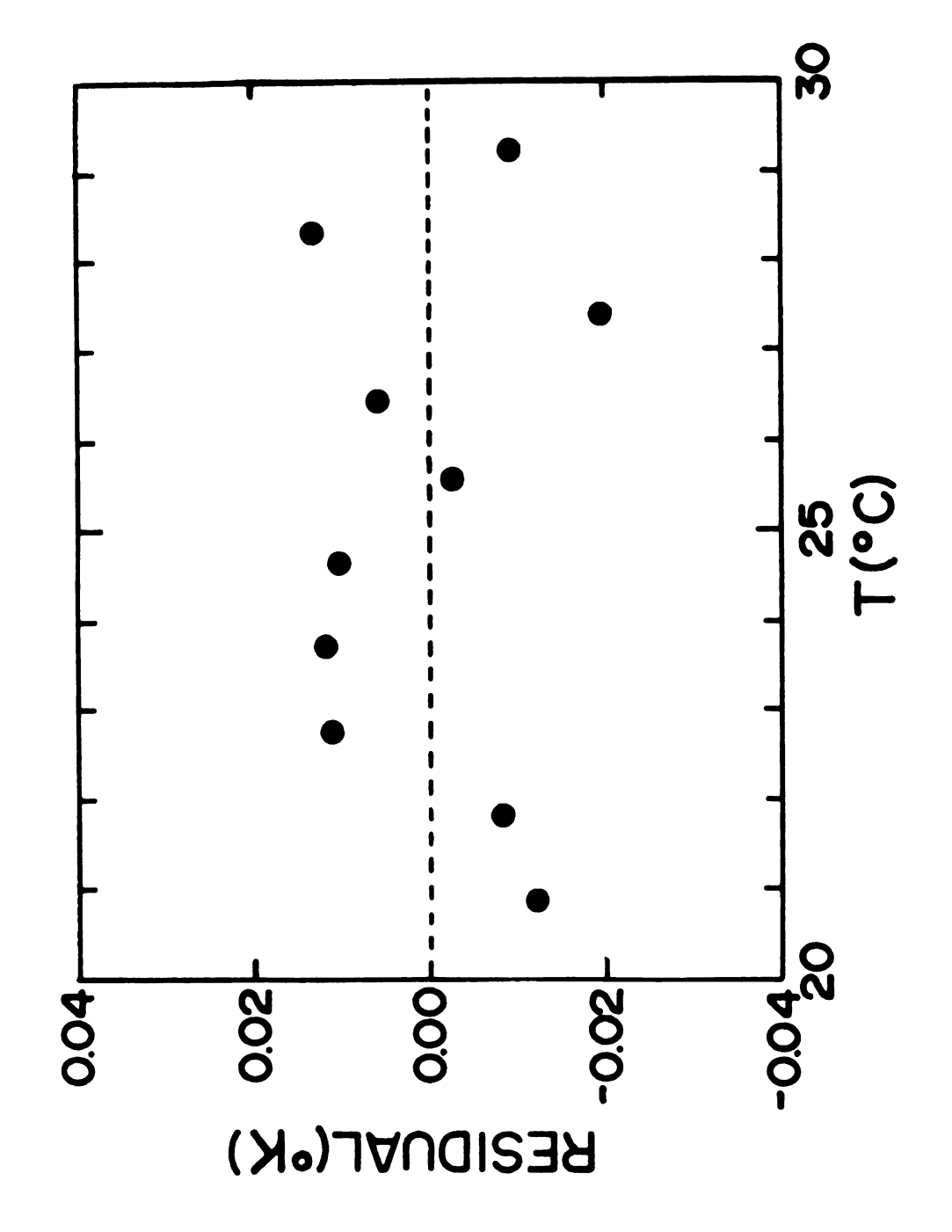


Figure 16. Fit of the Data of Figure 15 to the Equation: $T^{-1} = A + B$ in R.



Residual Plot for the Curve-fit of Figure 16. Figure 17.

accuracy of the temperature monitor could be reduced to the millidegree range if standards were available.

3. Data Acquisition and Analysis

Two major programs have been written for the routine acquisition of temperature data. The first and most versatile of these programs is the timed data acquisition routine. The operator of the temperature monitor has the option of specifying the number of data acquisitions per averaged data point, the total number of averaged data points (up to 400), and the time between data acquisition. In addition, a major branch point is provided in the program at which the operator may choose to reinitialize the data acquisition parameters, acquire another data set using the previously specified parameters, plot the current data on the graphics display terminal, write the current data into a permanent data file, or chain to another program.

The second of these programs is a very simple program which performs a single data acquisition in order to determine the temperature using any thermistor which has been previously calibrated by the procedure described above. These programs have proven to be extremely useful in fundamental investigations of small temperature changes occurring in stopped-flow mixing systems (73).

D. EVALUATION OF THE TEMPERATURE MONITOR

1. Accuracy and Precision

In order to evaluate the temperature circuit with respect to accuracy, two different thermistors were calibrated and mounted side-by-side next to a calibrated bomb calorimeter thermometer in the bath described above. The bath temperature was varied over the range 20-30°C and then readings of the temperature were taken with each thermistor at ten different temperatures. The results of the evaluation are shown in Table 1. The thermometer temperature, the mean temperature determined by each thermistor, and the deviations of both thermistors from the thermometer readings are listed. Although a few of the deviations are as large as 0.02 - 0.03°K, the mean deviation for thermistor number one is 0.011 °K and that of thermistor number two is 0.005 °K. These results are well within the ±0.05°K accuracy of the thermometer and consistent with the ±0.01°K precision of the available temperature bath.

The inherent precision of the circuit was evaluated by replacing the thermistor with a 10 $k\Omega$ resistor (DRB). In this way we simulated a thermistor at a constant temperature near the midrange point of the circuit. Data were collected and averaged using the various numbers of points per ensemble average shown in Table 2. Ten

Table 1. Accuracy of Temperature Circuit.

Thermometer (°C)	Thermistor #1 (°C)	Deviation (°K)	Thermistor #2 (°C)	Deviation (°K)
20.40	20.38	-0.02	20.41	+0.01
21.33	21.30	-0.03	21.33	00.00
22.27	22.26	-0.01	22.29	+0.02
23.20	23.19	-0.01	23.22	+0.02
24.15	24.14	-0.01	24.15	00.0
25.08	25.08	00.00	25.08	00.0
26.00	26.00	00.0	26.00	00.0
26.93	26.93	00.0	26.94	+0.01
27.86	27.88	+0.02	27.86	00.0
28.81	28.80	-0.01	28.80	-0.01
		mean 0.011		mean 0.005

Table 2. Precision of Temperature Circuit.

# Pts/Signal Average	Mean T (°C)	SD (°K)	S/N
1	24.3257	0.0017	14000
5	24.3260	0.0010	23000
10	24.3255	0.00076	32000
50	24.3248	0.00051	48000
100	24.3249	0.00016	149000
500	24.3242	0.00019	128000
1000	24.3244	0.00041	59000
2000	24.3236	0.00016	150000

such ensemble averages were then used to determine the mean temperature and its standard deviation. The signal-to-noise ratio (S/N) was calculated for each experiment, and the results are shown in the table.

We should note that the S/N was calculated simply as the ratio of the readout (Celsius temperature) to its standard deviation. Obviously, the variance of the readout depends upon the variance of the amplifier signals, the variance of the offset current generator, and the variance of the ADC. As Table 2 shows, the S/N increases approximately as the \sqrt{N} until the number of points per average reaches a few hundred, at which point non-random sources of instrumental variance become important. The precision of the temperature monitor is about 0.1 m°K at one hundred points per signal average.

2. Frequency Response

The frequency response of the circuit was evaluated by simulating a step temperature change which was faster than the fastest response that might be expected from a thermistor. This was accomplished by using a FET switch to switch alternately a 10 $k\Omega$ and an 11 $k\Omega$ resistor into the feedback loop of OAl at a frequency of 1 kHz. The resulting circuit response is depicted in Figure 18. There was no signal averaging of the data, and the data demonstrate that the circuit is able to track the rapid

1 KHZ SIMULATED T STEP

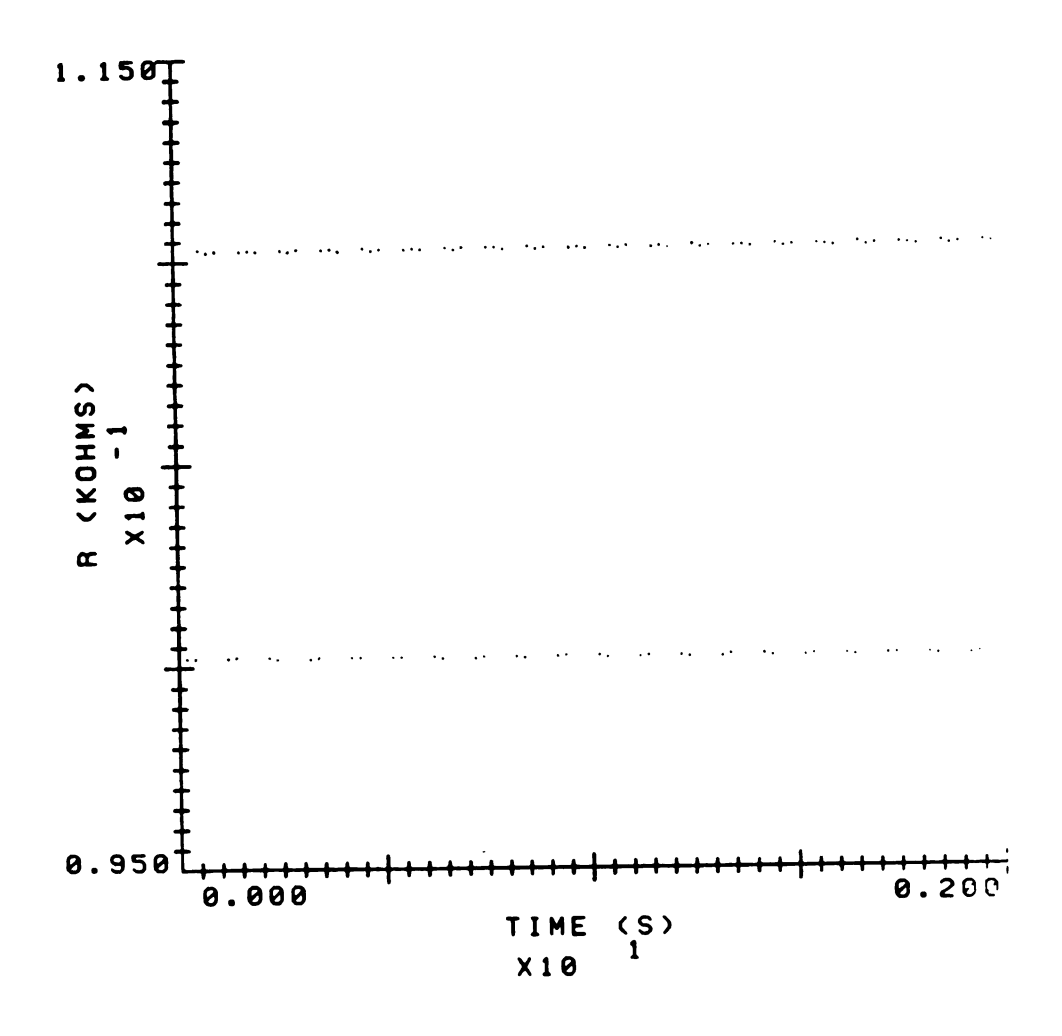


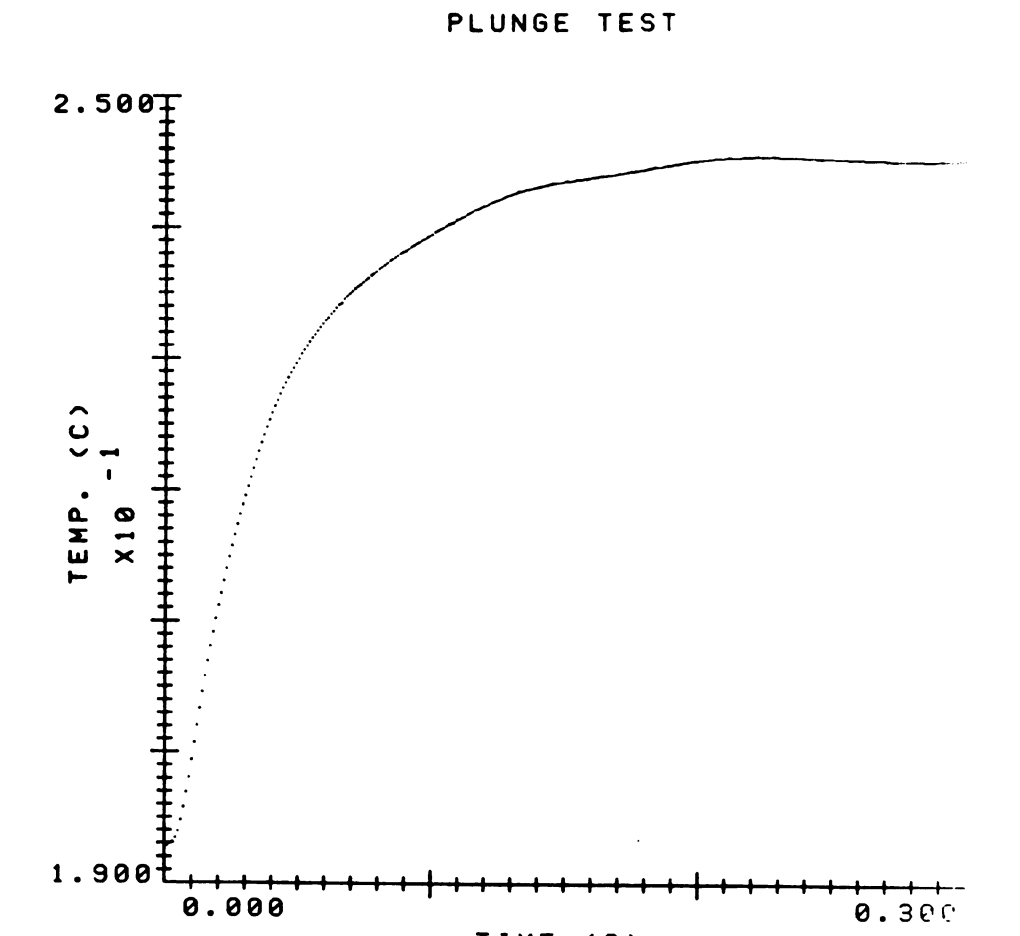
Figure 18. Rapid Temperature Change Simulated by Switching Two Different Resistors into the Feedback Loop of OAl.

signal change precisely.

A more practical test of the circuit was carried out by performing a plunge test of one of our fast thermistors in a manner similar to that described by Berger and Balko (74). The data resulting from the plunge test are plotted in Figure 19. From these data the time constant of the thermistor was found to be 24.8 ms. The circuit is ideally suited to performing such tests as long as the temperature changes which occur are within its range. It is important to note that the response time of the system is limited by available thermistors ($\tau \approx 3-7$ ms).

E. CONCLUSIONS

The temperature monitor which we have described has been shown to be accurate to ± 0.05 °K limited by available standards, precise to ± 0.002 °K, and capable of tracking a step temperature change in 200 μs given thermistors with such rapid response. The monitor has been demonstrated to be useful for problems requiring rapid, accurate measurement of temperature changes such as the measurement of the response times of fast thermistors. In addition, the circuit has found use in our laboratories in the investigation of the thermal characteristics of stopped-flow mixing systems (73). Other areas in which



TIME (S)

Figure 19. Thermistor Plunge.

the instrument may find use include enthalpimetric titrations, enthalpimetric reaction-rate methods, and other thermal and enthalpimetric methods (67).

CHAPTER IV

A COMPUTER CONTROLLED BIPOLAR PULSE CONDUCTIVITY SYSTEM FOR APPLICATIONS IN CHEMICAL RATE DETERMINATIONS

A. INTRODUCTION

Traditionally, the measurement of electrolytic conductance has been one of the most accurate and precise of all electrochemical techniques. Unfortunately, the laborious procedures often required to achieve such measurements have hindered its routine use in the analytical laboratory and its use in conjunction with other techniques such as stopped-flow mixing which require more rapid response. The electronic revolution of the past decade has made possible new instrumental methods which previously were difficult or impossible to carry out. Among these is the bipolar pulse technique which was first developed in our laboratories (75). The technique involves the sequential application of two voltage pulses of equal magnitude and duration but opposite polarity to a cell, followed by measurement of the instantaneous cell current at the exact end of the second pulse. In this way the voltage across the series capacitance of the cell electrodes is nearly zero and the parallel capacitances associated with the

conductivity cell and connections are drawing essentially no current at the time of measurement. A determination of the cell current at this time, therefore, allows an accurate measurement of the cell resistance. The measurement itself is then subject only to the limitations of the particular instrument and not to the cell design, chemical application, or solvent system employed. Subsequent work with this technique has demonstrated its wide dynamic range and sensitivity for various conductometric measurement problems (76,77), and variations on the technique have been developed by others (78,79).

In the sections which follow, we present a computerized version of the bipolar pulse instrument which provides for: computer control over the analog portions of the circuit; high speed readjustment of circuit parameters (<300 µs); optimization of each measurement in real-time; signal-to-noise enhancement by averaging and digital smoothing; rapid and sophisticated data analysis; and correction for temperature changes which may occur during the measurement process. In addition, we demonstrate the utility of the instrumental system by employing it as the detection system in a stopped-flow mixing apparatus. As examples of the types of chemical systems which may be studied with such an apparatus, fundamental investigations of the dehydration of carbonic acid and of the pseudo-first-order reaction of

nitromethane with base are presented.

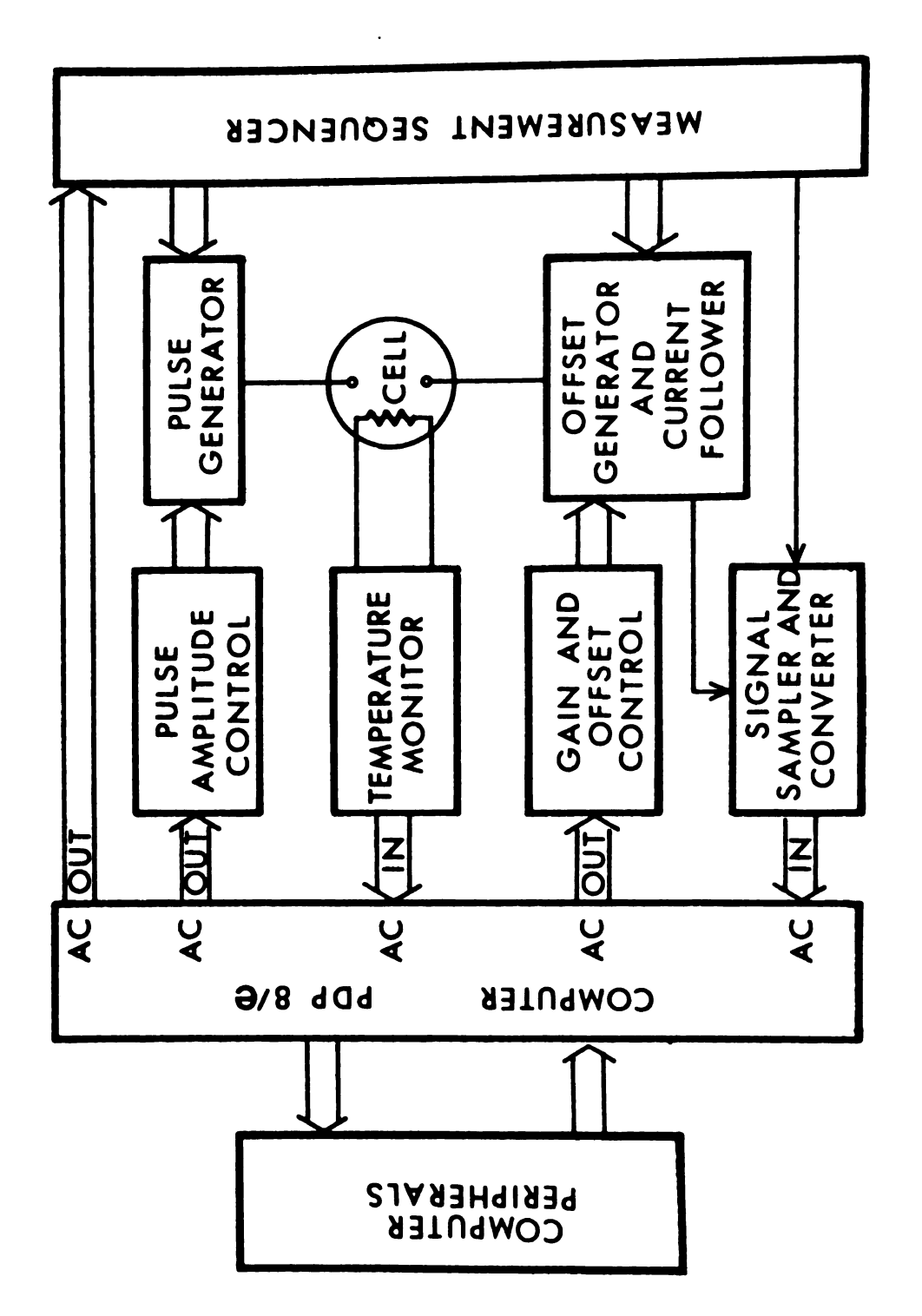
B. THE INSTRUMENT

A block diagram of the instrument system is shown in Figure 20. It includes the computer, the computer peripherals, and the bipolar pulse instrument. The computer is a Digital PDP 8/8 (51) with 16 K of memory. The peripherals available include a dual floppy disk system, a cartridge disk system, an extended arithmetic element, a mainframe real time clock, a DEC writer, and a graphics display terminal. The Heath EU-801E interface system was used. The structure of the bipolar instrument itself was organized to take advantage of the interactions available with this computer system.

The DEC OS/8 operating system was used for software development and program execution. It consists of a monitor, absolute and relocatable assembly languages and loaders, FORTRAN, and various utility routines.

Because of the availability of FORTRAN, as well as the ability to combine it with the assembly language, SABR, it was assumed, in the design and construction of the instrument, the programming of a sophisticated nature could be utilized.

The instrument is controlled by data transferred from the computer to the control circuits and the measurement sequencer. The computer may also supply the



Block Diagram of the Computerized Conductance Instrument. Figure 20.

triggering signal to the measurement sequencer which initiates pulsing. The pulse amplitude control module receives data from the CPU which determines the pulse height and provides the correct positive and negative voltage levels to the pulse generator. The gain and offset controls determine the amplification of the signal produced by pulsing the cell and the amount of that signal offset before amplification. The measurement sequencer, which supplies the signals that determine the length of the pulses and the timing of the measurement, contains a time base also controlled by the computer. The analog signal produced by combination of the cell and offset currents is tracked, held, and converted to a digital signal by the signal sampler and converter under control of the measurement sequencer. Finally, the digital information is transferred to the computer under software control and stored for later analysis.

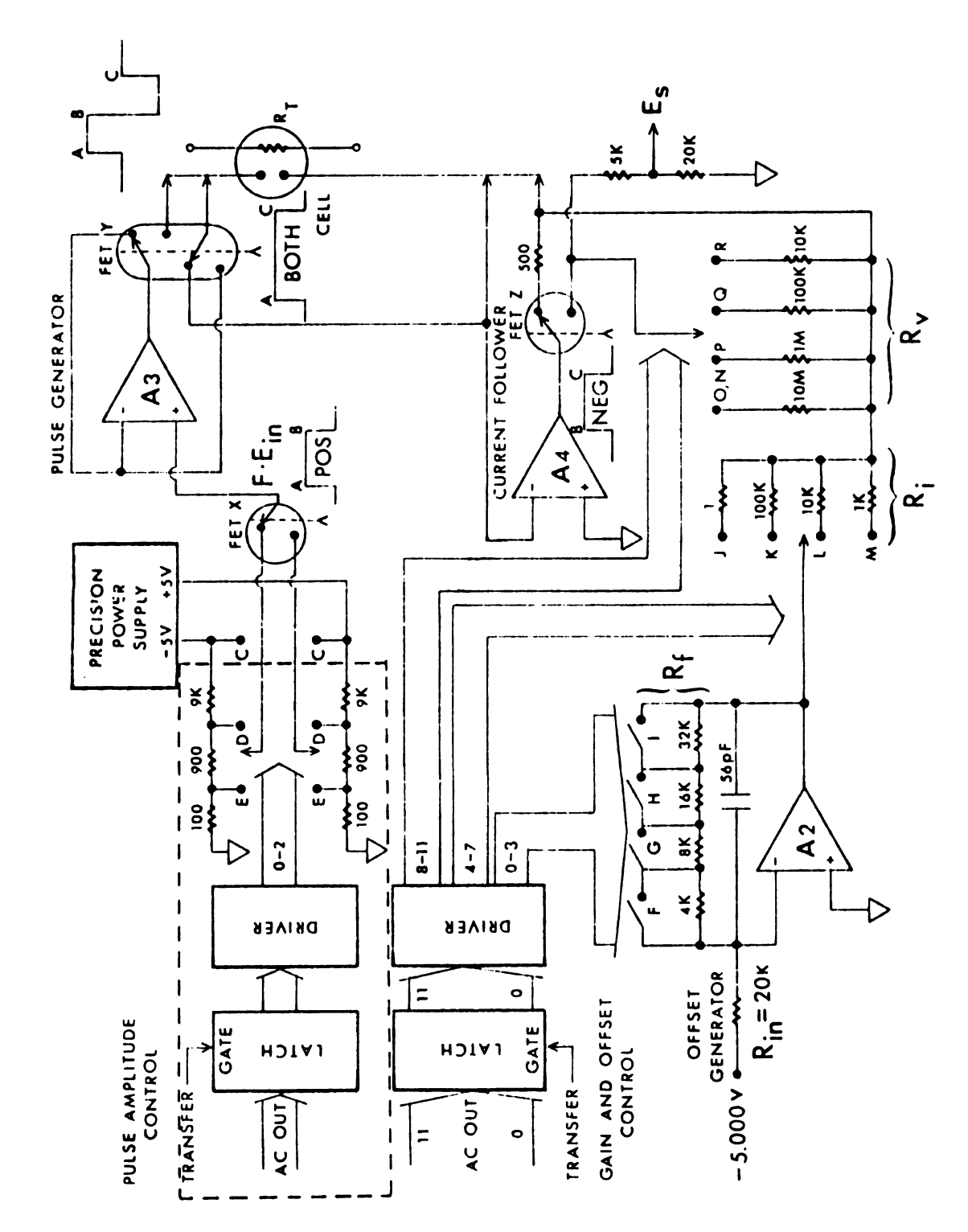
Cell temperature may be simultaneously followed by the computerized temperature monitor which has been described elsewhere (3) (see Chapter III).

1. The Analog Interactions

Since the present instrument was specifically designed for computer control and monitoring, it was possible to simplify the analog circuits by use of digital circuit adjustment techniques and a digital data

acquisition system.

The simplified schematic diagram of Figure 21 illustrates the interaction of the computer with the analog portion of the circuit. All of the precision voltages necessary for the operation of the instrument are derived from the precision +5 volt and -5 volt supplies which are regulated to 0.01%. These voltages are fed to the two voltage divider circuits of the pulse amplitude control shown inside the dashed line of the figure. The computer selects the amplitude of the bipolar pulse (± 5 , ± 0.5 , or ±0.05 V) by switching on one of the three DP T relays (C, D, or E). The pulse generator, amplifier A3, applies the chosen positive and negative pulses to the cell. Pulsing occurs during the timing sequence A-B-C on the switch control waveforms shown in Figure 21. The polarity of the pulse is determined by the state of field effect transistor (FET) switch X under control of the measurement sequencer waveform POS. The polarity is positive during time A-B and negative at all other times. output of amplifier A3 is connected to the cell during the total pulsing time (A-C) by FET switch Y which is controlled by measurement sequencer waveform both. Four cell leads are used; two to maintain the cell at the chosen voltage level and two to supply current for the cell. reduces the effect of contact resistance to the cell leads. The other electrode is similarly connected to the circuit by two cell leads from operational amplifier A4, the



Analog Circuits of the Conductance Instrument. Figure 21.

very fast (500 V/usec) current follower; one lead provides the control potential and the other the current Amplifier A4 controls the lower electrode to be always at virtual ground and sinks all currents to virtual ground when pulses are not being applied by connection to FET switch Y. When the current output of the cell is not being monitored, a 500 Ω resistor is switched into the feedback loop of amplifier A4 by FET switch Z to insure that the inverting input will be at virtual ground, and to prevent amplifier saturation during the positive pulse. During the time interval B-C (NEG), when the cell current is being sampled, the appropriate computerselected feedback resistance is switched into the circuit by FET switch Z under control of the measurement sequencer. The current follower output is divided to give a signal, E_s , to the sample and hold module, which is 4/5 of the actual output. To the analog circuit, then, the 0-10 volt analog-to-digital converter (ADC) appears to be a 0-12.5 volt converter. This was done to provide overlap at scale changes which eliminates the need for precise scale adjustments, as will be explained in the performance section. The voltage output, Es, is tracked and held at the exact end of the second pulse by the signal sampler and converter.

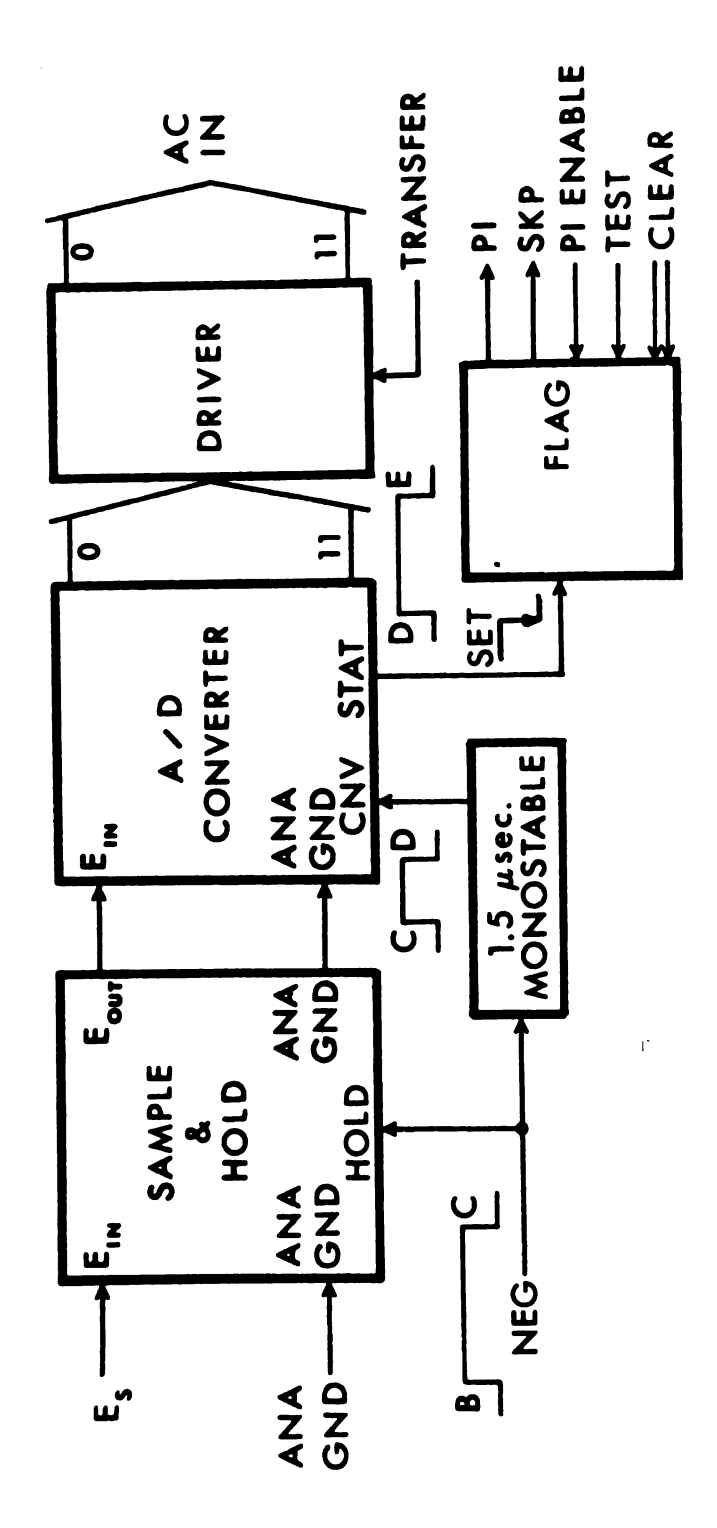
In order to provide additional resolution most of the cell current may be offset by a constant current supplied

by operational amplifier A2. The required amount of offset is selected by the computer through appropriate combination of feedback resistors and series resistors
(relays F-M). The offset current produced is added to
the cell current at the summing point of amplifier A4
producing up to four additional most-significant bits of
resolution in the conversion process (80).

2. The Digital Interactions

The digital measurement of the conductance information at the output of the current follower is made by the combination of a fast tracking sample-and-hold module and a 12 bit ADC (10 µsec conversion). Waveform NEG from the measurement sequencer causes the sample and hold module shown in Figure 22 to track during the negative pulse and hold the signal, E_S, at the exact end of the pulse (time C). The falling edge of waveform NEG triggers a 1.5 µs monostable which resets the ADC on its rising edge and initiates conversion on the falling edge at time D. The status output of the converter sets a skip flag at time E and, if desired, a program interrupt. The output of the ADC is transferred to the computer upon request. The flag is read and cleared by the computer and is automatically cleared at the start of the program.

It has been pointed out (75,76) that the timing of pulses is critical to the success of a conductance



Analog-toDigital Conversion Section of the Conductance Instrument. Figure 22.

measurement using the bipolar pulse technique. Thus, a precise internal timing system shown in Figure 23 was utilized to produce the waveforms. A synchronous 2-bit counter driven by a crystal oscillator-multiplexer is used to generate the POS, NEG, and BOTH waveforms shown in Figures 21, 22, and 23. The frequency of the single-cycle pulse generator is under computer control, and it may be triggered by the computer or an external event generated by another instrument. Pulse widths from 10 μs to 100 s are available, but only those from 10 μs to 10 ms are useful.

3. System Flexibility and Software

The component circuits of the instrument provide the sequence of events necessary to perform a measurement of conductance. These circuits are interconnected only to the extent required by these sequences. This was done with the intention of producing an instrument with the highest degree of internal flexibility, both in combination of functions and in timing these functions. The use of digital measurement and timing techniques places the computer's decision making abilities within the instrumental framework and requires the use of intelligent rather than fixed interactions between the various separate circuits. In this way, the instrument itself may be altered to better perform a chemical

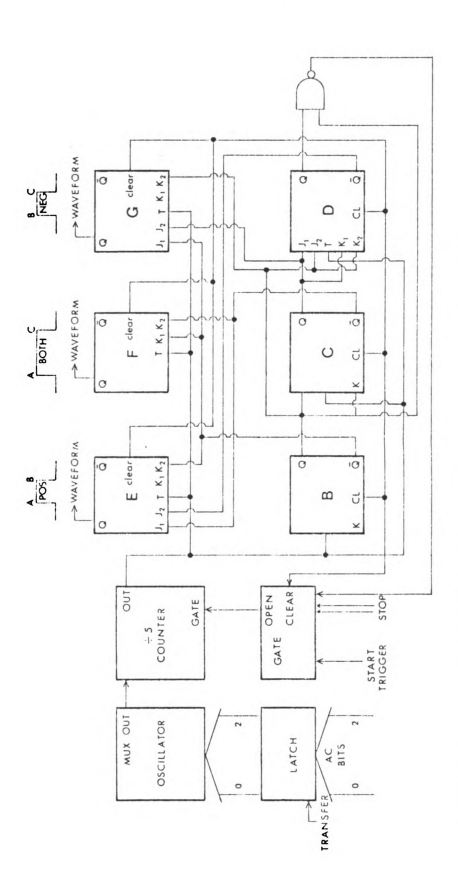


Figure 23. Measurement Sequencer of the Conductance Instrument.

measurement by a simple modification of the control software. The experiment itself may then be reconfigured during run time such that the data received as a result of the software-instrument-experiment correlation is the optimum data attainable by the technique.

The software for the computerized conductance instrument may be broadly classified into three categories: utility routines; data acquisition routines; and data analysis routines. A common element in both the utility and data acquisition categories is the preliminary routine which determines the optimum circuit settings for each of the four useful pulse widths according to the optimization rules which will be discussed in another section. The utility routines include provision for the automatic determination of signal-to-noise ratios, of accuracy with respect to standards, of optimum pulse width, and of pulse timing over the entire operating range of the instrument. In addition, routines are available for periodic exercising of the circuits and adjustment of the analog components, and built-in error messages are available to help diagnose instrument malfunctions.

The data acquisition routines include facility for the acquisition of a single signal average consisting of a user-specified number of discrete data points or of a specified number of such signal averages at precisely timed intervals. Additionally, it is possible to continuously acquire and analyze data at precisely timed intervals and output the data to the console device or to the DEC writer. A maximum data rate mode in which no time is sacrificed in making scale changes is also available for chemical processes which occur on a very fast time scale. A multiple data rate routine may be used to provide useful conductance information on both long and short time scales. Finally, in each data acquisition routine, it is possible to simultaneously acquire temperature data for use in correcting the conductance data for temperature changes which occur during the measurement process.

The data analysis routines vary somewhat with the type of experiment which is to be carried out, but most allow the following operations to be performed. Upon entry into the data analysis routine, the raw conductance data is calculated and stored in memory in preparation for subsequent manipulations. The operator may then choose to plot the data on the graphics display terminal, list it on the DEC writer, or correct it for temperature, dilution, or scale change effects. The data may also be stored in a file on the mass storage device for subsequent retrieval and analysis by the same or other programs.

The heart of each of the data analysis routines is an interactive graphics subroutine which has been

described elsewhere (see Chapter VII). This subroutine enables the operator to precisely and rapidly specify particular points or regions on the G-vs-time (or G-vs-volume) curves for each experiment. The operator may then request the average conductance (G) or temperature (T) over a region of the curve, the values of G and T at the specified points, or other more complex results such as the end point in a titration, the first order rate constant in a kinetics experiment, or a derivative smooth of either conductance or temperature data (81,82).

The instrument may, of course, be operated in other modes as are required by the particular experiment.

Since a large library of software has now been written for this instrument, it has been found that completely new programs can be developed in a few hours or derived from existing programs in even less time.

4. Measurement Optimization

An expression for the conductance, G, of the cell in the circuit of Figure 21 may be derived as follows:

$$G_{cell} = \frac{I_{cell}}{E_{cell}}$$
 where (IV-1)

But

$$I_{\text{meas}} = (\frac{5}{4}) \frac{E_s}{R_v} \text{ and } I_{\text{offset}} = \frac{R_f \cdot E_{\text{in}}}{R_{\text{in}} R_i}$$
 (IV-3)

where $E_{in} = 5.000$ V, and the factor (5/4) results from the voltage divider at the output of the circuit. Since $E_{cell} = E_{in} \cdot F$ where F is the pulse height multiplier determined by the voltage divider in the pulse amplitude control module, we then have

$$G_{cell} = \left(\frac{4E_{s}}{5R_{v}} - \frac{R_{f}E_{in}}{R_{in}R_{i}}\right) \frac{1}{FE_{in}}$$

$$= \frac{1}{F} \left(\frac{4E_{s}}{5E_{in}R_{v}} - \frac{R_{f}}{R_{in}R_{i}}\right).$$
(IV-4)

Obviously, for a given conductance, a number of circuit settings could be chosen which would yield a signal within the range of the ADC. Since estimates of the uncertainties of each component in the above equation are known, it is possible to calculate the error in the measured conductance for each different instrument setting and various values of E_S . A computer program was written to perform this task, and the results indicated that maximum accuracy could be attained at maximum pulse height, maximum feedback resistance in the current follower, maximum offset, and maximum E_S .

Based on these rules, an algorithm was built into the preliminary routine which maximizes resolution and accuracy by increasing the pulse height to its maximum value (<5 V) and if necessary the current follower gain until the ADC overranges. Current offset is then applied until the ADC is back on scale, thus providing the MSB's of the analog-to-digital conversion. This process is carried out at each of the four pulse widths and the circuit parameters for each are stored for later use. If the circuit parameters cannot be optimized, the appropriate error messages are output to the console device. These optimization rules are also used in the data acquisition routines at run time to maintain the instrument response within the range of the ADC. If, in the data acquisition routine, the ADC is found to be off-scale, an optimization routine is entered which changes the circuit parameters in the fastest possible manner to bring the response on-scale, and the change in the parameters is recorded in memory for the eventual calculation of G. Through the use of these algorithms, the bipolar pulse conductance system always makes the best measurement that is consistent with the quality of the components of the system.

C. PERFORMANCE

1. Scale Changes

The instrument, as initially designed, performed well over its entire range except in the regions of scale

changes. It was found to be impossible to perfectly align the pulse height, current follower gain, and offset so that there was no overlap or underlap of scales. The problem of underlap was most severe as it led to a "dead zone" in which data points were lost altogether, as the computer caused the instrument to oscillate between lower full scale and higher zero because of the area where the scales failed to meet. In addition, some non-linearity at the lowest current follower (A4) output was still present, even though additional time was allowed for cell relaxation. The problem was solved for both ends of the range of A4 by providing overlap at the upper end through the divider at the output of A4, and not allowing an A/D conversion below 0077g without a scale change. Any discontinuity occurring at the scale change was eliminated by allowing the computer to mathematically adjust the data at those points. The data acquisition routine stores parameters corresponding to the settings of the analog circuit for each measured conductance. When the data analysis routine senses a scale change, it computes and stores the difference between the value of the conductance before the scale change and the value after the scale change. This difference is then added to all subsequent measurements of conduc-It was found that the overlap combined with computer correction of data made instrumental adjustment

virtually unnecessary. Only infrequent trimming of the current follower (A4), to prevent non-linear response due to pulse asymmetry, is required.

2. Linearity and Range

Many of the operational amplifiers in the analog circuit have very fast response times and thus, a tendency to oscillate. A 56 pF capacitor prevents oscillation of the offset amplifier (A2) but causes the current follower response to become non-linear. However, since the noise band-width of the instrument is upper limited by the frequency response of the sample-and-hold module (500 kHz), the small 10 MHz oscillations of the current follower are transparent to the measurement and are allowed to occur.

The instrument was found to be linear over its entire operating range, which extends from 2.2 x 10^{-1} to 1.3 x 10^{-8} Ω^{-1} . Above 0.22 Ω^{-1} , the conductivity is so high that maximum offset is insufficient to put the conversion system on scale. Below 1.3 x 10^{-8} Ω^{-1} , conduction between the copper foil pattern through the glass epoxy printed circuit board becomes significant compared to the measured conductance.

3. Resolution and S/N

For measurements which do not involve averaging of discrete data, the resolution is limited by the conversion system, the maximum being at 8 or more offset "units" applied, yielding 16 bits of resolution. At very low conductances, less than 12 bits of conversion may be utilized with no offset applied, limiting resolution.

As can be seen in Table 3, averaging of data increases the signal-to-noise ratio to quite large values, also providing additional bits of resolution as has been pointed out (83). The region of maximum S/N occurs around $10^{-3} \, \Omega^{-1}$ where the noise on the signal (for an average of 2000 conductance data acquisitions per point) is only about 1.6 parts per million. All data represent sets of from 100 to 500 points taken at close intervals. Some measurements were limited by the stability of the standards available.

4. Accuracy

In making absolute conductance measurements a standard resistance is measured which requires the same instrumental scale settings as the conductance to be determined. Once the computer is given the true value of the standard, it can software correct any conductance measured at that scale setting since the error is constant

Table 3. Performance Characteristics.

Conductance	Number of Averages	Standard Deviation	Signal-to- Noise Ratio	Limited By
4.9 x 10 ⁻²	1	4.16 x 10 ⁻⁵	1.18 x 10 ³	Noise
4.9×10^{-2}	2000	2.17×10^{-6}	2.26 x 10 ⁴	Limit of Averaging
9.4×10^{-3}	7	1.41×10^{-5}	6.70×10^{3}	Noise
9.4 x 10	2000	3.23×10^{-8}	2.92×10^{5}	Limit of Averaging
9.9×10^{-4}	ч	1.50×10^{-7}	6.60×10^{3}	Noise
9.9×10^{-4}	2000	1.54×10^{-9}	6.40 × 10 ⁵	Stability of Standard
3.2×10^{-4}	ч	7.45×10^{-8}	4.34 x 10 ³	Noise
3.2×10^{-4}	2000	1.52×10^{-9}	2.13×10^{5}	Stability of Standard
9.9 x 10 ⁻⁵	ч	6.29×10^{-8}	1.43×10^{3}	Noise
9.9 x 10 ⁻⁵	2000	2.30×10^{-10}	4.20 x 10 ⁵	Limit of Averaging
9.9 x 10 ⁻⁶	ч	6.74×10^{-9}	1.47×10^{3}	Noise
9.9 x 10 ⁻⁶	2000	3.60×10^{-11}	2.74×10^{5}	Limit of Averaging
8.2×10^{-7}	г	1.27×10^{-9}	6.40×10^{2}	Noise
8.2×10^{-7}	2000	1.05 x 10 ⁻¹¹	7.77×10^4	Stability of Standard
9.0 x 10 ⁻⁸	1000	9.96 x 10 ⁻¹²	9.01 x 10 ³	Stability of Standard, Time Scale of Experiment

and linear within a particular scale setting. Instrumental drift was found to be an insignificant problem (less than 0.005% per day) over most of the range of operation. In the lower conductance region (less than $2 \times 10^{-7} \Omega^{-1}$) accuracy is limited by the relatively higher noise levels on the low current signals produced. In the highest conductance regions (greater than $10^{-1} \Omega^{-1}$) accuracy is limited by the relatively higher asymmetry in the lowest pulse height. Accuracy was, however, found to be predominantly a function of the series capacitance associated with the cell as can be seen from Table 4. This effect arises from pulse height asymmetry due to finite FET switching and amplifier settling times as well as the stability of the virtual ground supplied by the current follower. This stability decreases as the amount of current supplied to the summing point increases. The current reaches a maximum at the highest offset currents, corresponding to conductances of 2 x $10^{-3} \Omega^{-1}$, 2 x $10^{-4} \Omega^{-1}$, etc.

All values in Table 4 represent 30 µseconds allowed relaxation time between pulses except at 2 x 10^{-5} Ω^{-1} and 2 x 10^{-6} Ω where longer relaxation times were required to increase accuracy.

As a further test of the accuracy of the system for real conductance cells data was acquired both with the computerized instrument and with a high-quality Wheatstone

Table 4. Accuracy (in percent) for various conductance - series capacitance combinations. Allowed relaxation time is 30 $\mu seconds$ unless otherwise indicated.

	C(µF)			
$G(\Omega^{-1})$	10	5	1	
10 ⁻¹	0.17	4.4	19	
2×10^{-2}	0.0053	0.82	0.057	
10 ⁻²	0.0071	0.40	1.4	
2×10^{-3}	0.12	0.21	0.38	
10 ⁻³	0.026	0.059	0.13	
2×10^{-4}	0.074	0.38	0.15	
10-4	0.0069	0.0045	0.23	
2×10^{-5}	0.0073	0.0051	0.018	
10 ⁻⁵	0.0037	0.0012	0.28	
2×10^{-6}	0.049	0.072	0.095	
10 ⁻⁶	0.024	0.054	0.18	
2×10^{-7}	0.25	0.52	0.99	
10 ⁻⁷	0.38	0.45	0.76	

^{†9} msec between pulses.

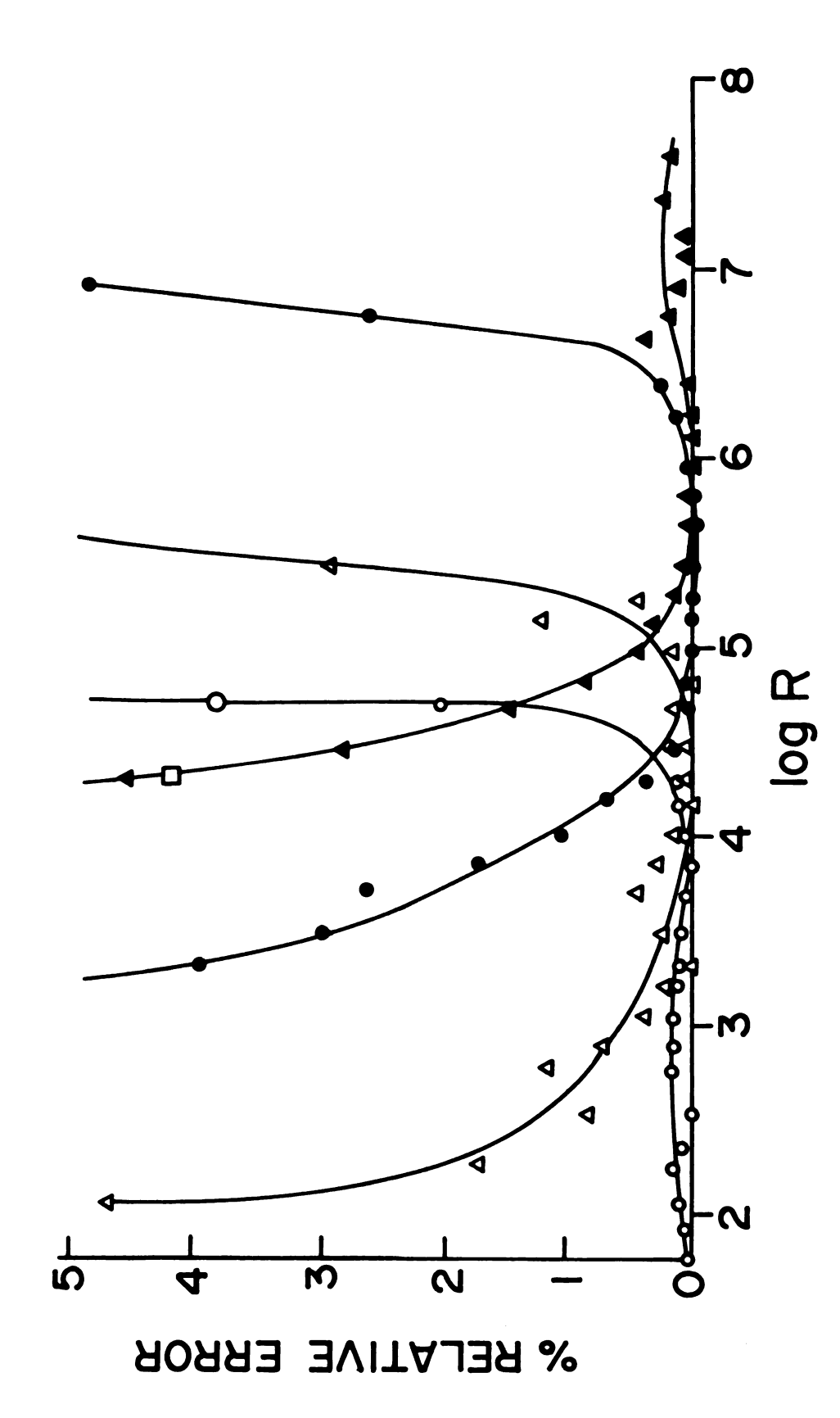
^{†30} msec between pulses.

bridge (84). Several solutions were carefully prepared from very pure fused KCl and double-distilled deionized water. The solutions which ranged in concentration from 0.1 M to 0.005 M were placed in a traditional conductivity cell and allowed to reach temperature equilibrium at 25.00 ± 0.01 °C in a thermostat (Neslab Model TV 45/250). The resistances of the solutions were determined with both instruments. The average difference in the resistances was 0.02% and in no case was the difference greater than 0.04%.

5. Pulse Width Selection

In the selection of a particular pulse width for use in a given conductance region, two factors must be considered. First, the pulse width must be short compared to the time constant of the series RC formed by the double layer and the solution resistance. Secondly, the pulse width must be long enough to allow the current follower to settle to its true output at the end of the pulsing. For low conductances the current follower gain must be increased, slowing the response of the amplifier. Thus longer pulse widths must be used at lower conductances.

A plot of percent relative error for a series capacitance of 5 μF \underline{vs} log (resistance), covering the entire operating range, was prepared and shown in Figure 24. It is seen from the plot that, for best accuracy, the



(o) PW = Percent Errors-vs-log (Resistance) at Various Pulse Widths: 01 ms; (Δ) PW = 0.1 ms; (Φ) PW = 1.0 ms; (Δ) PW = 10 ms. Figure 24.

pulse width should be chosen as follows: Above $10^{-4}~\Omega^{-1}$ (10 k Ω) the shortest PW (0.01 msec) is used, between $10^{-4}~\Omega^{-1}$ and $1.4~\times~10^{-5}~\Omega^{-1}$ (10 k Ω - 70 k Ω) the PW = 0.1 msec is used, between 1.4 x $10^{-5}~\Omega^{-1}$ and 1.4 x $10^{-6}~\Omega^{-1}$ (70 k Ω - 700 k Ω) the PW = 1.0 msec is used, and between 1.4 x $10^{-6}~\Omega^{-1}$ and the lower conductance end (700 k Ω = 80 M Ω), the PW = 10.0 msec is used. Similar curves were prepared for other series capacitances. The curves are all in approximate agreement with the data of Figure 24 with regard to the proper choice of pulse width for a particular solution conductance. The system was applied to two illustrative chemical studies, the results of which follow below.

D. DEHYDRATION OF CARBON DIOXIDE

Because of the role which carbon dioxide plays in all life processes, its reactions are among the most important and the most extensively studied in all of chemistry (85). Of particular interest is the dehydration of carbonic acid which is shown in Equation (IV-5)

$$\begin{array}{c}
k \\
\text{H}_2\text{CO}_3(\text{ag}) \xrightarrow{\text{H}_2\text{O} + \text{CO}_2(\text{ag})}
\end{array} (IV-5)$$

The reaction as usually studied is initiated by mixing: HCO_3^- and H^+ to form carbonic acid as shown in Equation (IV-6)

$$H_{(aq)}^{+} + HCO_{3(aq)}^{-} + H_{2}^{CO_{3(aq)}}$$
 (IV-6)

The progress of the dehydration reaction has been investigated by a host of techniques including thermal methods (86-88), optical methods (37,89-91), pH detection (92,93), quenching methods (94), tonometry (91), and conductometry (continuous flow) (93). Reaction IV-6 is extremely rapid with a rate constant of 10^8 s⁻¹ (95), but the dehydration reaction follows a time course which is in the stoppedflow time scale. This reaction presents an excellent opportunity to demonstrate the capabilities of the bipolar pulse conductance technique for studying moderately rapid reactions in solution.

The rate law expression for reaction (IV-5) has been developed by Brinkman, Margaria, and Roughton (91) and has the following form:

$$\left(1 + \frac{K}{[HCO_3^-]_{ex}}\right) \ln [H^+] + \left(1 - \frac{K}{[HCO_3^-]_{ex}}\right)$$

$$\ln [HCO_3^-]_{tot} = kt + C \qquad (IV-7)$$

where K is the equilibrium constant for reaction (IV-6) [HCO₃]_{ex} is the amount of bicarbonate in excess of the stoichiometric amount which is required to react with the acid, and C is a constant of integration. Saal (93) has derived a form of this equation for conductometric

detection which is:

$$\left(1 + \frac{K}{[HCO_3^-]_{ex}}\right) \ln \delta_t + \left(1 - \frac{K}{[HCO_3^-]_{ex}}\right)$$

$$\ln \left(\frac{[HCO_3^-]_{ex}}{\beta}\right) + \delta_t = kt + c' \qquad (IV-8)$$

where

$$\delta_{t} = \frac{G_{t} - G_{\infty}}{G^{\infty}}$$
 (IV-9)

$$= \frac{1000 \text{ G}_{\infty} \text{ K}}{\lambda_{\text{HCO}_3} - + \lambda_{\text{H}^+}}$$
 (IV-10)

and C' = C + ln . The other symbols have their usual significance: G is conductance; κ is the cell constant; and λ is the equivalent ionic conductance of the ion of interest.

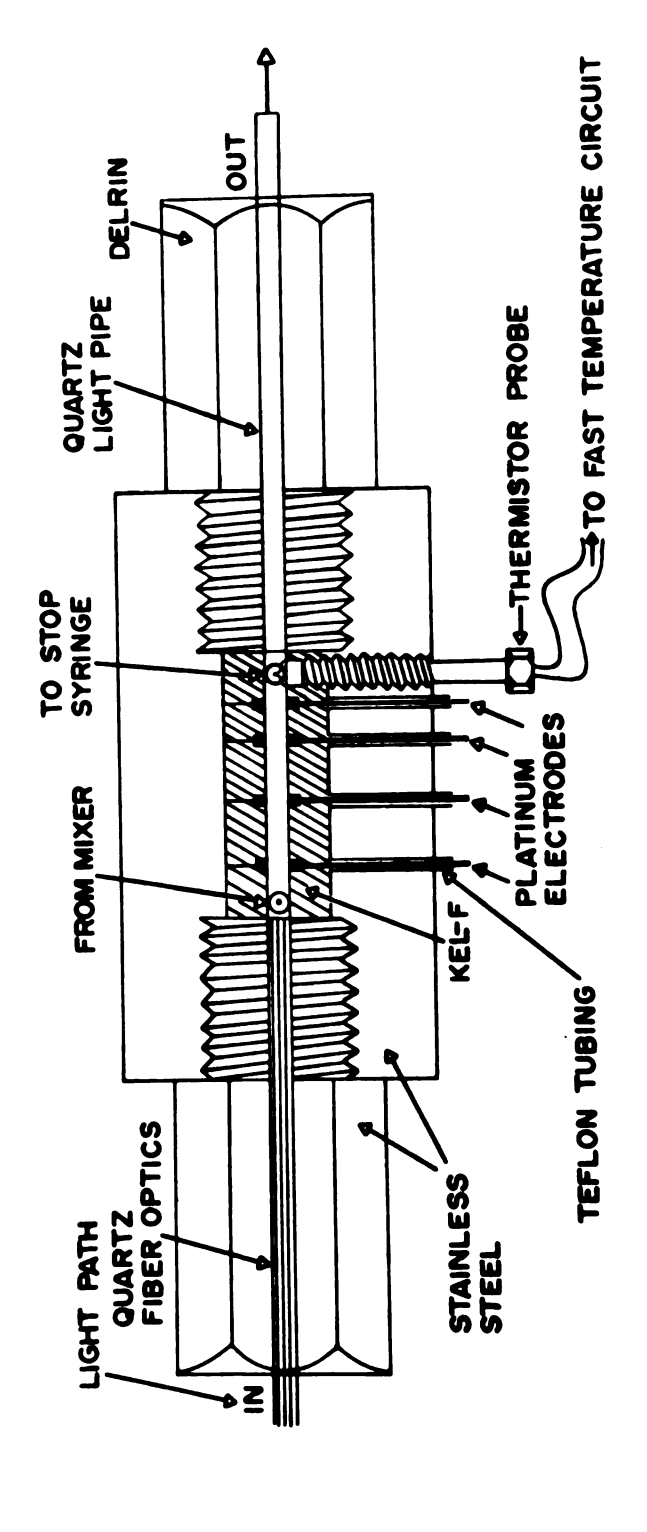
1. Experimental

A stock solution of hydrochloric acid was prepared from double distilled deionized water and was standardized against primary standard sodium carbonate. The concentration of the solution was found to be 0.0857 M. Reagent grade sodium bicarbonate was purified by recrystallization from double distilled-deionized water saturated with carbon dioxide (96). A solution 0.200 M in sodium

bicarbonate was then prepared. These solutions were used for all of the carbonic acid kinetics experiments.

The stopped-flow mixing systems developed by Beckwith and Crouch (43) was used with the following modification. Since the cell of the stopped-flow unit had no provision for conductometric detection or for thermal detection, the observation cell shown in Figure 25 was constructed and installed in the instrument. The cell is somewhat different from conductometric cells described by others (97-99) in that it supports electrical conductance, optical absorbance and thermal detection systems. conductance electrodes are torus-shaped and were formed by sandwiching platinum disks between the blocks of Kel-F (100) shown in the figure and drilling the 2 mm horizontal flow channel through the entire assembly. The observation cell is sealed at each end by the light pipes, and the Kel-F blocks are sealed by the pressure applied from each end by the two threaded pieces which also contain the light pipes. The electrode configuration was arranged so as to provide several different possible cell constants, but in practice the center two electrodes are usually used with the outer two available for use as guards.

The thermistor probe was constructed from a fast $(\tau = 7 \text{ ms})$ bead-in-glass thermistor (47) and was connected to the fast temperature circuit via a shielded, 2 conductor cable. The optical detection system of the



}

Multidetector Observation Cell for the Stopped-flow Module. Figure 25.

stopped-flow unit has been described elsewhere (101). The flow system has a dead time of ca. 3.5 ms (2).

The sodium bicarbonate and hydrochloric acid solutions were mixed rapidly in the stopped-flow module, and at or near the time of the stop, data acquisition was initiated by a signal from an opto-interruptor module affixed to the stopping mechanism (101). The averaged data were acquired and processed and the resulting plots of G-vs-time were displayed on the graphics display device. A sample data set is illustrated in Figure 26.

The choice of the interval over which the data was to be analyzed and the interval which was averaged to determine G value were chosen interactively from the terminal and the analysis of the data was initiated.

The slopes, intercepts, standard deviations, and correlation coefficients for the linear least squares analyses were then presented on the display device. Three experimental runs were made at each of five different temperatures. Temperature control was provided by a Neslab TV 45/250 constant temperature bath. Since, as we have shown elsewhere (73), the temperature in the stoppedflow module does not change appreciably over the ∿300 ms after the stop, no temperature compensation was necessary.

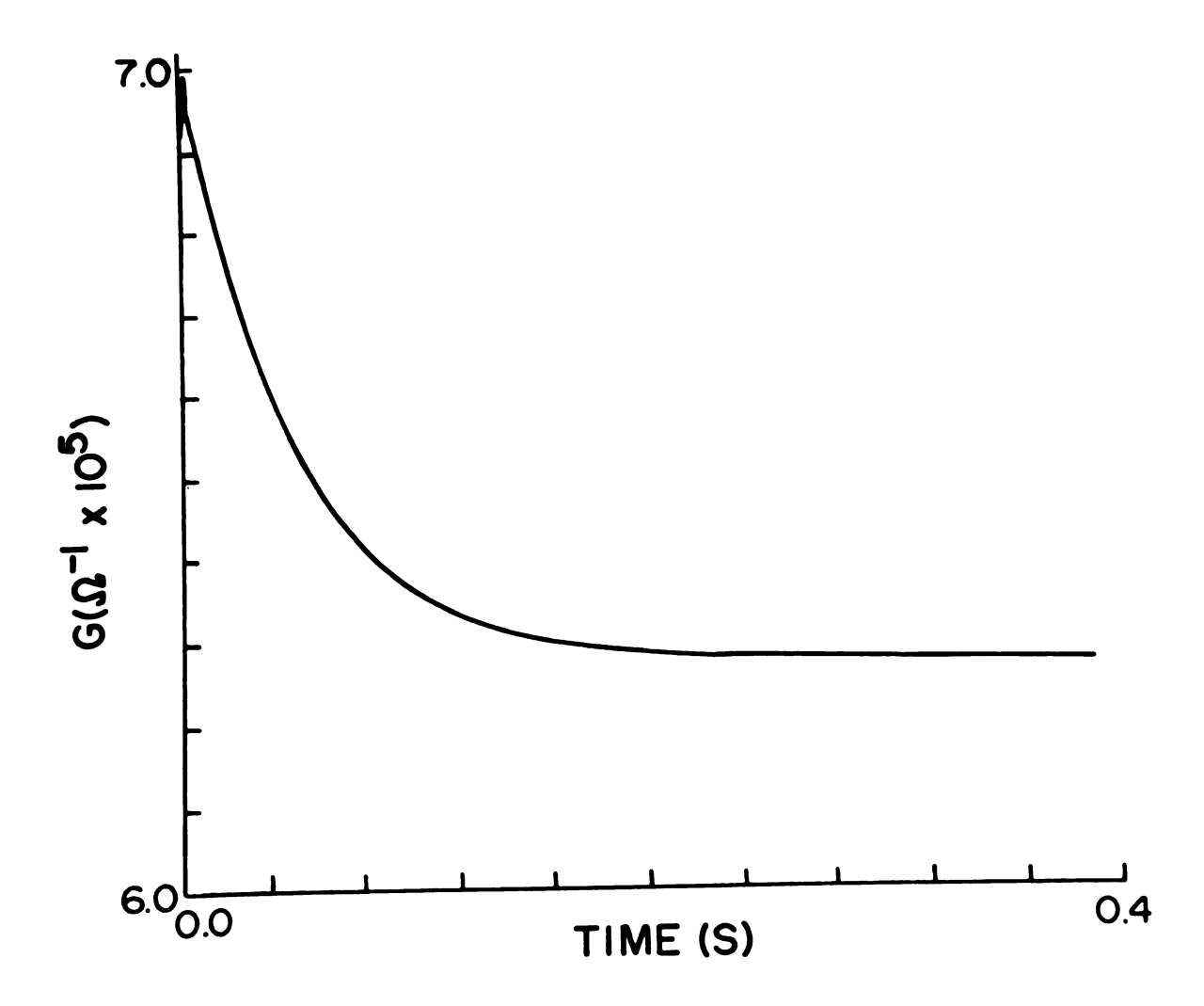


Figure 26. Reaction Curve for the Dehydration of Carbonic Acid by Conductometric Detection.

2. Results and Discussion

The first order rate constants determined at the five different temperatures are presented in Table 5. These data may be compared to the results of Berger (87) obtained by thermal and photometric stopped-flow techniques, the data of Roughton (86) resulting from continuous flow experiments with thermal detection, and the results of Dalziel (89) determined by continuous flow with photometric detection. These data along with the data from the present work are illustrated in Figure 27 in the form of an Arrhenius-type plot of ln k-vs-T⁻¹.

The values of ℓ n k from this work are seen to lie on or very close to the best fit line through all of the data points. The activation energy, E_a , resulting from a weighted linear least squares regression analysis of the composite curve is 15.32 ± 0.16 Kcal mol^{-1} , and E_a determined from the data which we have presented is 15.13 ± 0.18 Kcal mol^{-1} . The two slopes are essentially equal at the 95% confidence level. The precision of the rate constants was excellent as is shown in Table 3, and the linear correlation coefficients of the rate law regression equations were 0.999 or better in all cases.

Table 5. Calculated Rate Constants for the Dehydration of Carbonic Acid.

Temperature °C	k(s ⁻¹)	%RSD	
33.2	43.0	2.5	
29.2	33.0	1.5	
24.1	22.0	1.7	
19.0	14.3	2.0	
16.0	10.4	0.9	

Regression Equation for $\ln k - vs - T^{-1}$: $\ln k = [-7.61(\pm 0.09) \times 10^3]T^{-1} + 28.7 (\pm 0.3), r = 0.9994.$

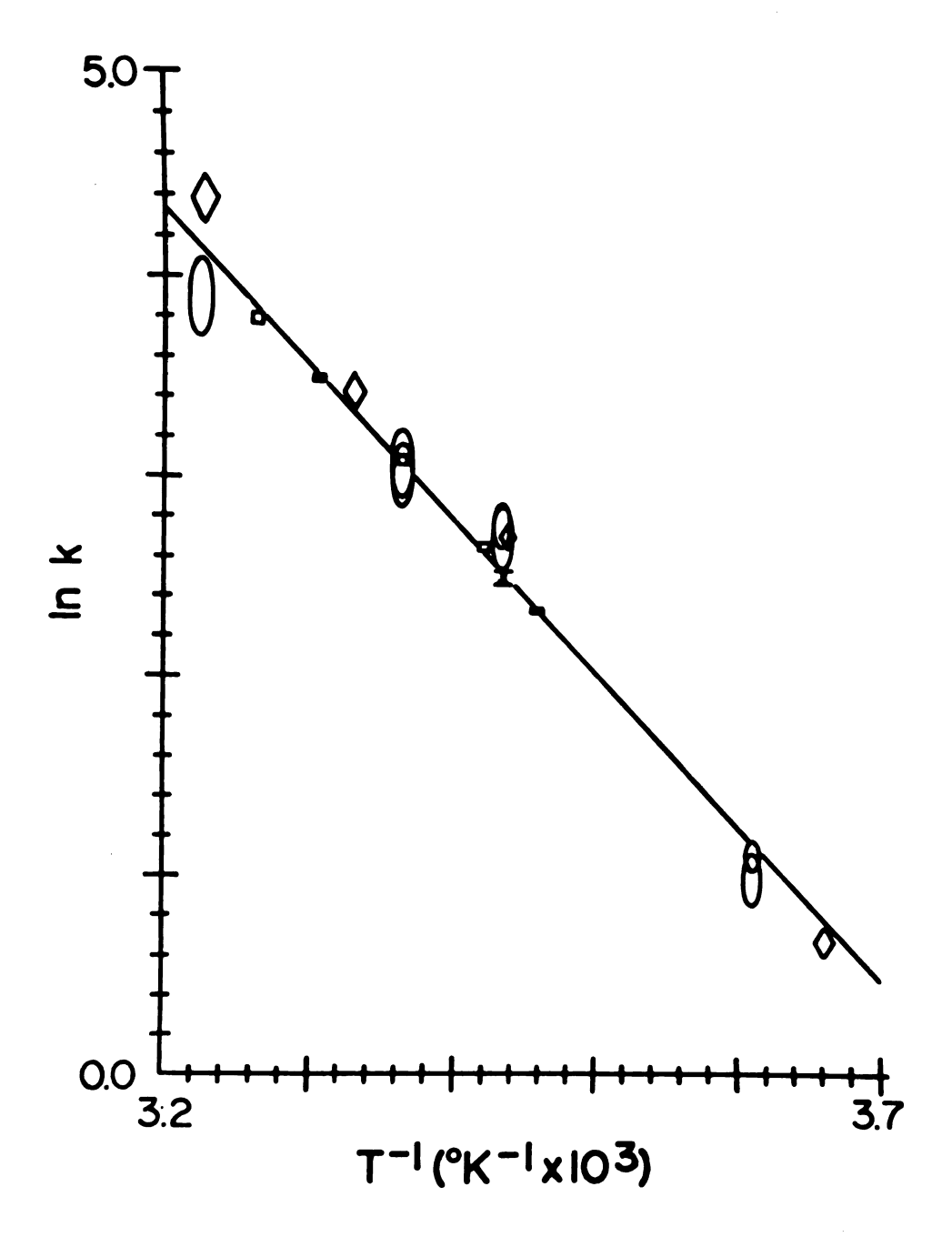


Figure 27. Arrhenius Plot of Rate Constants Obtained at Various Temperatures by Conductometry () and by Other Methods: () Roughton (86), Thermal; (o) Berger (87), thermal and photometric; (I) Dalziel (89), photometric.

E. TEMPERATURE COMPENSATION AND THE REACTION OF NITRO-

As we have suggested elsewhere (73) (see Chapter II) temperature effects may be particularly important in stopped-flow mixing systems when the time course of the reaction is comparable to the time constant of the return of the observation cell to thermal equilibrium following the temperature change which often occurs during the push. This is especially true of conductometric detection since the conductance of an electrolyte solution may change by 1-3% per degree change in the temperature. A number of electronic schemes have been suggested (75,102) for correcting conductivity measurements for temperature changes.

The computerized conductance instrument with the capability of simultaneously acquiring precise temperature data provides a unique opportunity for numerical correction of conductivity data.

The procedure for numerically correcting measured conductance requires knowledge of the temperature-conductance behavior of the chemical system of interest.

This is easily obtained by systematically varying the temperature of the reaction vessel (observation cell in the stopped-flow module) while simultaneously measuring the conductance and temperature of the reactant mixture as a function of time. The timed data acquisition program

discussed in the instrumental section forms the basis for this type of study.

Once the G-vs-T data have been acquired they are written into a data file on the disk. A special program is then called which performs a least squares polynomial curve fit on the data and stores the resulting coefficients in a file which may subsequently be read by other analysis programs. The temperature conductance curves are seldom very complex over a reasonably narrow temperature range, and they may often be fit with a first order equation. The fits are generally good to 0.05% of the measured conductance and are often good to better than 0.01% over narrow temperature ranges. Once the coefficients are obtained, all subsequent reactions in the same ionic medium may then be corrected by the analysis programs.

The temperature compensation process may be illustrated by the study of the reaction of nitromethane with base as shown in Equation IV-11.

$$CH_3NO_3 + OH^- \rightarrow CH_2NO_2 + H_2O$$
 (IV-11)

The reaction may be conveniently carried out under pseudofirst order conditions in excess base such that the time course of the reaction is <u>ca</u>. 40-60 s. This is about the same time scale as that of the thermal changes in our stopped-flow system (73).

1. Experimental

A standard solution of NaOH in double distilled deionized water was prepared and standardized against
primary standard KHP. The concentration was found to be
7.71 x 10⁻³ M. A solution 0.1 M in CH₃NO₂ was prepared
from spectroquality nitromethane (Aldrich) and diluted to
ca. 10⁻⁴ M. The solutions were combined and allowed to
react in the stopped-flow observation cell. The temperature of the thermostat was varied over ca. 10 K range, and
the conductance and temperature were measured at 300
discrete points during the temperature change. The
resulting data is shown in curve A of Figure 28. The curve
was fitted to a cubic equation, and the residuals for the
fit were all found to be less than ±0.05%.

Subsequent reactions with the same reactant solutions were carried out, and each measured conductance was corrected by using the coefficients from the curve fit, the measured temperature at each value of the conductance, and a standard temperature (usually the temperature over the first 100-300 ms of the reaction or the final equilibrium temperature) chosen interactively from the graphics terminal.

2. Results and Discussion

The success of the curve fitting technique may be illustrated by considering curve B in Figure 28. In this

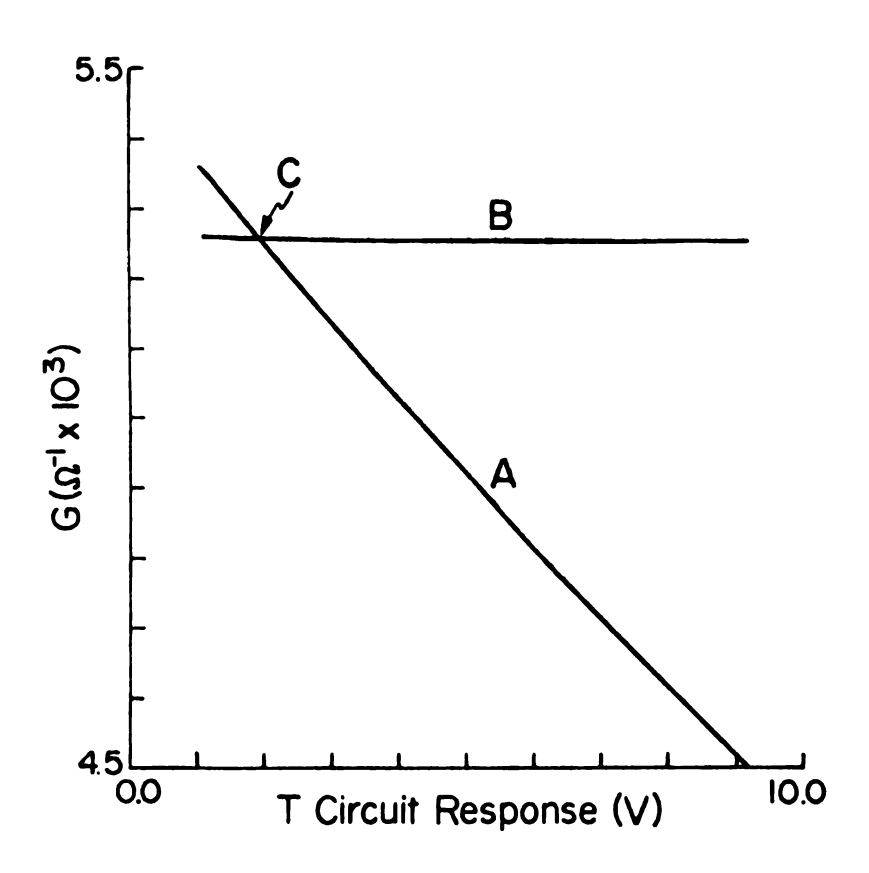


Figure 28. Conductance-vs-Temperature Circuit Response for a Mixture of 5 x 10^{-5} M NItromethane and 3.36×10^{-3} M OH.

ments were corrected was the temperature of the mixture when the conductance had the value of the crossover point (point C) of the two curves. Thus a correction performed on the complete data set should give a horizontal line passing through the point. As curve B shows the corrected conductance is constant to within ±0.1% of the measured conductance.

Figure 29 shows the result of a stopped-flow kinetics experiment on the same nitromethane system carried out at 25.0°C. The upper curve is the uncorrected conductance displayed as a function of time, and the lower is the conductance corrected for temperature changes which occurred during the progress of the reaction.

A number of interesting results may be obtained from these curves. Pseudo-first order rate constants calculated from a regression analysis of $\ln(G-G_{\infty})$ -vs-t for the two curves yield values of $7.36 \times 10^{-2} \text{s}^{-1}$ for the raw data and $7.72 \times 10^{-2} \text{s}^{-1}$ for the temperature corrected data. Since the concentration of base is known, the second order rate constant under these conditions may be computed from the expression: $k_2 = k_1[\text{OH}^-]$. This calculation yields values of 19.0 ℓ mol⁻¹s⁻¹ and 19.9 ℓ mol⁻¹s⁻¹ for the uncorrected and corrected rate constants respectively; the difference being 4.6%. Both values are in reasonable accord with the value of 27.1

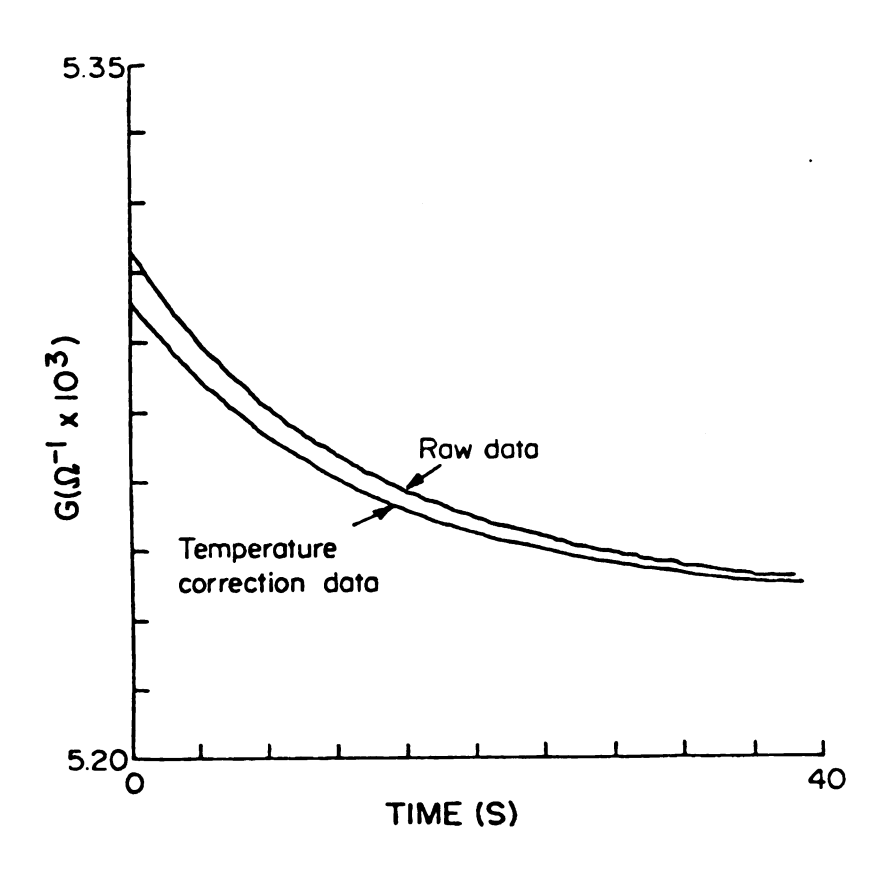


Figure 29. Conductometric Curve Showing the Progress of the Reaction of Nitromethane with Base.

\$\lambda\$ mol^{-1}s^{-1}\$ obtained by Knipe, et al. (24) under somewhat different conditions, the value of 26.4 obtained by McLean and Tranter (23), the value of 27.6 found by Bell and Goodall (25) by a pH-stat method, and the value of 17.1 obtained both by an amperometric method (106) and by a high frequency method (107).

In addition, recent results by Campbell et al. (108) by constant rate titrimetry yield values of 18.3, 21.7, and 35.6 at three different concentrations of nitromethane. The dependence of the rate constants on the concentration suggests that the reaction is probably not strictly pseudo-first order, and it is therefore not possible to assess which of the curves of Figure 29 is more accurate. However, it is clear that a critical study of such reactions via the stopped-flow conductance technique will require correction of the data for temperature errors.

An important comparison may be made of the initial rates as determined from the uncorrected and corrected curves. This is especially pertinent if conductometric detection is to be used in reaction rate methods for the measurement of <u>initial</u> rates. An analysis of the curves in Figure 29 shows the ratio of the initial rates to be 1.3. This is reasonable when it is realized that the temperature change inside the cell is changing at its maximum rate at this time as well (73) (see Chapter II).

F. CONCLUSION

A computerized-bipolar pulse conductivity instrument has been described. The instrument has been shown to possess high speed, high precision, high accuracy, wide dynamic range, and good versatility in the investigation of chemical reactions which involve a change in conductance over the course of the reaction. In addition to its application to chemical kinetics, the instrument should provide an excellent detection system for conductometric titrations, liquid chromatography, and other conductometric techniques.

CHAPTER V

PRECISION STEPPING MOTOR DRIVEN BURETS FOR AUTOMATED CHEMICAL ANALYSIS

A. INTRODUCTION

One of the most difficult problems in the automation of wet chemical analyses is the automatic delivery or preparation of reagents. A number of schemes have been reported for accomplishing this task (109-114). Renoe, et al. (109) have introduced a computer-controlled weight based solution handling system which utilizes an electronic weight sensor to measure quantities of solutions delivered. This system has the advantage of providing feedback to the computer as to the actual amount of solution delivered, but the system has a rather narrow range (10 q total with ± 1 mg error).

Mieling et al. (110), have developed a solution preparation module which delivers reagents via a timed peristaltic pump. The pump was calibrated and found to have good long term stability (0.14%). Although the system overcame some of the mechanical problems of syringe-based systems, it lacks precision (1% at 1 ml and 0.5% at 11 ml).

The syringe based system of Deming and Pardue (111) achieved good success in preparing and delivering

solutions over a rather narrow range of dilution (80:1 with 0.1% precision). Mechanical problems in the linkage between the stepping motors and the micrometer syringes detracted from the utility of the system.

Others have achieved reasonable success with syringe and stepping motor based systems (112-114), but some, particularly the commercial automatic burets, suffer from unacceptable precision, high initial cost (115), and costly and/or inaccessible replacement parts.

The purpose of this work was to design and construct an automated buret that would eliminate some of these problems. Two different burets which are pictured in Figure 30 were designed and constructed and are described in detail below.

B. MACRO-BURET

1. Details of Design

It was desirable to have a large buret which could be used for delivering relatively large solution volumes with high accuracy and precision. The design goals included: (1) simplified construction and machining; (2) easily and inexpensively replaceable parts; (3) easy attachment to other components of the delivery system; and (4) accuracy and precision comparable to "Class A" volumetric glassware. The macro-buret which was designed

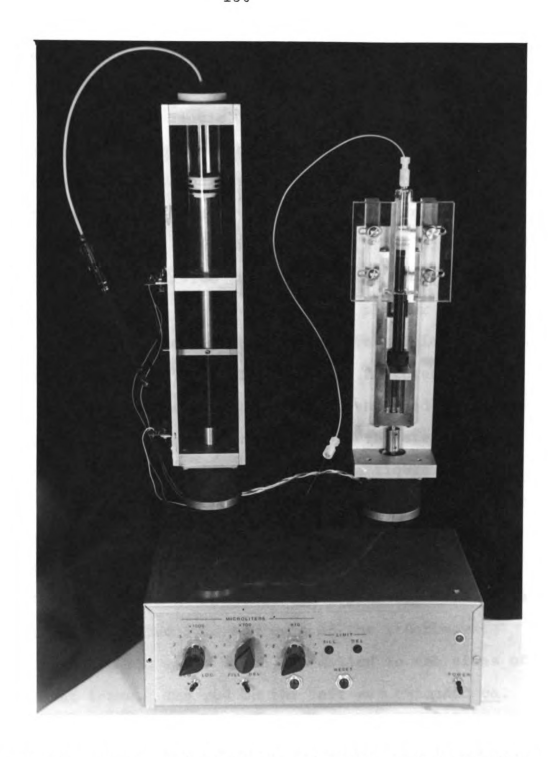


Figure 30. Photograph of Automated Burets and Controller.

to meet these goals is shown on the left side of the photo of Figure 30, and the mechanical details of the buret are illustrated in Figure 31. The design is similar in some ways to that of Megargle and Marshall (112), but possesses some characteristics which make it more useful.

The volumetric delivery of fluids is carried out by the teflon plunger shown in the figure. The plunger is moved up and down inside the glass sleeve made of heavywall precision bore glass tubing. The plunger is linked to the stepping-motor by the aluminum tube which is threaded approximately 1½" into its top (½ x 20 threads). The tube is mated with a length of ½ x 20 threaded stainless steel rod that is in turn connected to the stepping motor via the brass collar shown in the figure. The rotary motion of the motor is translated into the linear motion of the plunger by this arrangement.

Rotary motion of the aluminum tube is prevented by the T-shaped rider attached to the top of the tube. The small rods threaded into the ends of the rider move vertically in the slots which are milled in the sides of the buret frame. The rod on the left was extended <u>ca</u>.

0.5" to the left, and its diameter was reduced to 0.1" so that it could serve as the limit flag for the opto-interruptor modules which are installed near the extrema of travel of the rider. When the rod breaks the light beam of the opto-interruptor (see Chapter VI), a TTL

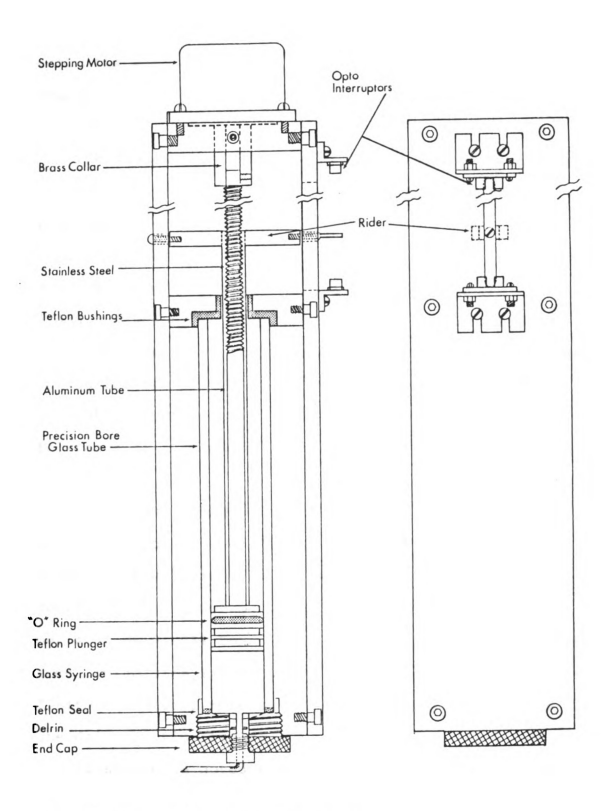


Figure 31. Detail of Macro-Buret.

signal is sent to the stepper motor controller that prevents additional pulses from being sent to the motor until the motor direction is reversed. This prevents damage to the buret due to driving the plunger beyond its maximum travel.

The diameter of the precision-bore glass tubing and the thread size for the drive screw were chosen to provide convenience in selecting multiples or fractions of 1 ml. The glass tubing was 2.2377 ± 0.0005 cm in diaeter which corresponds to a cross-sectional area of 3.933 ± 0.002 cm². Twenty revolutions of the stepping motor provide 1.0000 ± 0.0005" (2.540±0.0013 cm) of linear motion for the plunger. This corresponds to a volume of 9.989 ± 0.005 ml. This value is well within the tolerance of a "Class A" 10 ml transfer pipet which is 10.00 ± 0.02 ml.

The volume resolution of the buret is determined by the resolution of the stepping motor (117) which is 200 steps per revolution $\pm 3\%$ per step noncumulative. This corresponds to a volume resolution of 2.50 \pm 0.08 μ l per step or 0.005% for a full 50 ml delivery. In practice some imprecision is introduced by temperature changes, finite mechanical tolerances, and irreproducibility in the delivery tip itself.

It should be noted that the knurled end cap of the buret which holds the glass tube in place is threaded

to mate to the popular { x 28 high pressure liquid chromatography (HPLC) fittings. This is to provide versatility in connecting the buret to valves, teflon tubing, and other useful fittings.

2. Performance

The performance of the macro-buret was evaluated by weighing consecutively delivered portions of water in a stoppered flask and computing the volume from the density of water at its measured temperature.

This was done for both 10 ml and 1 ml portions to assess the accuracy, precision and the linearity along the bore of the tubing. Three sets of experiments were performed for the 10 ml increments and four sets were carried out for the 1 ml increments. The results are shown in Tables 6 and 7.

As Table 6 shows, the precision of delivery for any of the four tested 10 ml increments is much better than the ± 0.02 ml tolerance of "Class A" glassware. The precision of consecutive 10 ml deliveries is only slightly worse, less than 0.006 ml in all three trials. The overall standard deviation is 0.004 ml.

For the 1 ml increments four sets of experiments were performed, and the results are presented in Table

7. In only one of the five consecutive increments is the precision greater than 0.0012 ml, the overall standard

Buret Delivery Accuracy and Precision Ten Millimeter Increments. Table 6.

		Increment Number	Number			
Trial	1	2	3	4	Mean	S.D.
1	9.9947	10.0022	10.0035	10.001	9000.01	0.004
7	9.9987	10.0040	10.0057	10.9042	10.0032	0.003
m	9.9921	10.0034	10.0045	10.0033	10.0008	0.0059
Mean	9.9952	10.0032	10.0046	10.0032		
S.D.	0.0033	6000.0	0.0011	0.0010		

Overall mean 10.001 S.D. 0.004

Buret Delivery Accuracy and Precision - One Milliliter Increments. Table 7.

		Incr	ncrement Number	er.			
Trial	1	2	3	4	5	Mean	S.D.
н	0.9984	0.9961	0.9978	0.9981	0.9978	0.9976	0.0009
8		9666.0	0.9983	0.9969	0.9985	0.9983	0.0011
က	0.9982	0.9962	0.9992	0.9988	0.9994	0.9984	0.0013
4	0.9962	0.9993	0.9998	0.9991	0.9998	0.9988	0.0015
Mean	0.9976	0.9978	0.9988	0.9982	0.9989		
S.D.	0.0012	0.0019	0.00089	0.0000	6000.0		

Overall mean 0.9983 S.D. 0.0012

deviation for all of the 1 ml increments. The linearity along the tube for the 1 ml increments is equally good. These values compare very favorably with the "Class A" criterion of ± 0.006 ml for a 1 ml pipet.

This buret has several advantages over commercial burets of similar size. First, it is relatively inexpensive. The raw materials for the buret itself were approximately ten dollars. The design is very simple and requires a minimum of machining time. The most expensive parts are the stepping motor (\sim \$60.00) and the driver electronics and power supply (\sim \$150.00). These items are general purpose pieces of equipment, and may be used for other kinds of instrumentation.

The buret described above has been used frequently over the last 1.5 years and no mechanical instability or degradation of precision has been detected. The plunger was found to be sensitive to drastic temperature changes and tended to leak if the temperature in the laboratory dropped by 3-5°C. The installation of the O-ring seal illustrated in the figure prevented this from occurring.

C. INTERCHANGEABLE SEMI MICRO AND MICRO BURET

1. Design Considerations

In addition to the macro-buret described above, it

was desirable to have a buret that was capable of precisely delivering very small volumes of reagent and that could easily accommodate various sizes of precision bore tubes. The solution to this problem is shown on the right in the photo of Figure 30. The principles of operation are exactly the same as the macro-buret except that the translational motion is provided by a commercially available dovetail slide (118).

This design shown in some detail in Figure 32, has most of the advantages of the previous design plus the added advantage that very little machining is required. The glass portion of the buret is a gas tight syringe and may have any total volume from 100 µl to 5 ml depending on the desired delivery volume (119). A further advantage of this approach is that the syringe plungers may be purchased separately, and the syringes may be easily made from precision bore glass tubing with the HPLC fitting shown in Figure 32 sealed to the tubing by glassblowing.

2. Performance

The performance of the interchangeable buret was evaluated in much the same way as the macro-buret. The difference is that only the precision may be evaluated. Since the syringe diameter could not be chosen to give convenient values of delivered volume per revolution,

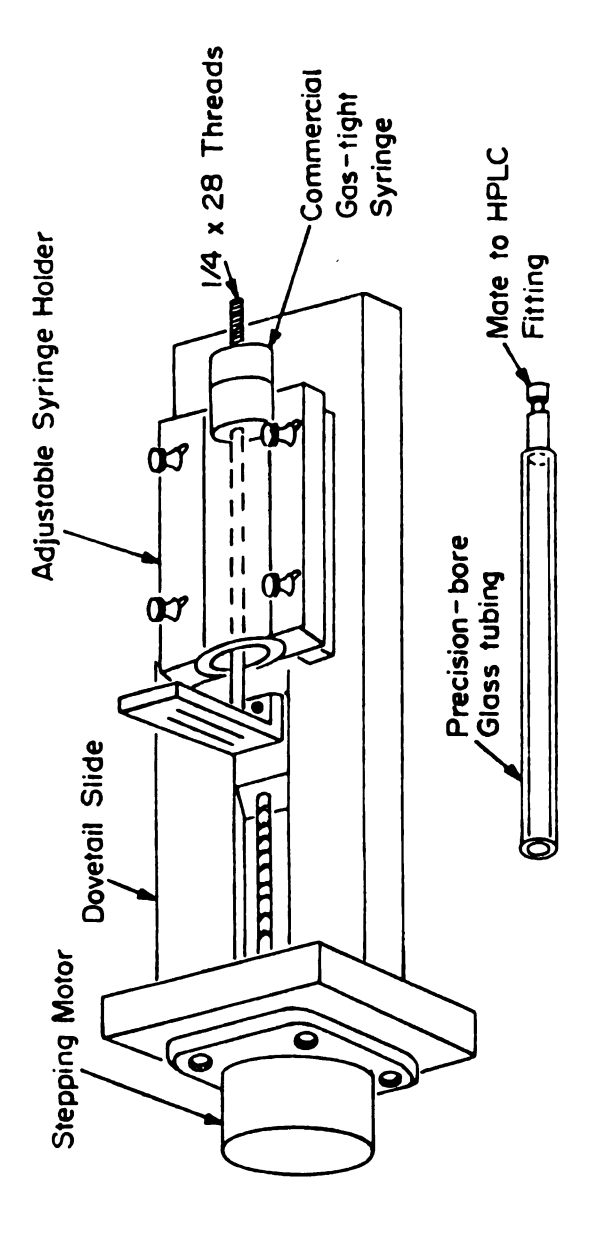


Figure 32. Detail of Interchangeable Buret.

each syringe must be calibrated. The number of steps per increment in the test was empirically chosen to give about 1 ml.

As the data in Table 8 show, the results for the interchangeable buret are much better than for the macroburet with the precision for a particular increment being no worse than 0.0006 ml (0.06%). The precision for consecutive increments was no worse than 0.0008 ml (0.08%) and the overall precision for all increments was 0.0006 ml.

Some improvement in this buret over the macro-buret is to be expected since the linear resolution of the dovetail slide is a factor of 2 better than the screw of the macro-buret. In addition, the mechanical tolerance of the dovetail lead screw is 0.0015" per foot of travel, certainly much better than that of the threaded rod of the macro buret. The two burets described above have exhibited excellent performance and should provide a versatile and economical method of automatically dispensing reagents. The macro-buret has already been successfully used in automated conductometric titrations with good results It should be noted that the stepping motor (120).controller and interface have been described in detail elsewhere (112,116,121-123). In the section below an automated solution preparation module is discussed which will utilize the two automated burets discussed here.

Table 8. Precision of Interchangeable Buret - One Milliliter Increments.

		Inc	Increment Number	ber			
Trial	1	2	3	4	5	Mean	S.D.
1	1.0056	1.0061	1.0059	1,0061	1.0060	1.0059	0.0002
7	1.0045	1.0059	1.0059	1.0062	1.0053	1.0056	0.0007
m	1.0042	1.0062	1.0059	1.0051	1.0060	1.0055	0.0008
4	1.0052	1.0058	1.0068	1.0050	1.0057	1.0057	0.0007
S	1.0050	1.0056	1.0058	1.0055	1.0055	1.0055	0.0003
Mean	1.0049	1.0059	1,0061	1.0056	1.0057		
S.D.	9000.0	0.0002	0.0004	9000.0	0.0003		

Overall mean 1.0056 S.D. 0.0006

D. SOLUTION PREPARATION SYSTEM

As was mentioned above, the automation of dilution and solution preparation tasks has been the object of much creative effort. This section describes an automated solution preparation module shown in Figure 33 which is capable of providing versatile dilutions over a wide concentration range and which can serve as the front end for stopped-flow mixing systems (see Chapter I).

1. Control and Sequencing

Even though the solution preparation step is the slow step in fundamental characterization of chemical reactions, and automation may increase the speed of preparation by at least an order of magnitude, it is still a very slow process. It is difficult to justify dedicating an expensive minicomputer with all its peripheral hardware to such a slow task. One solution to this dilemma is to utilize a foreground-background mode of operation to allow other tasks to be performed concurrently with the slow solution preparation task. Although this frees the minicomputer to some extent, the complexity of interleaving real-time tasks prevents full utilization of the CPU time.

Another possible solution to this problem is the hierarchical mini-micro computer system (110) shown in

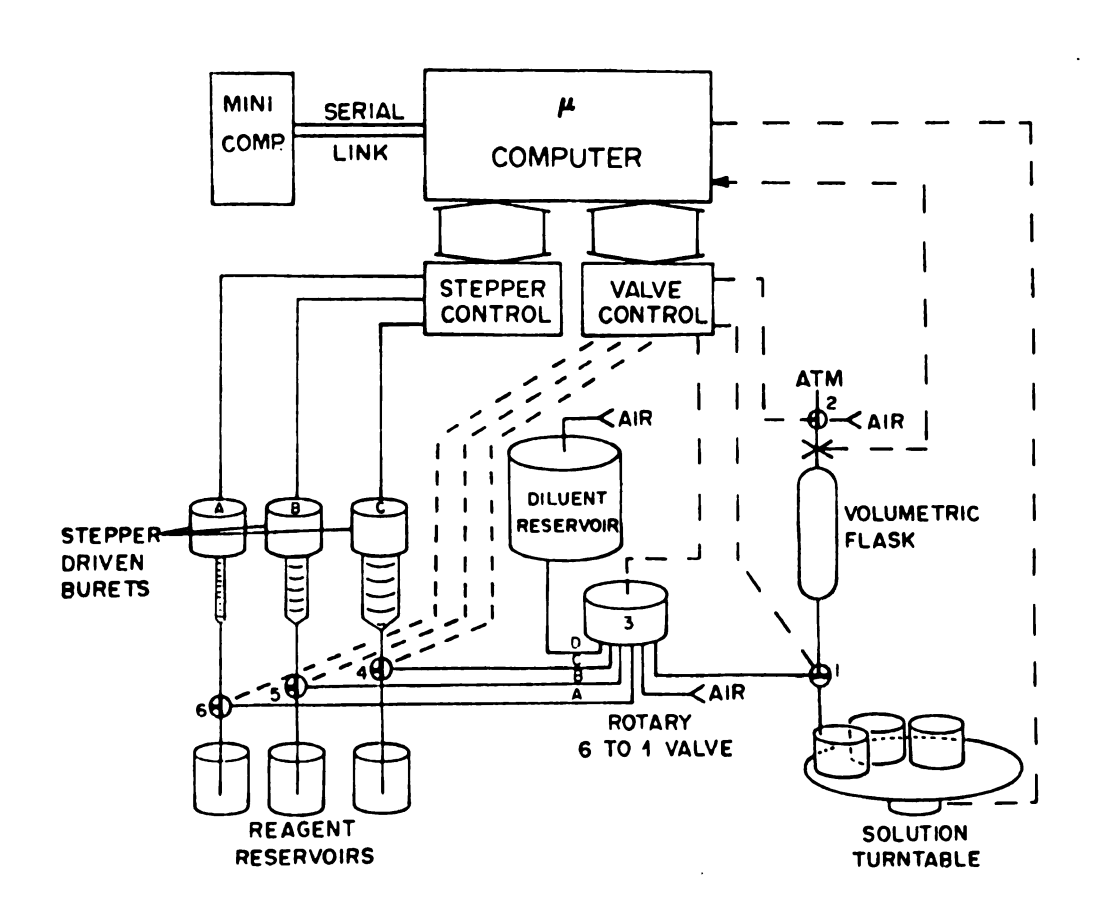


Figure 33. Automated Solution Preparation System.

Figure 33. In this arrangement a microprocessor (MPU) is connected to a minicomputer via an asynchronus link. Program development and debugging can be carried out on the minicomputer, and routines may then be loaded into the memory of the MPU via the link. The control functions of the MPU may then be carried out without wasting any minicomputer CPU time. Another advantage of this type of arrangement is that high level computations (ionic strength, dilution factors, volumes, etc.) may be carried out in the minicomputer, and then only the raw numbers need to be shipped to the MPU for its tasks. As soon as the MPU has finished the solution preparation, it can raise a flag indicating that it is ready to execute a new task. When the minicomputer finishes its current high priority task, it can check the MPU for completion, and reinitialize it with a new set of parameters.

2. System Components

The solution preparation module of Figure 33 consists of the following components. Precision delivery of reagents is carried out by the automated burets described above (A, B, and C in the figure). Each of these is connected to a reagent reservoir and the rotary 6-way valve (#3 in the figure) via the zero dead volume 3-way

HPLC valves (#4, #5, and #6).

The common channel of the 6 to 1 valve is connected through another 3-way valve (#1) to the volumetric flask and the final solution container on the turntable. Any one of the reagents or the diluent may be forced through valves #3 and #1 into the volumetric flask. When the liquid level reaches the optical sensor at the top of the flask, valve #1 may then be switched so that the solution in the flask is expelled into its container.

3. Solution Preparation

After initializing the system, which rinses the volumetric flask, fills the tubing between valve 3 and the flask with diluent, and fills the tubing between valves 4, 5 and 6 and valve 3 with appropriate reagents, the operation is as follows:

- 1. Valves 4, 5 and 6 are turned to connect the 3 burets to their corresponding reagent reservoirs.
- 2. Burets A, B, and C are loaded simultaneously with their respective reagents. The end of loading a buret is indicated when a opto-interruptor internal to the buret is broken by a flag on the buret carriage.
- 3. Rotary valve 3 is turned to position A, valve 6 to the deliver position, and a predetermined volume (number of steps of stepper motor) of reagent A is delivered.
 - 4. Rotary valve 3 is turned to position B, valve 5

to the deliver position, and a predetermined volume of reagent B is delivered.

- 5. Reagent C is delivered in a manner similar to reagents A and B.
- 6. Rotary valve 3 is turned to position D and air is used to force diluent through the line and into the volumetric flask until a level trip occurs.
- 7. Valve 1 is turned to connect the volumetric flask to the solution reservoir on the turntable, valve 2 is turned to the air position and solution is allowed to drain into the reservoir on the solution turntable.

4. System Performance

Although the solution preparation system is not complete, several components have been evaluated, and it is possible to project reasonable estimates for the precision of a dilution performed by the system. Rothman (116) investigated the precision of the volumetric flask which is to be used in this system. He found that the blowout procedure yielded a precision of delivery by the flask of $\pm 0.03\%$, well within the "Class A" criterion. In order to obtain an estimate of the range of dilutions which may be carried out with at least 0.1% precision, let us assume that we may deliver 500 μ £ from a 5 ml syringe with a relative precision of 0.1%. This is not unreasonable in light of the precision obtained for

1 ml increments of 0.06% discussed in Section C.2 above.

An estimate of the precision of the dilution $\sigma_{\mbox{dil}}{}'$ may be obtained from:

$$\sigma_{\text{dil}}^2 = \sigma_{\text{flask}}^2 + \sigma_{\text{buret}}^2$$

$$\sigma_{dil}^2 = (0.0003)^2 + (0.001)^2$$

$$\sigma_{dil} = 0.00104 \text{ or } 0.1$$
%

If we assume that the volumetric flask has a volume of 1000 ml, then the dilution ratio is 2000:1. It is hoped that the range of possible dilutions will be even greater than this value with equivalent precision for a 100 ml volumetric flask. The delivery precision for very small syringes has not yet been evaluated, and the ability of the rotary valve to shear volume elements of solution reproducibly has not been determined.

As soon as the system is completely assembled, a wide range of dilution experiments will be performed in order to assess the precision of the overall system. It is hoped that the system will become a very useful tool in the fundamental investigation of problems in solution chemistry, both as a "stand alone" solution preparation system and as a front end for stopped-flow mixing modules.

CHAPTER VI

Reprinted from ANALYTICAL CHEMISTRY, Vol. 48, Page 1429, August 1976
Copyright 1976 by the American Chemical Society and reprinted by permission of the copyright owner

Transducer for Measurement of Flow Rates in Stopped-Flow Mixing Systems

F. J. Holler, S. R. Crouch and C. G. Enke*

Department of Chemistry, Michigan State University, East Lansing, Mich. 48824

We have developed a simple method for directly determining the relative position of the syringe drive block in a stopped-flow mixing system as a function of time. This note describes the principles of the method as well as experimental results which indicate its accuracy and ease of application.

Reliable and accurate measurements of the kinematics of the drive syringes in stopped-flow mixing systems are often difficult to accomplish. The measurements are made difficult because the motion is seldom uniform over its brief duration of less than 50 ms. The information obtained in this type measurement is important for diagnosing mechanical problems in the drive mechanism and for the calculation of the mixing system dead time; that is, the time necessary for the observed mixture to flow from the point of initial contact of the reactants to the center of the observation cell (1–3), which in a properly operating system, corresponds to the age of the reaction mixture at the time of observation (4). The dead time must be known accurately in order to verify that a significant portion of the reaction in question has not occurred before observation begins.

In the system described here, a transparent rule is attached to the drive block of the stopped-flow apparatus, and an opto-interrupter module (General Electric H13B1 or Optron OPB803) is positioned so that the rule moves through the slot during the push (Figure 1a). The marks on the rule block the beam from the light emitting diode as they pass through the slot causing the photo darlington transistor switch (Figure 1b) to turn alternately off and on. When the output of the circuit is connected to a storage oscilloscope, a trace similar to that shown in Figure 2 is obtained. The rule may be any semitransparent ruling such as an inexpensive plastic centimeter rule or a Ronchi ruling (Edmund Scientific No. 30 511), both of which have been used with excellent results. The rule may be attached to the stop syringe to provide greater resolution if the bore of the stop syringe is the same as that of the drive syringes. The distance between each mark is known accurately (0.0508 cm for the ruling used to obtain Figure 2), and the times between each pair of marks may be obtained from the scope trace by noting the time of each positive and negative peak. The flow velocity may then be calculated as a function of time.

The information that may be obtained from the positiontime data plot is illustrated in Figure 2 for one of the mixing systems in our laboratory (5). The relative distance, and the velocity of the drive block are plotted as functions of time. Although the position and velocity plots may be obtained from the oscilloscope photograph by a simple graphical procedure, the curves in Figure 2 were obtained by first fitting the experimental points to a fourth-degree polynomial and then taking the first derivative of the resulting equation. We should also note that for situations in which the stopped-flow apparatus is already interfaced to a minicomputer, the data from the flow velocity transducer may be acquired by standard A/D conversion techniques, analyzed, and displayed in a form suitable for routine checks on system performance.

The plots in Figure 2 show that the flow velocity becomes constant to within a few percent about two thirds of the way through the push and that the average velocity over the last 5 ms of the push, v_{av} , is about 17 cm/s. It is necessary that v_{av} be taken over a period approximately equal to the dead time, t_d , since v_{av} should be the average velocity of the observed solution as it flows into the observation cell immediately before the stop. To calculate t_d , it is necessary to know the cross sectional area, A, of the drive syringes and the dead volume, V_d , between the point of initial contact of the solutions and the center of the observation cell $(1.22 \pm 0.02 \text{ cm}^2 \text{ and } 0.119 \pm 0.005 \text{ cm}^3 \text{ in our case})$. The dead time in this case is then $t_d = V_d/v_{av}A = 5.8 \text{ ms}$.

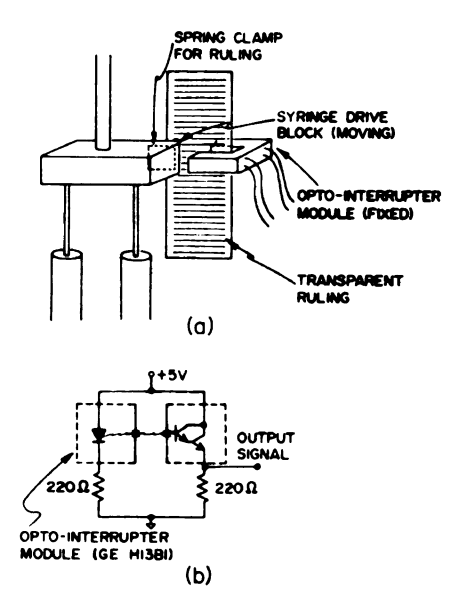


Figure 1. Displacement transducer. (a) Attachment to stopped-flow mixing system. (b) Schematic diagram

ANALYTICAL CHEMISTRY, VOL. 48, NO. 9, AUGUST 1976 . 1429

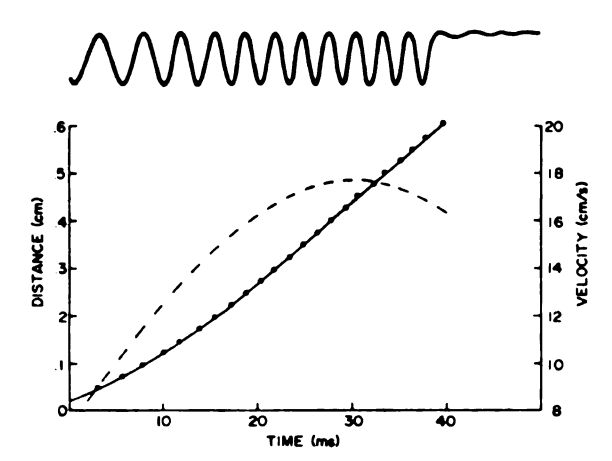


Figure 2. Upper curve: Oscilloscope trace. (@) Experimental points obtained from upper curve. (---) Fitted curve: distance vs. time. (- - -) Velocity vs. time

The most common method of determining dead times is the extrapolation method (1). It consists of carrying out a chemical reaction in a stopped-flow apparatus, recording the absorbance of the reaction mixture as a function of time, and extrapolating the resulting curve back to zero absorbance. The elapsed time between the time of zero absorbance and the stopping time of the syringes (the intersection of the extrapolated line and the experimental curve) is $t_{\rm d}$. The quantity td' includes the effects of mixing and stopping times as well as temperature, cavitation, and other artifacts which may degrade the performance of stopped-flow mixing systems. Stewart (1) has shown that t_d approaches t_d in properly operating stopped-flow systems as the reaction half life becomes long with respect to t_d .

Under conditions similar to those used to obtain the data shown in Figure 2, the extrapolation method and the flow velocity method were simultaneously used to acquire data for eight separate pushes of our stopped-flow instrument. The precision of the flow velocity method depends primarily on the precision of the measurement of the period between two peaks in the oscilloscope trace since the dimensions of the stopped-flow unit and the transducer are relatively constant during a push. Replicate determinations of the period of the last two cycles of the transducer (distance = 0.102 cm) before the stop yielded a mean value of 5.25 ± 0.09 ms (± 1 S), and thus a mean value for $v_{\rm av}$ of 19.3 \pm 0.5 cm/s. The mean dead time is then 5.08 ± 0.09 ms.

The precision of the extrapolation method of determining

td' depends on how precisely the reaction rate curve may be extrapolated to zero absorbance. The mean value of the dead time obtained by this method in the comparative study was 5.4 ± 0.4 ms. Thus the precision of the extrapolation method was ±8%, about four times worse than that of the flow velocity method.

The determinant error in the flow velocity method depends upon the accuracies of the time base of the oscilloscope, the dead volume, the ruling, and the cross sectional area of the drive syringes. By estimating tolerances for these quantities and applying the usual propagation of error procedures, we are able to calculate an upper bound of ±11% for the range of the accuracy of our method of obtaining t_d . This value could be improved by using a more accurate time standard such as a crystal controlled period meter for measuring the time between pulses of the transducer or by determining the dimensions of the stopped-flow system more accurately.

The ability to assign an upper limit to the determinant error in a dead time measurement is a definite advantage of the flow velocity method over methods requiring calibration procedures such as the initial absorbance method (1), the vane method of Gibson (6), and the potentiometer method of Chance (7). These last two techniques, however, give absolute direction and magnitude indication, and may provide higher resolution. An advantage of optical coupling is that nothing is attached to the drive mechanism of the stopped-flow apparatus that would impede its motion.

It should be emphasized that the extrapolation method and the flow velocity method are complementary diagnostic aids in the development and maintenance of stopped-flow mixing systems. A comparison of the times obtained by both methods may reveal mixing, stopping, temperature, or cavitation effects and facilitate their elimination. This flow velocity detector is extremely simple to attach to the drive system, either temporarily or permanently, and it requires only modest and common equipment for implementation.

LITERATURE CITED

- J. E. Stewart, "Durrum Application Notes No. 4", Flow Deadtime in Stopped-Flow Measurements, Durrum Instrument Corp., Palo Alto, Calif.
- J. M. Sturtevant, in "Rapid Mixing and Sampling Techniques in Biochemi Britton Chance, et al., Ed., Academic Press, New York, N.Y., 1964.
 Q. H. Gibson and L. Milines, Biochem. J., 91, 161 (1964).

- R. M. Reich, Anal. Chem., 43 (12), 85A (1971).
 P. M. Beckwith and S. R. Crouch, Anal. Chem., 44, 221 (1972).
 Q. H. Gibson, Discuss. Faraday Soc., 17, 137 (1954).
 B. Chance, J. Franklin Inst., 229, 455 (1940).

RECEIVED for review February 13, 1976. Accepted April 23. 1976. This work was supported in part by NSF Grant No. MPS75-03650.

CHAPTER VII

SOFTWARE DEVELOPMENT

A. INTRODUCTION

Basically, there are two different software sets which were developed during the course of this work: software for the operation of the pulsed thermistor circuit (3) (see Chapter III) and software for the operation of the bipolar pulse conductance instrument (53,124) (see Chapter IV). Following a brief description of the computer and operating system that were used in this work, these two software sets are briefly described. Finally, the interactive graphics package that was developed is described in some detail.

B. THE COMPUTER

The computer system that was utilized in this work is illustrated in Figure 36. It consists of a PDP 8/e minicomputer, 16K memory, RKØ5 cartridge disk, dual floppy disk, DEC writer, graphics terminal, alphanumeric terminal, and a Heath EU801E Computer Interface buffer. The combination of the cartridge disk and the floppy disk provided maximum flexibility, particularly when one of the systems was inoperable, and compatibility with other

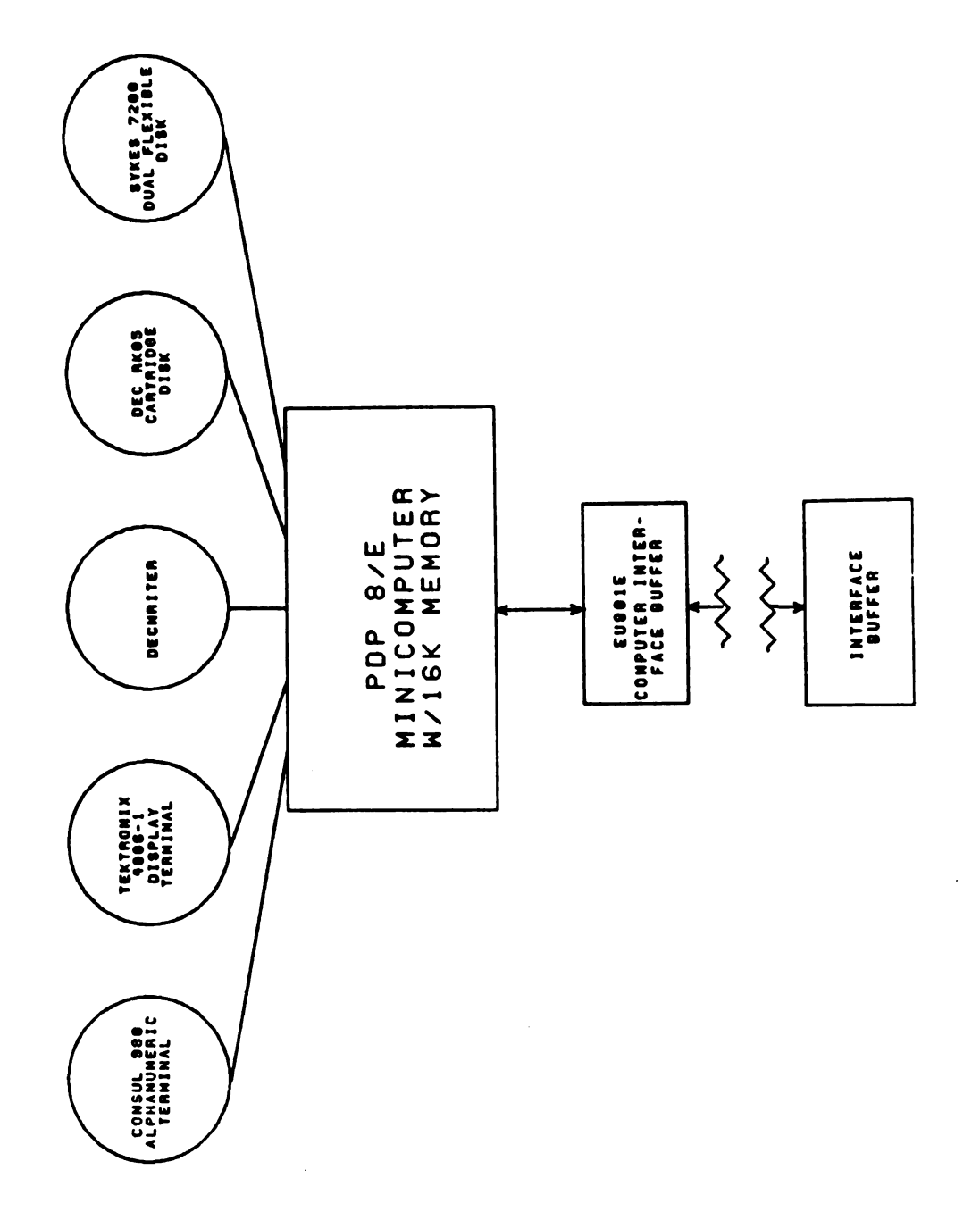


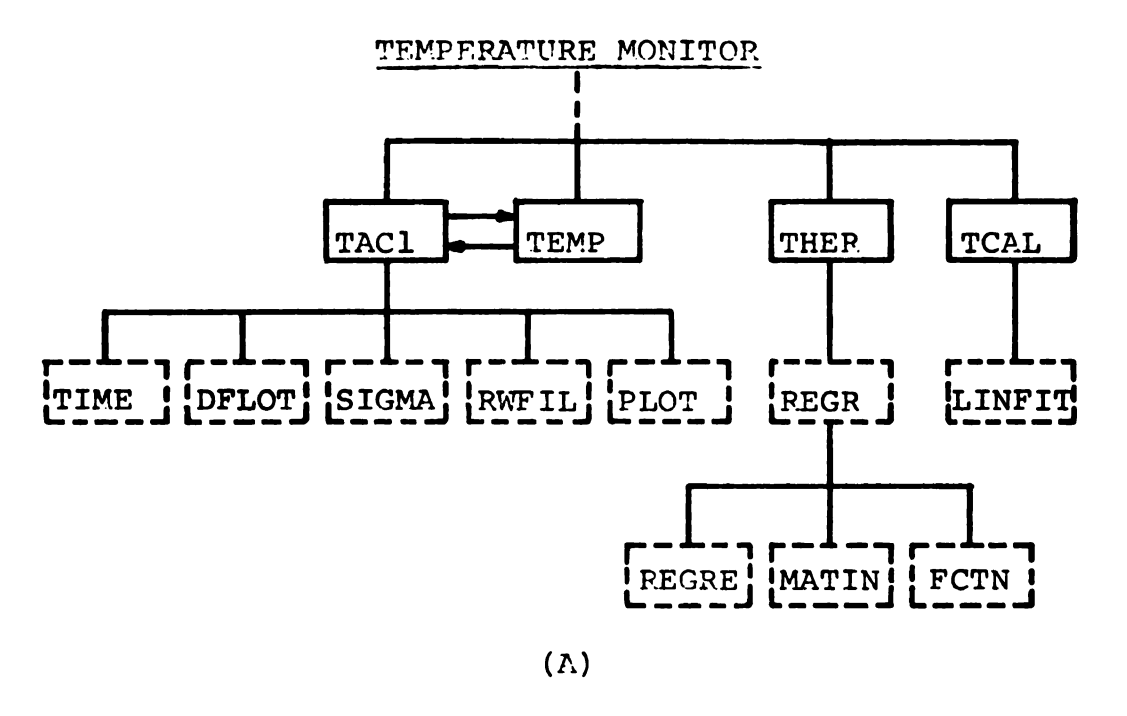
Figure 36. Block Diagram of Computer System.

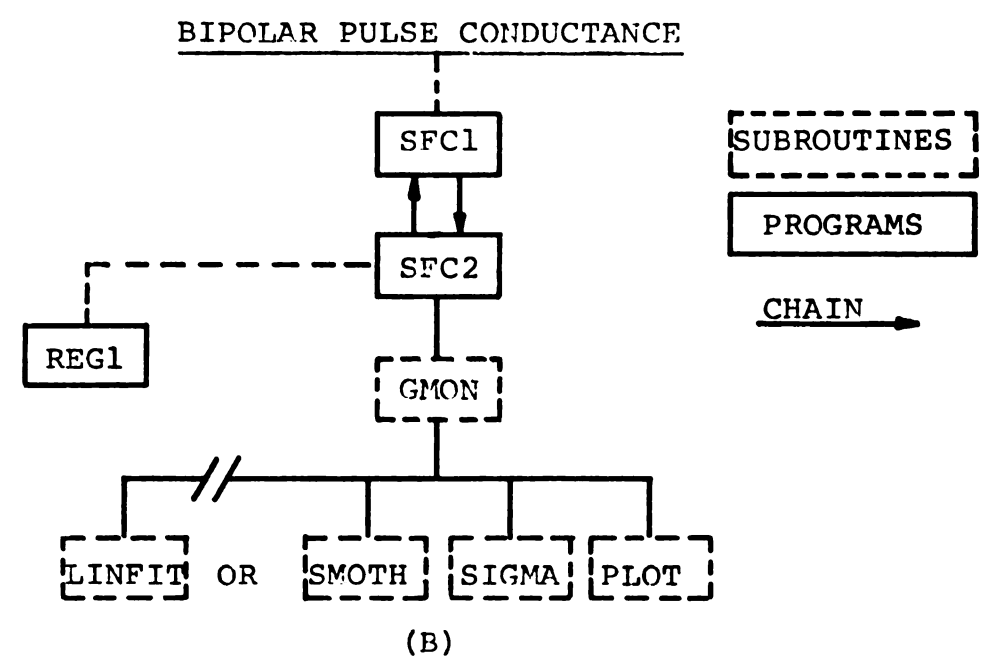
computers in the chemistry department.

The operating system that was utilized was OS/8, version III. The system is equipped with several assemblers, a BASIC interpreter, a FORTRAN II compiler, a FORTRAN IV compiler, and a large number of useful utility programs such as editors, debuggers, a monitor, etc. Until the version III software became available (125).at about the halfway mark in this work, only FORTRAN II was available, and all of the software to that point was written in this language. Since the two compilers were incompatible and a rather large library of useful software had accumulated, it was decided to retain use of the FORTRAN II compiler. In the long run the additional power and versatility of FORTRAN IV probably outweigh any inconvenience resulting from the changeover. All of the programs described were written in FORTRAN II and SABR, the FORTRAN II assembler.

C. TEMPERATURE MONITOR SOFTWARE

A diagram of the temperature monitor software is shown in Figure 37(a). The program TACl is a timed data acquisition program (see Appendix) which allows the operator to acquire any number of ensemble-averaged data points at equally spaced time intervals. Subroutine TIME is used to convert a real number of seconds into two





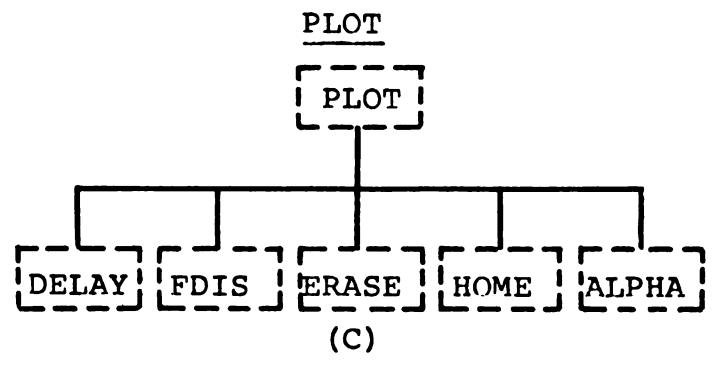


Figure 37. Block Diagram of Computer Software.

12-bit binary words that are used to control the clock.

DFLOT (126) converts the 24 bit, double precision, binary numbers resulting from the data acquisition into real numbers. Subroutine SIGMA is a mean, variance, and standard deviation routine and RWFIL reads and writes data files. Finally PLOT is a general purpose interactive graphics display routine that is described below.

TCAL (see Appendix) is a very simple data acquisition and calibration program that acquires ADC conversions when a series of precision resistors are in turn connected to the temperature monitor. Once the binary numbers are acquired a linear regression analysis is performed on the R-vs-binary number curve by subroutine LINFIT (127), and the resulting slope and intercept are written into a data file for retrieval by other programs.

Program THER is a thermistor calibration program that acquires an operator-specified number of data acquisition on a given thermistor, reads the actual temperature from the keyboard, and when all points have been acquired, writes the data into a file. The file may then be read by a general purpose, non-linear, least squares curve fitting program called REGR. This program utilizes subroutines REGRE (128), MATIN (129), and FCTN to fit the circuit response to a function specified by the function subroutine, FCTN. The coefficients from the fit may then be written in a data file for later use.

Finally, program TEMP is a simple data acquisition program that computes the temperature by performing an operator-specified number of data acquisitions on any calibrated thermistor.

D. BIPOLAR PULSE CONDUCTANCE SOFTWARE

The data acquisition software originally written for the bipolar pulse instrument by Caserta (124) was used with very little modification. This program, SFC1, and its relationship to the data analysis routines are shown in Figure 37(b). A software bug which plagued Caserta was the inability to utilize either the device independent I/O or chaining facility of the OS/8 operating system. In order to circumvent this difficulty, he used the RTAPE and WTAPE functions to store data on DECtape. Since in this work, the bipolar pulse conductance instrument was operated on a computer without DECtape, it was necessary to find the cause of the difficulty and fix it.

Caserta suspected (124) that his use of the locations 74_8-103_8 in field zero had some connection with this problem. This was confirmed, and it was found that the device independent I/O and chaining functions use some or all of these locations. As soon as the locations were changed to 125_8-134_8 , all of the functions worked

properly.

Prior to the solution of the problem, each program had to be called individually, often wasting much time. In addition, only 8K of memory was available, and thus, three different programs had to be called before data could be viewed. The consolidation of all of the data analysis and plotting functions greatly facilitated the operation of the conductance instrument.

Caserta's program CCLMLS was used as the basis for the analysis program SFC2. This program calculates conductivities and temperatures from the data generated by SFCl and stores them in an array in the subroutine GMON which contains the main branch point in the program. From this branch point, the operator may choose to perform a derivation smooth on the data using subroutine SMOTH (5,81), average a series of points using subroutine SIGMA, or plot the data as described below. A linear least squares regression analysis can also be carried out on any portion of the data. Conductance and temperature data can be written into a file and analyzed in order to determine the G-vs-T characteristics via a modification of REGR called REG1. The coefficients of the curve fit carried out by REG1 are written into a file from which they may be retrieved by SFC2 and used to make temperature corrections of conductance measurements.

The software set for the conductance instrument has

been written to provide flexibility by allowing function subroutines and other analysis subroutines to be easily incorporated into the programs. It suffers from the limitations of the FORTRAN II compiler itself, and would benefit from the high-level characteristics of FORTRAN IV and its capability to incorporate overlays.

E. PLOT - The Interactive Plotting Routine

One of the most difficult tasks in the automation and computerization of instrumentation at the research level is the design of software algorithms that perform specific tasks and yet are flexible enough to treat unpredictable differences in data sets. As an example of such a difficulty, let us consider the temperature-vs-time profiles shown in Figure 9 in Chapter II, and suppose that for some reason we would like to determine the difference between the temperatures at points A and C.

The following alternatives are available by performing such tasks. The data could be printed by the hard copy printer, a very slow or possibly expensive (fast line printer) procedure. The data could be plotted and the difference determined graphically, or finally, a specific algorithm could be designed to carry out the task. These alternatives lack both versatility and economy of time and money.

The most versatile method of carrying out the task

is via interactive graphics. If the data points of interest can somehow be pointed out to the computer, then it can easily carry out the numerical task and print only the desired result.

Fortunately (for the author), a storage-type graphics display terminal has recently become available that enables the rapid and accurate plotting of data. Although neither a hardware cursor nor a light pen were available for specifying points on data curves, it was possible to write a plotting program that performs the functions of a cursor and that in many cases provides superior performance. The assembly level plotting subroutines shown in Figure 37(c) were obtained from the DECUS Program Library (51) and were used without modification. Subroutine DECAY is a software timing routine that is called to provide a delay when the screen is erased so that points are not lost.

The basic principle of operation of the plotting routine is that it first plots the data array of interest, and then it replots it. The keyboard of the terminal is checked after each point to see if commands have been issued by the operator. All of the possible commands are shown in Table 9; all other keys are ignored. A typical plotting sequence is described below for interactively determining the difference between points A and C in Figure 9 as suggested above.

Table 9. Interactive Graphics Commands.

Command	Function
F	Move cursor to the right until stop command encountered
S	Stop and blink
R	Move cursor to the left until stop command encountered
CNTRL/F	Move single point to right
CNTRL/R	Move single point to left
1,2,3, or 4	Store index # of current point in storage location corresponding to the number typed (four are available)
CNTRL/G	Ring the bell and leave the inter- active mode

First, the data are scaled and plotted on the screen. Following this the beam is returned to the location of the first point, and it is plotted. The keyboard is then checked for control characters. If no character has been struck, the current point is plotted again. This recurs until a control character is struck. If F or R is struck the beam plots consecutive points in the indicated direction until any other character is struck. As soon as any other character is recognized, the beam stops and blinks as before.

If the CNTRL key is depressed with F or R, the beam moves a single point to the right or left and resumes blinking. If any of the numerals 1-4 are depressed, the index corresponding to the point currently being plotted is stored in a FORTRAN integer location. These four integers are returned to the calling program when the return from subroutine PLOT is made following the CNTRL/G command. The integers are then the indices of the data points in the FORTRAN data array that were selected in the interactive mode.

Following the initial plotting of the data of Figure 9, the blinking cursor can be moved until it blinks exactly on point A. The numeral 1 is depressed and the F command given to move the cursor to point C where the numeral 2 is depressed. Following a CNTRL/G command, the FORTRAN calling program can easily find the

difference between the Y values at the two points.

This subroutine which is listed in the Appendix has been extremely valuable in the precise determination of slopes between specified points on various response curves or differences between points as suggested above (see Chapter II). This method of interactive graphics display provides a versatile and economical means for carrying out unusual manipulations with graphical data.

APPENDIX

PROGRAM LISTINGS

```
PROGRAM NAME: TCAL.FT(V2.1) PROGRAMMER: J.HOLLER
                                                                       DATE: 3/26/77
C
          THIS PROGRAM IS DESIGNED TO ACQUIRE CALIBRATION DATA FOR THE
C
          FAST TEMPERATURE CIRCUIT. SINCE THE CIRCUIT IS LINEAR WITH THERMISTOR RESISTANCE, THE PROGRAM STORES RESISTANCE(R(I)) AND A/D CONVERSION(AD(I)) DATA ON THE DISK AS WELL AS THE SLOPE AND
Č
                                                    THE CALIBRATION IS CARRIED OUT BY
          INTERCEPT OF THE WORKING CURVE.
Č
          ATTACHING AN ACCURATE DRB(ESI DB52) TO THE CIRCUIT, VARYING THE RESISTANCE OVER THE RANGE OF INTEREST, AND ENTERING THE R VALUES VIA THE KEYBOARD. THE DATA IS WRITTEN INTO A FILE CALLED TCAL.DA
C
C
C
          IN A6 FORMAT.
Ċ
                    DIMENSION R(20), AD(20), SGMAY(20)
5
          READ(1,1) IAV, IPTS, MODE
1
          FORMAT('*PTS/AVE:'16,/,'*AVERAGES:'16,/,'WEIGHTING MODE:'16)
C
          THIS LOOP ACQUIRES ALL OF THE POINTS
C
C
          DO 4 J=1, IPTS
          DATA=0
          READ(1,6)R(J)
          FORMAT( 'R= 'E16.8)
6
C
C
          THIS LOOP ACQUIRES AND AVERAGES EACH POINT
Ğ
          DO 2 I=1, IAV
S
          6352
                               CLEAR FLAGSGATE DRIVER JUST IN CASE
8
          CLA CLL
                               /PULSE THE TEMPERATURE CIRCUIT
8
          6354
S
  CK,
                               /CHECK THE TEMP. FLAG
          6341
                               NOT FINISHED, CHECK AGAIN
8
          JMP CK
                               FINISHED, DRIVE THE DATA INTO THE AC TURN OFF THE SEQUENCER
8
          6352
8
          6332
                               /CONVERT TO 2'S COMPLEMENT
8
          TAD (4000
S
                               /PUT IT IN A FORTRAN LOCATION
          DCA \IDATA
S
          CLL
                               ALWAYS CLEAR THE LINK
          DATA=DATA+FLOAT(IDATA)
2
          CONTINUE
          AD(J) = (DATA/FLOAT(IAV)) + 2048.
C
4
          CONTINUE
C
C
          CALCULATE M AND B (X1 AND Y1)
C
          CALL LINFI(AD, R, SGMAY, IPTS, MODE, X, X1, Y, Y1, CC)
C
C
          WRITE OUT THE DATA
          DO 9 I=1, IPTS
          CALC=X+AD(I)*Y
          PCRES=((CALC-R(I))/R(I))*100.
          WRITE(1,3) AD(1), R(1), CALC, PCRES
          WRITE(3,3) AD(1), R(1), CALC, PCRES
          FORMAT(4(F11.5,4X))
          CONTINUE
9
          WRITE(3,7)Y,Y1,X,X1,GC
          WRITE(1,7)Y,Y1,X,X1,CC
      FORMAT(' SLOPE',2X,E16.8,4X'SD'2X,E16.8,/,' INCPT',2X,E16.8,4X'S +D'2X,E16.8,4X,'CORR.COEFF.',2X,E16.8)
CALL OOPEN('RKB0','TCAL')
7
          WRITE(4,8)X,Y
          WRITE(4,8)(R(I),AD(I),I=1,IPTS)
8
          FORMAT(A6)
          CALL OCLOSE
          STOP
          END
```

PROGRAM: TAC1.FT(V2.4) PROGRAMMER: J. HOLLER 4/8/77
THIS IS A DATA ACQUISITION PROGRAM FOR THE TEMPERATURE CIRCUIT
WHICH ALLOWS THE COLLECTION OF UP TO 400 AVERAGES OF UP TO 2047
POINTS EACH. THE DATA IS STORED (DOUBLE PREC.) IN COMMON AND
IS LATER RETRIEVED, FLOATED, AND WRITTEN INTO ARRAY R.
THE DATA MAY THEN BE PLOTTED ON THE TEK TERMINAL OR WRITTEN
INTO A FILE IN STANDARD C.G.ENKE CROUP FORMAT FOR ANALYSIS
ON THAT GROUP'S PDP 11/40 OR THE DEPARTMENTAL 11. IT SHOULD BE
NOTED THAT THIS VERSION OF THE PROGRAM USES THE REAL-TIME CLOCK
FOR TIMING RATHER THAN THE HARDWARE SEQUENCER. THE DATA MAY
BE WRITTEN INTO A FILE IN EITHER A6 OR F15.7 FORMAT AS
SPECIFIED BY THE USER.

SUBROUTINES CALLED: TIME--RETURNS CLOCK PARAMETERS
DFLOT--FLOATS THE DOUBLE PRECISION DATA
PLOT--TEK PLOTTING SUBROUTINE
SIGMA--AVERAGE AND STANDARD DEVIATION
RWFIL--FILE READER AND WRITER

VARIABLES OF INTEREST:

S

8

8

8

88

8

8

8

8

8

8

IAVES= OF AVERAGED DATA ACQUISITIONS
IPTS= OF DESCRETE POINTS PER AVERAGE
TMBTP=TIME BETWEEN POINTS (SECONDS)
ITMB=CLOCK MODE WORD OBTAINED FROM TIME
IPOT2= CLOCK TICKS FROM TIME
TYME=COMPUTED TIME AT THE CENTER OF EACH AVERAGE
TINC=TIME INCREMENT BETWEEN AVERAGES

LOADING SEQUENCE:

LO JHTAC1, JHSIGM, JHTIME, RWFILE, DFLOT, DELAY, PLOTIT(IOG)
(ASSUMING THAT TEKLIB.RL IS INCLUDED IN LIBB.RL AND THAT
LIBB.RL HAS BEEN MODIFIED TO UTILIZE THE DECWRITER)

NOTE: THE DATA IS ACQUIRED AT A CONSTANT DATA RATE DETERMINED BY TMBTP.

COMMON IDATA DIMENSION IDATA(800), R(400), C(6) PULSE BEGIN THE TEMP. PULSE AND CONVERT OPDEF 6354 SKIP ON TEMPERATURE FLAG SKPDF TEMCK 6341 /GATE THE TEMP. DRIVER AND CLEAR THE FLAG/HALT THE SEQUENCER **OPDEF** TEMDR 6352 **OPDEF** STSEQ 6332 /CHECK START FLAG SKPDF **GOCHK** 6362 OPDEF **CLZE** 6130 /CLEAR CLK ENABLE REG PER AC SKPDF CLSK 6131 SKIP ON CLK INTERRUPT OPDEF CLOE 6132 /SET CLK ENABLE REG PER AC CLAB **OPDEF** AC TO CLK BUFFER PRESET 6133 CLK STATUS TO AC (CLEARS FLAG)
READ THE DATA FIELD **OPDEF** CLSA 6135 **OPDEF** RDF 6214 **OPDEF** CDF 6201 **∕CHANGE TO DATA FIELD ● /AUTO INCREMENT REGISTER ABSYM** AINC 0012

```
C
       DETERMINE THE OPTION
C
C
33
          READ(1,35) IDEC
          IDEC= IDEC+1
         FORMAT( '0= IN, 1=RS, 2= IT, 3=PL, 4=AV, 5=WF, 6=RF, 7=EX, 8=CH: ', I3)
35
          GO TO (1000, 1001, 991, 50, 60, 40, 800, 19, 1002), IDEC
C
          READ TEMPERATURE COEFFICIENTS FROM 'DSK'
C
C
          CALL IOPEN('DSK', 'TCAL')
1000
          READ(4,2)B
          READ(4,2)EM
         CALL IOPEN('DSK', 'TRCOEF')
READ(4,3)(IDUMY,C(I),I=1,6)
          WRITE(1, 1003)(C(I), I=1,6)
1003
          FORMAT(2(2X, E16.8))
1001
          READ(1,777) IDEC1
         FORMAT('FAST(1), SLOW(2), OR SUPER SLOW(3): ', I1)
GO TO (778, 779, 781), IDEC1
777
778
          A0=C(1)
          A1=C(2)
          CO TO 780
          A0=C(3)
779
          A1=C(4)
          GO TO 780
781
          A0=C(5)
          A1=C(6)
         FORMAT(A6)
3
         FORMAT(A2, A6)
C
Č
         READ IN DATA ACQUISITION PARAMETERS
C
         READ(1,993) IDEC1
FORMAT('NU=300, IN=.0002, IA=5, T OUT?(0=Y, 1=N)', I2)
780
993
          IDEC1=IDEC1+1
          GO TO(999,998), IDEC1
         READ(1,1) IPTS, IAVES, TMBTP, IDEC
FORMAT('PA=',14,/,'AV=',14,/,'TI=',F10.6,/,'T/R(1/0):',I3)
998
          GO TO 992
999
          IPT8=5
          IAVES=300
          TMBTP=.0002
          IDEC= 1
          CALL TIME(TMBTP, ITMB, IPOT2)
992
          APTS= IPTS
C
          ITERATE WITH THE SAME PARAMETERS FROM HERE
č
991
          CONTINUE
```

```
C
         SET UP FOR DATA ACQUISITION
  GOUN, CLA CLL
888
                           /CLOCK TIME BASE: PRESET MODE
         TAD \ITMB
                           STORE IT ON DATA ACQUISITION PAGE
MAKE THE AC ALL ONES
         DCA I TMB0
         CMA
8888886668886668888
         CLZE
                           /INITIALIZE THE CLOCK
         CLA CLL
         TAD \IPOT2
                           BRING UP THE NUMBER OF TICKS
                           /MAKE IT NEGATIVE
/LOAD THE PRESET REGISTER
         CIA
         CLAB
         CLA CLL
         SET UP THE NUMBER OF AVERAGES
                           /SIZE OF THE ENSEMBLE TO BE AVERAGED
         TAD \IAVES
                           /MADE IT NEGATIVE
         CIA
         DCA I SNDP
                           STORE IT OFF-PAGE
         SET UP THE NUMBER OF POINTS PER AVERAGE
                           /SIZE OF THE ENSEMBLE TO BE AVERAGED
         TAD \IPTS
         CIA
                           NEGATIVE OF THE DIVISOR
         DCA I ANAQ
                           /STORE OFF-PAGE
         TAD (0177
DCA AINC
                           /SET UP ADDRESS OF FIRST DATA WORD
                           BEGIN TDA RUN
         JMP I SA09
 ANAQ, NAQ
                           NUMBER OF AVERAGES POINTER TO TDA
                           STARTING ADDRESS OF TDA RUN
NUMBER OF POINTS/AVE POINTER
8
 SA09, QA09
8 SNDP, NDP
                           /TIME BASE LOCATION
S TMBO, TMB1
```

```
S /THIS IS THE TDA. DATA ACQUSITION ROUTINE
         PAGE
         LAP
  TMB1,
                            /TIME BASE WORD
8
         •
  QA09,
         RDF
                            /READ THE DATA FIELD
8
                           ADD THE INSTRUCTION
PUT THE RESULTING CDF IN PLACE
         TAD CDF I
8
8
         DCA CDFX
  GO,
                            LOOK FOR START FLAG
8
         COCHK
8
         JMP GO
                            ∕NOT READY YET
         TAD TMB1
                            BRING UP THE MODE WORD
8
                            /ENABLE THE CLOCK
8
         CLOE
8
         TEMDR
                            /GATE IN THE GARBAGE AND CLEAR FLAG
                            /A GOOD SPOT TO CLEAR AC AND LINK
  QL09, CLA CLL
8
         DCA TLSB
DCA TMSB
                            ZERO LSB WORD
8
                           ZERO MSB WORD
S
                            /SET UP # OF POINTS/AVE POINTER FOR THIS RUN
8
         TAD NAQ
S
         DCA LNAQ
                           /CHECK THE CLOCK FLAG
8
  CNE,
         CLSK
                           NOT READY, CHECK AGAIN
BONG!!! CLEAR THE FLAG
         JMP GNE
8
8
         CLSA
8
         CLA CLL
  QA13, PULSE
                           /PULSE AGAIN
8
  QA14, TEMCK
                            /TEST TEMP FLAG
                            NOT READY
8
         JMP QA14
8
         STSEQ
                            /STOP THE SEQUENCE
                           CLEAR FLAG, GATE DRIVER ADD IN PREVIOUS LSB VALUE
8
         TEMDR
8
         TAD TLSB
         DCA TLSB
8
                            /SET LINK INTO LSB
8
         RAL
8
         TAD TMSB
                           /ADD IN MSB
8
         DCA TMSB
                           /ALL N POINTS/THIS AVE? /NO, RETURN FOR MORE
. 8
         ISZ LNAQ
         JMP GNE
8
         TAD TLSB
8
                            YES, AVERAGE
8
         6211
                            /AUTO-INCREMENT AND STORE DATA
8
         3412
         TAD TMSB
                            BRING IN THE MOST SIGNIFICANT WORD
8
         3412
                            /STORE IT
  CDFX, 0000
                            /REPLACED BY CHANGE TO DATA FIELD X
8
                            /HAVE ALL AVERAGES BEEN ACQUIRED?
         ISZ NDP
         JMP QL09
                            /NO, DO IT AGAIN
8
                            YES, GO ANALYZE THE DATA
         JMP I ANAL
                           /LEAST SIG. WORD
/MOST SIG. WORD
  TLSB,
8
  TMSB,
S NAQ.
                            NUMBER OF POINTS
  LNAQ,
                            /-#POINTS
8
  NDP,
                            /NUMBER OF AVERACES
  ANAL,
                           /THE WAY OUT
         \500
8
                           /TWO'S COMP. <> BINARY CONVERTER
  C4000, 4000
  CDFI, CDF
                           /CDF INSTRUCTION
8
S
         EAP
8
         PAGE
```

```
C
C
         START TO CALC. T OR R AND STORE IN ARRAY R
C
500
         CONTINUE
         IB=0
         TYME=((APTS-1.)/2.)*TMBTP
         TINC=APTS*TIBTP
         DO 30 I=1, IAVES
         IB= IB+2
         IA= IB-1
         CALL DFLOT( IDATA( IB) , IDATA( IA) , RDATA)
         RDATA=RDATA/APTS
         R(I) = EM * RDATA + B
         IF(IDEC)30,30,11
         CONTINUE
11
         R(I) = (1./(A0+(A1*ALOG(R(I))))-273.16
30
         CONTINUE
         GO TO 33
C
         WRITE FILES
40
         CALL RWFIL(R, 1, IAVES, TYME, TINC)
         GO TO 33
C
         PLOT DATA ON THE TEK TERMINAL
C
50
         CALL PLOT(R, IAVES, 0, 2, IA, IB, IC, ID, AMAX, AMIN)
         GO TO 33
C
         AVERAGE SECTIONS OF THE CURVE AS SPECIFIED FROM PLOT
C
60
         CALL PLOT(R, IAVES, 0, 1, IA, IB, IC, ID, AMAX, AMIN)
997
         DO 996 J=1,2
         CALL SIGMA(0,R(1),AV,VAR,SIG)
         DO 995 I= IA, IB
         CALL SIGMA(1,R(I),AV,VAR,SIG)
CALL SIGMA(2,R(I),AV,VAR,SIG)
995
         WRITE(1,994) IA, IB, AV, SIG
         WRITE(3,994) IA, IB, AV, SIG
FORMAT(' AV(', I3,'-', I3,'): ',E16.8,4X,'SD: ',E16.8)
994
         IA= IC
         IB= ID
996
         CONTINUE
         CO TO 33
C
         READ FILES FOR FURTHER ANALYSIS
800
         CALL RWFIL(R,2, IAVES, TYME, TINC)
         GO TO 33
C
Ċ
         CHAIN TO DETERMINE TEMPERATURE
1002
         CALL CHAIN('JHTEMP')
C
C
         GET OUT QUICKLY
C
19
         CALL EXIT
         STOP
```

END

PROGRAMMER: J. HOLLER PROGRAM: PLOT. FT(VS. 0) DATE: 8/24/77

CCCCCC

C

00000000000

THE PURPOSE OF THIS PROGRAM IS TO PROVIDE A PLOTTING SUBROUTIME THAT IS CAPABLE OF SCALING AND PLOTTING DATA CONTAINED IN A FORTRAN II ARRAY IN THE CALLING PROGRAM. IN ADDITION, THE SUBROUTINE PROVIDES THE CAPABILITY OF INTERACTIVELY CHOOSING POINTS ON A DATA CURVE FOR SUBSEQUENT ANALYSIS IN THE CALLING PROGRAM.

THE POINTS ARE SPECIFIED IN THE INTERACTIVE MODE AFTER THE DATA HAVE BEEN PLOTTED. THE BLINKING DOT (CURSOR) MOVES TO THE INITIAL POINT, AND WAITS FOR A COMMAND AS FOLLOWS.

S=STOP AND BLINK F=PLOT FORWARD R=PLOT REVERSE CNTRL/F=PLOT 1 POINT FORWARD CNTRL/R=PLOT 1 POINT REVERSE 1,2,3,
CNTRL/G=RETURN TO THE CALLING PROGRAM 1,2,3,4=STORE INDEX 1,2,3, OR 4

WHEN CONTROL IS RETURNED TO THE CALLING PROGRAM, THE INDICES OF THE SPECIFIED POINTS ARE AVAILABLE AS ARGUMENTS IX, X=1,2,3, AND 4 AND MAY THEN BE USED FOR PERFORMING CALCULATIONS ON THE DATA IN THE ARRAY.

OTHER IMPORTANT VARIABLE NAMES ARE AS FOLLOWS:

IPTS=THE NUMBER OF POINTS IN THE DATA ARRAY ISKP=# REJECTED POINTS DATA=THE NAME OF THE DATA ARRAY IMODE=CONTROL VARIABLE AS FOLLOWS:

IMODE=1, SCALE, PLOT, AND INTERACT IMODE=2, SCALE AND PLOT IMODE=3, SPLOT ONLY

IMODE=4. INTERACT ONLY USING LAST SCALING FACTORS

IX(X=1,2,3,4) = INDICES OF DATA SPECIFIED INTERACTIVELY JSKP-INDEX OF FIRST POINT TO BE PLOTTED J=INDEX OF LAST POINT TO BE PLOTTED AMAX=MAXIMUM IN ARRAY DATA AMIN=MINIMIM VALUE IN ARRAY DATA INCX=INTERVAL ON X AXIS YSCAL=SCALING FACTOR FOR DATA

SUBROUTINES CALLED:

IF:

ERASE-ERASES SCREEN OF TEK TERMINAL DELAY-CAUSES SOFTWARE WAIT FOR SLOW BLINK FDIS-PLOTS POINTS ALPHA-RETURNS TEK TERMINAL TO ALPHA MODE HOME-MOVES CURSOR TO HOME POSITION

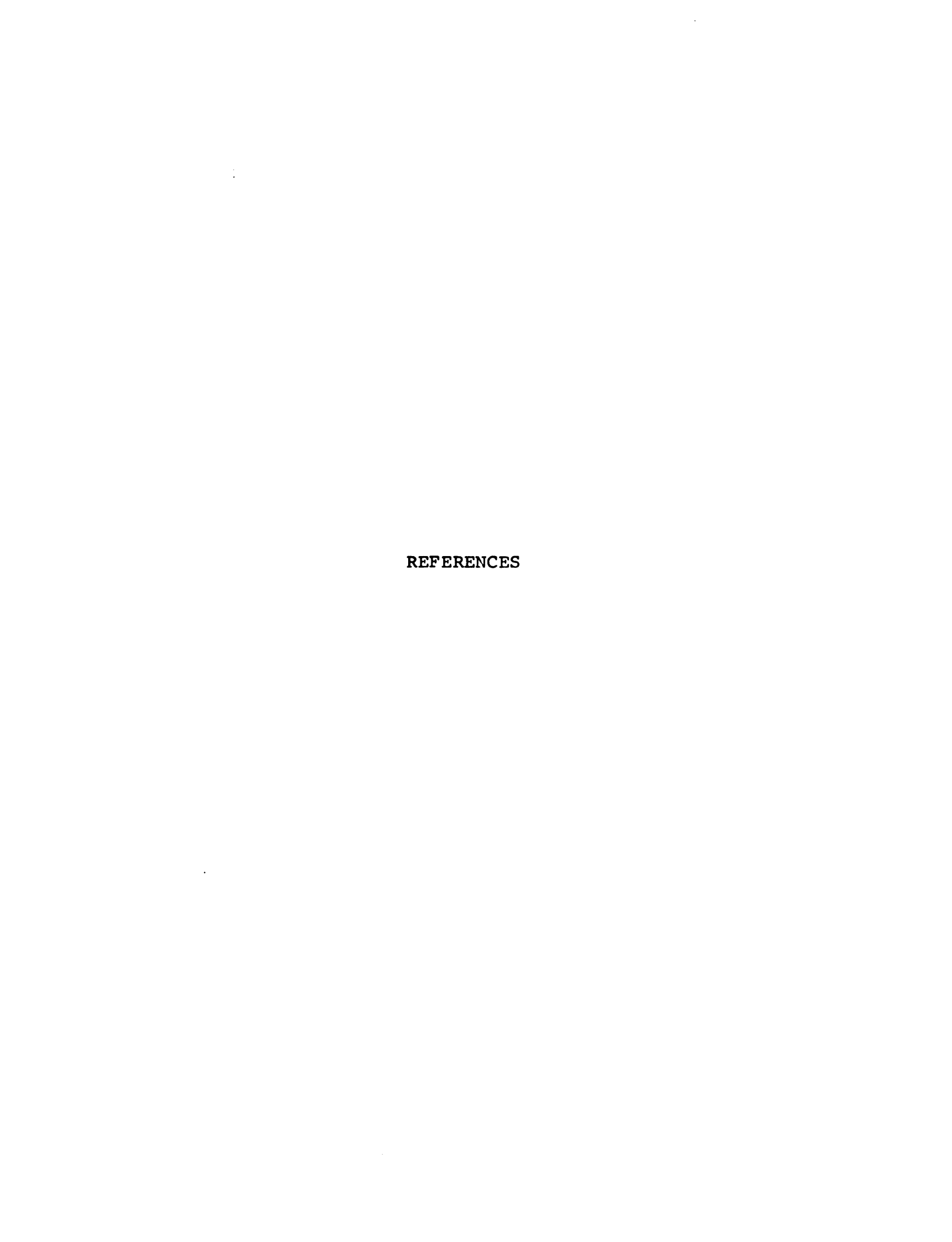
```
SUBROUTINE PLOT (DATA, IPTS, ISKP, IMODE, I1, I2, I3, I4, AMAX, AMIN)
        DIMENSION DATA(400)
C
         INITIALIZE
        GO TO (100, 100, 200, 16), IMODE
        JSKP= ISKP+1
100
        AMAX=DATA(JSKP)
        AMIN= AMAX
        J= IPTS-ISKP
        SCALES THE DATA
C
        DO 1 I=JSKP,J
        IF(AMAX-DATA(I))2,2,3
        AMAX=DATA(I)
3
         IF(AMIN-DATA(I))1,1,4
        AMIN=DATA(I)
1
        CONTINUE
        WRITE(1,7) AMAX, AMIN
FORMAT(' MAX='E16.8,/,' MIN='E16.8,/)
7
C
C
        FIND WHETHER TO SCALE OR OVERPLOT
C
200
        READ(1,8) IDEC1, IDEC2
        FORMAT('CHANGE SCALE? (1=YES, 0=NO)'I1,/,'OVERPLOT?'I1)
8
         IF (IDEC1)5,5,9
        READ(1,7) AMAX, AMIN
5
         YSCALE=ABS(768./(AMAX-AMIN))
         INCX=1024./FLOAT(IPTS-1)
         IF(IDEC2) 10, 10, 11
10
        CALL ERASE
        CALL DELAY(100)
C
        PLOT CRUDE AXES
C
C
        CALL FDIS(0,0,768)
        CALL FDIS(1,0,0)
        CALL FDIS(1, 1024,0)
C
Ċ
        PLOTS THE POINTS
C
11
        IX=-INCX
        DO 6 I=JSKP,J
         IX= IX+ INCX
         IY=((DATA(I)-AMIN)*YSCALE)
        CALL FDIS(-1, IX, IY)
        CONTINUE
6
        CALL ALPHA
        CALL HOME
C
        PROCEED TO INTERACT OR RETURN TO CALLING PROGRAM
C
        GO TO (12, 16, 16, 12), IMODE
```

```
Č
        BEGIN INTERACTIVE ROUTINE
C
                          BRING IN INDEX OF BEGINNING POINT
8
  \12,
        TAD \JSKP
8
        DCA I COUNT
                          STORE IT
8
        TAD ("S
                          /BRING IN AN "S"
                          /REPLACE THE OLD CHARACTER WITH IT
8
        DCA CHAR
        JMP STOP
                          START PLOTTING
                          /CET RID OF CARBAGE
8
  \13.
        CLA CLL
                          /CHECK THE KEYBOARD
8
        KSF
8
        JMP GOON
                          /CO ON
S
        KRB
                          /READ IT
                          STORE IT /GET IT AGAIN
8
        DCA CHAR
 GOON,
8
        TAD CHAR
                          /IS IT A CNTRL F?
S
        TAD (-206
8
        SNA CLA
                          /SKIP IF NOT
8
        JMP FORW1
                          /CO PLOT ONE POINT FORWARD
8
                          /GET IT AGAIN
        TAD CHAR
        TAD (-"F
                          /IS IT AN F? (306)
888
                          /NOPE
        SNA CLA
                          YES, INCREMENT AND PLOT /GET IT AGAIN
        JMP FORW
8
        TAD CHAR
8
                          /IS IT CNTRL R?
        TAD (-222
                          SKIP IF NOT
        SNA CLA
8
        JMP REVER1
                          /CO PLOT ONE POINT BACKWARD
                          CET IT AGAIN
        TAD CHAR
8
        TAD (-"R
                          /IS IT AN R? (322)
88
        SNA CLA
                          /NOPE
                          YES, DECREMENT AND PLOT /GET IT AGAIN
        JMP REVER
8
        TAD CHAR
                          /IS IT A CONTROL C? (207)
8
        TAD (-207
8
                          /NOPE
        SNA CLA
        JMP F15
                          /RETURN
        TAD CHAR
                          /GET IT AGAIN
                          /IS IT AN S?
8
        TAD (-323
                          /SKIP IF IT ISN'T
/MUST BE S, PLOT THEN GO LOOK FOR NUMBERS 1-4 ON KB
8
        SNA CLA
8
        JMP F14
                          /MUST BE 1-4, CO CHECK
        JMP STOP
 FORW1, TAD ("S
                          /STOP AFTER INCREMENTING IF
8
                          /CNTRL/F
8
        DCA CHAR
8
 FORW. TAD I \IPTS
                          /MAKE SURE IPTS NOT EXCEEDED
8
        CIA
                          ✓ NEGATE IT
        TAD I COUNT
8
                          /ADD # POINTS
                          /SKIP IF IPTS.LE.COUNT
8
        SMA CLA
8
        JMP LIMIT
                          /GO MAKE BLIPS IF IPTS.EQ. COUNT
                          /INCREMENT THE COUNTER
         ISZ I COUNT
         JMP F17
                          ∕GO PLOT THE POINT
S LIMIT, TAD ( "S
                          /323
                          /STORE "S" FOR STOP
        DCA CHAR
                          /GO BLIP
8
         JMP F14
                          STOP AFTER DECREMENTING IF
SREVER1, TAD ( 'S
        DCA CHAR
                          /CNTRL/R
8
S REVER, STA

∠MAKE THE AC −1

        TAD I COUNT
8
                          ADD TO THE COUNTER
                          /IS COUNTER > 0?
8
        SPA SNA
                          /NO, GET ANOTHER CHARACTER
        JMP F14
8
                          /NET EFFECT: DECREMENTS COUNTER
8
        DCA I COUNT
         JMP F17
                          /GO PLOT
```

```
/CHECK FOR CHARACTER
S STOP, TAD CHAR
        AND (0007
                          /GET RID OF BITS 0-8
                          ∠ADD -1
        TAD MINUS1
8
                          /SKIP IF NOT 1
        SNA
8
        JMP LOC1
                          /GO STORE INDEX IN I1 IF 1
                          /ADD -1
/SKIP IF NOT 2
8
        TAD MINUSI
8
        SNA
                          STORE INDEX IF 2
        JMP LOC2
8
                          /ETC. FOR 3
        TAD MINUSI
        SNA
8
        JMP LOC3
                          /AND FOR 4
        TAD MINUS1
        SNA CLA
JMP LOC4
8
8
        JMP F14
                          /TRY IT AGAIN
 LOC1, CLA CLL
                          /CLEAR EVERYTHING
8
                          BRING UP THE INDEX OF CURENT POINT
8
        TAD I COUNT
8
        DCA I \I1
                          /PUT IT IN FORTRAN II
                          /PLOT AGAIN 8 RETURN
        JMP F14
 LOC2, CLA CLL
TAD I COUNT
8
                          /SAME FOR 2
8
8
        DCA I \12
8
        JMP F14
 LOC3, CLA CLL
                          /SAME FOR 3
        TAD I COUNT
8
8
        DCA I \13
        JMP F14
8
 LOC4, CLA CLL
                          /SAME FOR 4
        TAD I COUNT
8
        DCA I \I4
        JMP F14
SCOUNT, \ICOUN
                          /ADDRESS OF INDEX
S CHAR, 0000
                          /CHARACTER HOLDER
                          CLEAR THE LINK LOCATION BEFORE
S F14,
        CLL
        JMP \14
                          ∕COING TO FORTRAN
S
S F15,
        CLL
                          /DITTO
        JMP \15
8
8 F17,
        CLL
8
        JMP \17
                          /-1
SMINUS1,7777
C
C
14
        CONTINUE
C
C
        DELAY MAY BE PLACED HERE TO SLOW BLINK
C
17
        IX=(ICOUN-JSKP)*INCX
        IY=(DATA(ICOUN)-AMIN)*YSCALE
C
        CHECK FOR LIMITS OF TEK SCREEN
C
C
        IF(IX-1024) 19, 19, 18
18
        IX= 1024
        IF(IX)20,20,21
19
20
        I X= 0
        IF( IY-768) 23,23,22
21
22
        IY=768
23
        IF(IY)24,24,25
24
        IY=0
        REPLOT CURRENT POINT
\mathbf{C}
C
25
        CALL FDIS(-1, IX, IY)
        CALL ALPHA
        GO TO 13
15
        CALL HOME
        RETURN
16
        END
```



REFERENCES

- S. R. Crouch, F. J. Holler, P. K. Notz, and P. M. Beckwith, Appl. Spectroscopy Rev., submitted.
- F. J. Holler, S. R. Crouch, and C. G. Enke, Anal. Chem., 48, 1429 (1976).
- 3. F. J. Holler, S. R. Crouch and C. G. Enke, Chem. Instrum., in press.
- 4. T. A. Nieman, F. J. Holler, and C. G. Enke, Anal. Chem., 48, 899 (1976).
- 5. T. A. Nieman, Ph.D. Thesis, Michigan State University 1975.
- 6. H. B. Mark, Jr. and G. A. Rechnitz, "Kinetics in Analytical Chemistry", Wiley-Interscience, New York, 1968.
- 7. K. B. Yatsimerskii, "Kinetic Methods of Analysis", Pergamon Press, Oxford, 1966.
- 8. G. A. Rechnitz, Anal. Chem., 36, 453R (1964).
- 9. G. A. Rechnitz, Anal. Chem., 38, 513R (1966).
- G. A. Rechnitz, Anal. Chem., <u>40</u>, 455R (1968).
- 11. G. G. Guilbault, Anal. Chem., <u>38</u>, 527R (1966).
- 12. G. G. Guilbault, Anal. Chem., 40, 459R (1968).
- 13. G. G. Guilbault, Anal. Chem., <u>42</u>, 334R (1970).
- 14. R. A. Greinke and H. B. Mark, Jr., Anal. Chem., 44, 295R (1972).
- 15. R. A. Greinke and H. B. Mark, Jr., Anal. Chem., 46, 413R (1974).
- 16. R. A. Greinke and H. B. Mark, Jr., Anal. Chem., 48, 87R (1976).
- 17. M. M. Fishman and H. F. Schiff, Anal. Chem., 44, 543R (1972).

- 18. S. R. Crouch in "Computers in Chemistry and Instrumentation".)H. D. Mattson, H. B. Mark, Jr., and H. C. McDonald, Jr., Eds.), Vol. 3, Dekker, New York, 1973, pp. 107-207.
- 19. G. G. Guilbault, in "MTP International Review of Science, Physical Chemistry Series One" (A. D. Buckingman Consult. Ed., T. S. West, Ed.), Vol. 12 Butterworths, London, University Park Press, Baltimore, 1973, pp. 161-191.
- 20. K. B. Yatsimerskii, in "MPT International Review of Science, Physical Chemistry Series One", (A. D. Buckingham, Consult. Ed., T. S. West, Ed.) Vol. 12, Butterworths, London, University Park Press, Baltimore, 1973, pp. 193-215.
- 21. H. V. Malmstadt, E. A. Cordos and C. J. Delaney, Anal. Chem., 44, 26A (1972).
- 22. H. V. Malmstadt, C. J. Delaney and E. A. Cordos, Anal. Chem., <u>44</u>, 79A (1972).
- 23. H. V. Malmstadt, C. J. Delaney and E. A. Cordos, CRC Critical Rev. Anal. Chem., 2, 559 (1972).
- 24. H. B. Mark, Jr., Talanta, 19, 717 (1972).
- 25. H. L. Pardue, in "Advances in Analytical Chemistry and Instrumentation", (C. N. Reilley and F. W. McLafferty, Eds.,), Vol. 7, Wiley-Interscience, New York, 1968, pp 141-207.
- 26. W. J. Blaedel and G. P. Hicks, in "Advances in Analytical Chemistry and Instrumentation" (C. N. Reilley, Ed.) Vol. 3, Wiley-Interscience, New York, 1964, pp. 126-140.
- 27. H. B. Mark, Jr., L. J. Papa and C. N. Reilley, in "Advances in Analytical Chemistry and Instrumentation" (C. N. Reilley, ed.) Vol. 2, Wiley-Interscience, New York, 1963, pp. 255-385.
- 28. H. O. Mottola, CRC Critical Rev. Anal. Chem., 5, 229 (1975).
- 29. J. D. Ingle, Jr. and S. R. Crouch, Anal. Chem., 43, 697 (1971).
- 30. S. R. Crouch and H. V. Malmstadt, Anal. Chem., 39, 1090 (1967).

- 31. J. B. Pausch and D. W. Margerum, Anal. Chem., <u>41</u>, 226 (1969).
- 32. A. C. Javier, S. R. Crouch, and H. V. Malmstadt, Anal. Chem., <u>41</u>, 239 (1969).
- 33. E. F. Caldin, "Fast Reactions in Solution", Wiley, New York, 1964.
- 34. H. Hartridge and F. J. W. Roughton, Proc. Roy. Soc. Series A, 104, 376 (1923).
- 35. F. J. W. Roughton, Discussions Faraday Soc., 17, 116 (1954).
- 36. F. J. W. Roughton in "Rapid Mixing and Sampling Techniques in Biochemistry", (B. Chance, R. Eisenhardt, Q. H. Gibson, and K. Lonberg-Holm, Eds.)
 Academic Press, New York, 1964, pp. 5-13.
- 37. B. Chance, J. Franklin Inst., 229, 455, 613, 737 (1940).
- 38. K. R. O'Keefe and H. V. Malmstadt, Anal. Chem., 47, 707 (1975).
- 39. Q. H. Gibson in "Rapid Mixing and Sampling Techniques in Biochemistry", (B. Chance, R. Eisenhardt, Q. H. Gibson, and K. Lonberg-Holm, Eds.) Academic Press, New York, 1964, pp. 115-116.
- 40. M. L. Miller and G. Gordon, Anal. Chem., <u>48</u>, 778 (1976).
- 41. P. K. Chattopadhyay and J. F. Coetzee, Anal. Chem., 44, 2117 (1972).
- 42. P. K. Notz, private communication.
- 43. P. M. Beckwith and S. R. Crouch, Anal. Chem., 44, 221 (1972).
- 44. P. K. Notz and S. R. Crouch, manuscript in preparation.
- 45. Q. H. Gibson and L. Milnes, Biochem. J., <u>91</u>, 161 (1964).
- 46. J. E. Stewart, Durrum Application Notes #4, "Flow Deadtime in Stopped-Flow Measurements".
- 47. Thermometrics, Inc., 15 Jean Place, Edison, NJ 08817.

- 48. Victory Engineering Corp., Victory Road, Springfield, NJ 07081.
- 49. Yellow Springs Instrument Co., Yellow Springs, OH.
- 50. Sargent-Welch Scientific Co., Skokie, IL 60076.
- 51. Digital Equipment Corporation, Maynard, MA 01754.
- 52. J. W. Frazer, A. M. Kray, W. Selig, and R. Lin, Anal. Chem., 47, 869 (1975).
- 53. F. J. Holler, K. J. Caserta, S. R. Crouch, and C. G. Enke, Anal. Chem., submitted.
- 54. N. Papadakis, R. B. Coolen, and J. L. Dye, Anal. Chem., <u>47</u>, 1644 (1975).
- 55. E. F. Caldin, J. E. Crooks, and A. Queen, J. Phys. E: Sci. Instrum., 6, 930 (1973).
- 56. R. M. Wightman, R. L. Scott, C. N. Reilley, R. W. Murray, and J. N. Burnett, Anal. Chem., 46, 1492 (1974).
- 57. S. W. Benson, "The Foundations of Chemical Kinetics", McGraw-Hill, New York, 1960, p. 66.
- 58. J. L. Dye, personal communication.
- 59. L. Bowie, F. Esters, J. Bolin and N. Gochman, Clin. Chem., 22, 449 (1976).
- 60. M. L. Miller and G. Gordon, Anal. Chem., <u>48</u>, 778 (1976).
- 61. B. Balko and R. L. Berger, Anal. Chem., <u>41</u>, 1506 (1969).
- 62. R. L. Berger, W. S. Friauf, and H. E. Cascio, Clin. Chem., 20, 1009 (1974).
- 63. S. H. Praul and L. V. Hmurcik, Rev. Sci. Instrum., 44, 1363 (1973).
- 64. H. B. Sachse, "Semiconducting Temperature Sensors and Their Applications", Wiley-Interscience, New York, 1975.
- 65. M. Sapoff, in "Temperature, Its Measurement and Control in Science and Industry", Vol. 4, Part 3,

- Instrument Society of America, Pittsburgh, 1973, pp. 2109-2121.
- 66. Reference 6, page 199.
- 67. J. Jordan, J. K. Grime, D. H. Waugh, C. D. Miller, J. M. Cullis and D. Lohr, Anal. Chem., 48, 427A (1976).
- 68. H. V. Malmstadt, C. G. Enke and S. R. Crouch, "Electronic Measurements for Scientists", W. A. Benjamin, Menlo Park, 1973.
- 69. "National Anthem", No. 3, May 1976, National Semi-Conductor Corp.
- 70. Reference 6, page 180.
- 71. P. R. Bevington, "Data Reduction and Error Analysis for the Physical Sciences", McGraw-Hill, New York, 1969, pp. 171-176.
- 72. H. W. Trolander, D. A. Case, and R. W. Harruff, in "Temperature, Its Measurement and Control in Science and Industry", Vol. 4, Part 2, Instrument Society of America, Pittsburgh, 1973, pp. 997-1009.
- 73. F. J. Holler, C. G. Enke, and S. R. Crouch, Anal. Chem, submitted.
- 74. R. L. Berger and B. Balko, in "Temperature, Its Measurement and Control in Science and Industry", Vol. 4, Part 3, Instrument Society of America, Pittsburgh, 1973, pp. 2169-2192.
- 75. D. E. Johnson and C. G. Enke, Anal. Chem., <u>42</u>, 329 (1970).
- 76. D. E. Johnson, Ph.D. Thesis, Michigan State University (1970).
- 77. Frank M. Hussey, Master's Thesis, Michigan State University (1971).
- 78. P. H. Daum and D. F. Nelson, Anal. Chem., 45, 463 (1973).
- 79. S. G. Ballard, Rev. Sci. Instrum., 47, 115 (1976).
- 80. S. N. Deming and H. L. Pardue, Anal. Chem., 42, 1466 (1970).

- 81. C. G. Enke and T. A. Nieman, Anal. Chem., <u>48</u>, 705A (1976).
- 82. A. Savitzky and M. J. E. Golay, Anal. Chem., <u>36</u>, 1627 (1964).
- 83. H. V. Malmstadt, C. G. Enke, S. R. Crouch, and G. Horlick, "Optimization of Electronic Measurements, Module 4", W. A. Benjamin, Inc., Menlo Park, CA 1974.
- 84. H. Thompson and M. Rogers, Rev. Sci. Instrum., <u>27</u>, 1079 (1956).
- 85. D. M. Kern, J. Chem. Educ., 37, 14 (1960).
- 86. Roughton, F. J. W., J. Am. Chem. Soc., <u>63</u>, 2930 (1941).
- 87. Berger, R. L. And Stoddart, L. C., Rev. Sci. Instrum., 36, 78 (1965).
- 88. B. Balko, R. L. Berger, and Walter Friauf, Anal. Chem., 41, 4506 (1969).
- 89. K. Dalziel, Biochem. J., <u>55</u>, 79 (1958).
- 90. R. L. Berger, B. Balko, W. Borcherdt, and W. Friauf, Rev. Sci. Instrum., 39, 486 (1968).
- 91. R. Brinkmann, R. Margaria, and F. J. W. Roughton, Trans. Roy. Soc. (London), A232, 65 (1933).
- 92. J. A. Sirs, Trans. Faraday Soc., <u>54</u>, 207 (1958).
- 93. R. Saal, Rev. Trav. Chim., 47, 264 (1928).
- 94. C. Faurholt, J. Chim. Phys., 21, 400 (1924).
- 95. M. Eigen, K. Kustin, and G. Mass, Z. Physik, Chem., 30, 130 (1961).
- 96. T. Shedlovsky and D. A. McInnes, J. Am. Chem. Soc., 57, 1705 (1935).
- 97. J. A. Sirs, Trans. Faraday Soc., 54, 201 (1958).
- 98. R. H. Prince, Ibid, 54, 838 (1958).
- 99. M. A. Wolfe, Chem. Instrum., 5, 59 (1973).
- 100. 3-M Corporation.

- 101. P. K. Notz, Ph.D. Thesis, Michigan State University, 1977.
- 102. T. R. Mueller, R. W. Stelzner, D. J. Fisher, and H. C. Jones, Anal. Chem., 37, 13 (1965).
- 103. D. McLean and R. L. Tranter, J. Phys. E. Sci. Instrum., 4, 455 (1970).
- 104. A. C. Knipe, D. McLean, and R. L. Tranter, J. Phys. E: Sci. Instrum., 7, 586 (1974).
- 105. R. P. Bell and D. M. Goodall, Proc. Roy. Soc. A., 294, 272 (1966).
- 106. E. W. Miller, A. P. Arnold, and M. J. Astle, J. Amer. Chem. Soc., 70, 3971 (1949).
- 107. P. J. Elving and J. Lakritz, Ibid, 77, 3217 (1955).
- 108. B. H. Campbell, L. Meites, and P. W. Carr, Anal. Chem., 46, 386 (1976).
- 109. B. W. Renoe, K. R. O'Keefe, and H. V. Malmstadt, Anal. Chem., 48, 661 (1976).
- 110. G. E. Mieling, R. W. Taylor, L. G. Hargis, J. English, and H. L. Pardue, Anal. Chem., 48, 1686 (1976).
- 111. S. N. Deming and H. L. Pardue, Anal. Chem., 43, 192 (1971).
- 112. R. Megargle and J. Marshall, Chem. Instrum., $\underline{4}$, 29 (1972).
- 113. K. A. Mueller and M. F. Burke, Anal. Chem., 43, 641 (1971).
- 114. E. C. Toren, Jr., R. N. Carey, A. E. Sherry, and J. E. Davis, Anal. Chem., 44, 339 (1972).
- 115. Models E412-G and E415, Brinkman Instruments, Inc., Westbury, NY 11590.
- 116. L. D. Rothman, Ph.D. Thesis, Michigan State University, 1974.
- 117. Model 23D-6102, Computer Devices of California, Santa Fe Springs, CA 90670.
- 118. Model Al506C, Velmex, Inc., Bloomfield, NY 14443.

- 119. Model 19925-X gas-liquid syringes, Glenco Scientific, Houston, TX 77007.
- 120. E. B. Bradt, Undergraduate project, Michigan State University, 1976.
- 121. M. B. Denton, M. W. Routh, J. D. Mack, and D. B. Swartz, Amer. Lab., 8, 69 (1976).
- 122. F. J. Holler, T. V. Atkinson, T. G. Kelly, and C.
 G. Enke, Amer. Lab., 8(9), 9 (1976).
- 123. "Sigma Stepping Motor Handbook", Sigma Instruments, Inc., Braintree, MA 02184, 1972.
- 124. K. J. Caserta, Ph.D. Thesis, Michigan State University, 1974.
- 125. "OS/8 Handbook", Digital Equipment Corporation, 1975.
- 126. E. J. Darland, Ph.D. Thesis, Michigan State University, 1977.
- 127. Reference 71, pp. 104-106.
- 128. <u>Ibid</u>, pp. 171-176.
- 129. <u>Ibid</u>, pp. 301-303